PORTIONS OF THIS DOCUMENT ARE ILLEGIBLE

DOE/PC/30026--T3

DE82 008312

80PC30026-5

STUDY OF EBULLATED-BED FLUID DYNAMICS FOR H-COAL

QUARTERLY PROGRESS REPORT NO. 5
July 1, 1981 - Sept. 30, 1981

R. J. Schaefer, D. N. Rundell, D. A. Halbert

DATE PUBLISHED: NOVEMBER, 1981

CONTRACT DE-AC22-80PC30026

Research and Development Department
Amoco Oil Company
P.O. Box 400
Naperville, Illinois
60566

p

p

STUDY OF EBULLATED BED FLUID DYNAMICS FOR H-COAL

QUARTERLY PROGRESS REPORT NO. 5
July 1 - September 30, 1981

R. J. Schaefer, D. N. Rundell, D. A. Halbert

AMOCO RESEARCH CENTER
NAPERVILLE, ILLINOIS 60566

PREPARED FOR THE UNITED STATES
DEPARTMENT OF ENERGY
UNDER CONTRACT DE-AC22-80PC30026

DATE PUBLISHED: NOVEMBER, 1981

p p

TABLE OF CONTENTS

p p

FOREWORD

The H-Coal process, developed by Hydrocarbon Research, Incorporated (HRI), involves the direct hydroliquefaction of coal to low-sulfur boiler fuel or synthetic crude oil. The 200-600 ton-per-day H-Coal pilot plant is being operated next to the Ashland Oil, Incorporated, refinery at Catlettsburg, Kentucky, under DOE contract to Ashland Synthetic Fuels, Incorporated. The H-Coal ebullated bed reactor contains at least four discrete components: gas, liquid, catalyst, and unconverted coal and ash. Because of the complexity created by these four components, it is desirable to understand the fluid results of prior cold flow model experiments (1) to the operating H-Coal PDU reactor in Trenton, New Jersey. Studies are also planned to examine the coalescence behavior of gas bubbles in three-phase ebullated beds.

The work to be performed is divided into four parts: fluid dynamics measurements on the PDU reactor, gas bubble coalescence studies at Northwestern University, cold flow and mixing tests at Amoco's Naperville Research Center, and model implementation. The objective of this quarterly progress report is to outline progress in the first two areas.

p p

SUMMARY

Modification of the Amoco pilot plant was completed to permit performing cold flow tests at high gas rates without gas entrainment in the recycle line. A total of thirty-seven additional tests measuring the fluidization of a bed of HDS-2A catalyst by nitrogen and a kerosene/coal char slurry were completed

Analysis of the H-Coal PDU sample viscosity and density data from Battelle was started. Some inconsistency between this data and corresponding H-Coal PDU liquid physical property measurements from Oak Ridge National Laboratory was noted.

Northwestern University installed pressure drop transducers on their test column to permit calibration of their optical and capacitance probes. Test holographic images of gas bubbles in the column were also obtained. The literature search for the liquid mixing experiments was completed.

INTRODUCTION

The fluid dynamics of the H-Coal reactor has been previously studied in a cold flow unit. Reference 1 provides details of the construction of the unit and results of tests with a variety of gases, liquids, and catalyst sizes. A semi-theoretical model was developed to predict the volume fractions occupied by the gas, liquid, and catalyst phases. The aims of this new contract are fourfold:

1) The model developed using cold flow unit test results will be extended to apply to the operating H-Coal PDU reactor.

2) Because gas bubble dynamics are crucial in determining the nature of the flow, studies of bubble flow will be performed at Northwestern University using optically clear beds.

3) Liquid mixing tests will determine the residence time distribution of liquid in the reactor. Under the previous contract, it was determined that the coal char fines (simulating the unreacted coal and ash) were uniformly distributed throughout the bed. Hence, the measurement of liquid data is essential for modeling the residence time and knetic parameters associated with the unreacted coal.

4) The model will be implemented into a readily usable format.

DATA COLLECTION

HRI PDU Fluid Dynamics Study

Viscosity of PDU Reactor Liquid.-- All data received from Battelle's study of the viscosity and density of the PDU reactor liquid samples were stored in a computer for analysis and plotting. A final repo: (2) was also received from Oak Ridge National Laboratories detailing results o: their tests on four PDU liquid samples.

Amoco Cold Flow Fluid Dynamics Tests.-- After the Amoco cold flow unit was repiped to the configuration shown in Figure 1, fluid dynamics tests were continued with a kerosene/ coal char slurry, Previous tests in this series (3) were inconsistent with similar tests performed under a prior H-Coal contract (1), suggesting that the catalyst particles were incompletely soaked. The test series was therefore extended

p p

to cover the complete range of gas and liquid velocities. New slurry samples were taken under flow conditions to verify the coal char concentration in the kerosene.

Bench scale experiments were also performed to measure the apparent density of the coal char fines. A known weight of coal char was placed in a graduated cylinder. After addition of a measured volume of kerosene to the cylinder, the mixture was capped to prevent evaporation and allowed to soak for a week. Measurement of the final volume permits calculation of the fines density.

Bench scale experiments were performed to measure the terminal velocity of a variety of catalyst particles of differing sizes and shapes. The goal of these studies is to improve the ability to predict if parameters in the Richardson Zami correlation for non-spherical particles. Data analysis is in progress.

NORTHWESTERN UNIVERSITY

Gas Bubble Dynamics

The experimental effort at Northwestern University involved a variety of experimental tests to measure gas bubble behavior in a three phase fluidized bed. The holography studies continued; although pictures were taken over the entire cross-section of the test column, some interference problems were encountered when photographing the holographic image. A new lens system was designed and ordered to correct this problem. Pressure drop transducers were attached to the test column to measure the average gas holdup. This data will then be used for probe calibration. A single mode optical fiber was used in the light beam probe, allowing an easier alignment and eliminating undesirable light propagation modes. Data reduction programs are currently being developed to account for the effect of small gas bubbles (0.05-0.10mm diameter) which only partially interrupt the light beam. The impedance probe was employed to measure the variation of gas holdup across the radial position of the test column.

Northwestern's three monthly progress reports appear in Appendix A.

Liquid Mixing Tests

The literature search for articles describing experimental methods for measuring liquid despersion in a three phase fluidized bed was completed. The report appears in Appendix B and C.

DATA ANALYSIS

HRI PDU Fluid Dynamics Study

Viscosity of PDU Reactor Liquid.--A summary of the PDU liquid density and viscosity results from the Battelle testing appears in Table I. In some cases, Battelle repeated the measurements after modifying the viscometer in January, 1981. Table I therefore includes the data of the analysis.

Values in Table I were derived from interpolation of data plotted in Appendix D (slurry density), E (plastic viscosity) or F (yield stress). Density and yield stress were correlated by equations of the form

$$\rho = a + bT \qquad (1)$$

$$\tau_y = c + dT \qquad (2)$$

while the plastic viscosity was represented by the equation

$$N_{pl} = g \exp [h/T] \qquad (3)$$

The solid lines on each graph represent the best fit line.

Also included in Table I are the corresponding values obtained from Oak Ridge National Laboratories testing of four PDU liquid samples. (2) There are some substantial differences between the Battelle and ORNL values, as may be seen in the comparison of shear stresses at a 300 sec^{-1} shear rate. Because previous reports (3) documented the changes in physical properties with time, it is likely that both temperature and time effects are implicitly included in the data in Appendeces D-F. Further analysis is necessary to estimate the magnitude of these effects.

Amoco Cold Flow Fluid Dynamics Tests

After repiping of the Amoco cold flow unit the liquid slurry was recirculated to thoroughly mix the coal char and the kerosene. Table II documents the measured concentration determined by millipore filtration of coal char in the various liquid samples. A higher concentration was seen than previously reported; this was probably associated with more thorough mixing.

The results of the repeat measurements of coal char fines density appear in Table III. The density reported here is an apparent skeletal density, and does not include the pore volume which may be filled with kerosene.

The catalyst bed expansions and liquid and gas velocities are tabulated in Table IV. Because the bed expansions on the initial seventeen tests were inconsistent with prior data (3), these tests have been removed from the series. Bed expansion vs liquid and gas flow rate is plotted in Figure 2. No bed contractions were observed.

The volume fractions occupied by the gas, liquid and catalyst are tabulated in Table V for the dense phase in the catalyst bed and in Table VI for the dilute phase region above the bed.

Figure 3 presents the Darton Harrison drift flux versus gas holdup. The drift flux V_{cd} is defined by the expression

$$V_{cd} = \left(\frac{U_g}{E_g} - \frac{U_l}{E_l + E_f} \right) (E_g)\ (1 - E_g) \qquad (4)$$

The solid line in Figure 3 represents a composite of the ideal bubbly line data from previous experiments. A slight offset is seen in the data points, but only one or two low liquid velocity tests appear to depart from ideal bubbly behavior. Because the bed expansion was less than 10% for these two experiments, it is unclear if complete bed fluidization had been achieved. Figure 4 contrasts the drift flux results of this test series with those from run 204, a prior series with 5.1 vol % coal char fines. Within the data scatter, both systems appear similar.

PLANS FOR NEXT PERIOD

1) Continue analysis of Battelle data to determine effect of time and

temperature on PDU reactor liquid samples

2) Continue cold flow fluid dynamics tests at higher coal char concentration

3) Continue analysis of HRI PDU fluid dynamics data.

4) Continue efforts at Northwestern University

5) Begin preparations for liquid tracer test.

REFERENCES

1) I.A. Vasalos, et al., Final Progress Report, "Study of Ebullated Bed Fluid Dynamics for H-Coal," Contract DE-AC05-77ET-10149, February, 1980.

2) Letter, J. R. Hightower (ORNL) to R. J. Schaefer (Amoco) "Final Report-H-Coal Product Physical Properties Measurement" July 8, 1981

3) R. J. Schaefer et al. Quarterly Progress Report #4 "Study of Ebullated Bed Fluid Dynamics for H-Coal" Contract DE-AC22-80PC-30026 July 15, 1981.

NOMENCLATURE

Symbol	Description	(UNITS)
$\dot{\gamma}$	Shear rate	Sec^{-1}
η_{pl}	Plastic viscosity	$N.S/m^2$
τ	Shear stress in viscometer	N/m^2
τ_o	Yield stress	N/m^2
ϵ	Volume fraction of component	
a	Correlation parameter for density	g/cc
b	Correlation parameter for density	g/cc-deg K
c	Correlation parameter for yield stress	N/m^2
d	Correlation parameter for yield stress	N/m^2-deg K
g	Correlation parameter for plastic viscosity	$N.S/M^2$
h	Correlation parameter for plastic viscosity	deg K
u	Superficial velocity	Ft/Sec
V_{cd}	Darton-Harrison drift flux	mm/Sec

Subscripts

b	Bed (dense) phase value	
c	Catalyst	
g	Gas	
l	Liquid	
γ	Determined by γ-ray absorption	
ΔP	Determined by ΔP measurement	

TABLE 1

PDU REACTOR LIQUID VISCOSITIES AND DENSITIES (11)

Sample ID		Period Sample Was Taken	Sample Date	Battelle Date of Analysis	Battelle To (1)	Battelle η_{pl} (2)	Battelle ρ (3)	ORNL To (4)	ORNL η_{pl} (5)	ORNL ρ (6)	ORNL T* (7)	Battelle T* (7)
Amoco-1		130-93-04A	7/30/80	3/81	0.114	1.49	0.790					
-2		130-93-04A	7/30/80	5/81	0.201	1.78	0.772					
-3		130-93-10A	8/05/80	3/81	0.134	2.28	0.883					
-4		130-93-20A	8/28/80	5/81	0.052	1.52	0.867					
-5	ORNL-1	130-93-27A (8)	9/04/80	2/81	0.056	2.18	0.904	0.1270	1.683	0.908	0.632	0.710
-6	ORNL-2	130-93-34A	9/11/80	2/81	0.142	2.71	0.945	3067	3.027	0.985	1.215	0.955
-7 (9)		130-93-41B	9/19/80 AM	---	----	----	-----					
-8		130-93-42A	9/19/80 PM	4/81	0.117	3.01	0.855					
-9	ORNL-3	130-93-42A	9/19/80 PM	4/81	0.062	1.76	0.857	0.2324	1.730	0.882	0.751	0.590
-10		130-93-42B	9/20/80 AM	4/81	0.072	1.27	0.841					
-11	ORNL-4	130-93-43A	9/20/80 PM	2/81	0.308	2.49	0.945	0.1911	1.070	0.838	0.512	1.055
-12		130-93-43B	9/21/80 AM	2/81	0.065	1.67	0.874					
-13 (10)		130-93-44A	9/21/80 PM	----	-----	----	-----					
-14		130-93-44B	9/22/80 AM	3/81	0.002	0.77	0.872					
-15		130-93-45A	9/22/80 PM	3/81	0.302	2.24	0.928					
-16		130-93-45B	9/23/80 AM	3/81	0.048	2.24	0.957					

Notes

(1) N/m^2 interpolated to 719°K from Appendix F
(2) mPa.s (cp), interpolated to 719°K from Appendix E
(3) g/cc, interpolated to 719°K from Appendix D
(4) N/m^2 from Reference 2.
(5) mPa.s from Reference 2.
(6) g/cc from Reference 2.
(7) N/m^2 at 300 Sec^{-1} shear rate.
(8) Amoco-5 taken 9/4/80 at 1600 hours (Period 27A). ORNL-1 taken 9/4/80 at 1830 hours (Period 27F).
(9) Sample was contaminated during testing and discarded. See Appendix A of Reference [3]
(10) Sample bomb contained only gas.
(11) These values are preliminary only. See text for discussion.

TABLE II

COAL CHAR CONCENTRATIONS IN KEROSENE SLURRY, RUN 221

Sample ID	Sample location	Wt% Coal fines	
AU-77-156	First spool piece(reactor base)	7.21	
AU-77-157	Recycle Line from recyclecup	7.54	(1)
AU-77-158	2nd spool piece (60" from reactor base)	6.97	
AU-77-159	3rd spool piece (120" from reactor base)	7.08	
AU-77-160	4th spool piece (180" from reactor base)	7.19	
AU-77-161	Reactor liquid overhead line	(2)	
	Average	7.11 ± 0.11	

Notes

(1) Not included in average

(2) Sample lost in processing

TABLE III

MEASUREMENT OF COAL CHAR FINES DENSITY

	(A)	(B)	(C)
(1) Mass of empty graduated cylinder;gm	647.5	693.0	683.5
(2) Mass of dry coal fines added, gm	80.5	119.5	240.0
(3) Volume of kerosene added, ml	500	500	500
(4) Final volume of slurry, ml	555	580	670
(5) Final mass of cylinder & slurry gm	1131	1220	1329.5
(6) Apparent density of fines, g/cc	1.46	1.49	1.41

Note: $6 = \frac{2}{4-3}$

TABLE IV

% BED EXPANSION FOR RUN 221

CATALYST : HDS2A
GAS : NITROGEN
LIQUID : KEROSENE
COAL CHAR CONC: 4.0 VOL %
TEMPERATURE : 73. DEG F

Run No.	Liquid Flow Rate, Ft/Sec	Gas Flow Rate Ft/Sec	Catalyst Bed Height (In.)	% Bed Expansion
221-18	0.053	0.0	47.	2.
-19	0.079	0.0	50.	9.
-20	0.103	0.0	56.	22.
-21	0.128	0.0	65.	41.
-22	0.156	0.0	73.	59.
-23	0.171	0.0	86.	87.
-24	0.163	0.0	96.	109.
-25	0.052	0.049	48.	4.
-26	0.055	0.079	49.	7.
-27	0.053	0.103	47.	2.
-28	0.052	0.128	49.	7.
-29	0.080	0.047	55.	20.
-30	0.080	0.077	58.	26.
-31	0.080	0.104	59.	28.
-32	0.079	0.129	59.	28.
-33	0.106	0.048	66.	43.
-34	0.106	0.080	66.	43.
-35	0.106	0.108	66.	43.
-36	0.107	0.134	68.	48.
-37	0.131	0.050	70.	52.
-38	0.132	0.083	73.	59.
-39	0.134	0.111	76.	65.
-40	0.132	0.136	64.	39.
-41	0.161	0.053	81.	76.
-42	0.159	0.087	84.	83.
-43	0.158	0.116	87.	89.
-44	0.177	0.052	92.	100.
-45	0.191	0.086	97.	111.
-46	0.206	0.052	106.	130.
-47	0.201	0.077	106.	130.
-48	0.102	0.068	66.	43.
-49	0.102	0.106	67.	46.
-50	0.102	0.134	68.	48.
-51	0.131	0.135	81.	76.
-52	0.050	0.0	47.	2.
-53	0.176	0.0	84.	83.
-54	0.201	0.0	97.	111.

TABLE V

CALCULATED HOLDUPS, RUN 221: DENSE PHASE

CATALYST : HDS2A
GAS : NITROGEN
LIQUID : KEROSENE
COAL CHAR CONC: 4.0 VOL %
TEMPERATURE : 73. DEG F

Run No.	Liquid Flow Rate, Ft/Sec	Gas Flow Rate, Ft/Sec	ϵ_{cs}	$\epsilon_{\ell,\gamma}$	$\epsilon_{\ell,\Delta P}$	$\epsilon_{g\gamma}$	Vcd (Mm/Sec)
221-18	0.053	0.0	0.54	0.44	0.58	0.0	0.0
-19	0.079	0.0	0.51	0.46	0.55	0.0	0.0
-20	0.103	0.0	0.45	0.52	0.60	0.0	0.0
-21	0.128	0.0	0.39	0.56	0.64	0.0	0.0
-22	0.156	0.0	0.35	0.62	0.67	0.0	0.0
-23	0.171	0.0	0.29	0.67	0.70	0.0	0.0
-24	0.163	0.0	0.26	0.69	0.71	0.0	0.0
-25	0.052	0.049	0.53	0.37	0.0	0.09	10.2
-26	0.055	0.079	0.52	0.37	0.0	0.10	18.1
-27	0.053	0.103	0.54	0.35	0.0	0.10	24.4
-28	0.052	0.128	0.52	0.37	0.0	0.10	31.4
-29	0.080	0.047	0.46	0.45	0.0	0.07	9.8
-30	0.080	0.077	0.44	0.43	0.0	0.12	15.0
-31	0.080	0.104	0.43	0.41	0.0	0.15	20.0
-32	0.079	0.129	0.43	0.40	0.0	0.15	26.2
-33	0.106	0.048	0.38	0.55	0.47	0.05	11.5
-34	0.106	0.080	0.38	0.49	0.42	0.10	16.2
-35	0.106	0.108	0.38	0.45	0.38	0.15	19.4
-36	0.107	0.134	0.37	0.44	0.38	0.17	24.4
-37	0.131	0.050	0.36	0.56	0.50	0.06	10.6
-38	0.132	0.083	0.35	0.52	0.47	0.11	15.6
-39	0.134	0.111	0.33	0.50	0.48	0.14	19.6
-40	0.132	0.136	0.40	0.39	0.29	0.20	17.5
-41	0.161	0.053	0.31	0.61	0.56	0.06	11.1
-42	0.159	0.087	0.30	0.58	0.52	0.10	16.8
-43	0.158	0.116	0.29	0.56	0.50	0.12	22.0
-44	0.177	0.052	0.28	0.65	0.63	0.05	11.0
-45	0.181	0.086	0.26	0.63	0.60	0.09	17.3
-46	0.206	0.052	0.24	0.67	0.68	0.06	9.5
-47	0.201	0.077	0.24	0.64	0.65	0.09	13.7
-48	0.102	0.068	0.38	0.51	0.46	0.08	14.8
-49	0.102	0.106	0.38	0.46	0.41	0.14	20.1
-50	0.102	0.134	0.37	0.45	0.40	0.16	25.7
-51	0.131	0.135	0.31	0.50	0.45	0.16	24.0
-52	0.050	0.0	0.54	0.43	0.52	0.0	0.0
-53	0.176	0.0	0.30	0.64	0.69	0.0	0.0
-54	0.201	0.0	0.26	0.69	0.72	0.0	0.0

TABLE VI

CALCULATED HOLDUPS, RUN 221--DILUTE PHASE

CATALYST : HDS2A
GAS : NITROGEN
LIQUID : KEROSENE
COAL CHAR CONC: 4.0 VOL %
TEMPERATURE : 73. DEG F

Run No.	Liquid Flow Rate, Ft/Sec	Gas Flow Rate, Ft/Sec	ϵ_{ℓ}, γ	$\epsilon_{\ell}, \Delta P$	ϵ_g, γ
221-18	0.053	0.0	0.93	0.93	0.0
-19	0.079	0.0	0.93	0.93	0.0
-20	0.103	0.0	0.93	0.93	0.0
-21	0.128	0.0	0.94	0.93	0.0
-22	0.156	0.0	0.93	0.93	0.0
-23	0.171	0.0	0.93	0.93	0.0
-24	0.163	0.0	0.93	0.93	0.0
-25	0.052	0.049	0.87	0.92	0.10
-26	0.055	0.079	0.82	0.88	0.14
-27	0.053	0.103	0.79	0.85	0.17
-28	0.052	0.128	0.77	0.83	0.20
-29	0.080	0.047	0.86	0.91	0.11
-30	0.080	0.077	0.81	0.86	0.15
-31	0.080	0.104	0.77	0.83	0.19
-32	0.079	0.129	0.75	0.81	0.21
-33	0.106	0.048	0.85	0.90	0.11
-34	0.106	0.080	0.80	0.85	0.16
-35	0.106	0.108	0.77	0.81	0.20
-36	0.107	0.134	0.73	0.79	0.24
-37	0.131	0.050	0.84	0.90	0.12
-38	0.132	0.083	0.80	0.84	0.17
-39	0.134	0.111	0.76	0.82	0.21
-40	0.132	0.136	0.72	0.78	0.25
-41	0.161	0.053	0.86	0.91	0.11
-42	0.159	0.087	0.80	0.86	0.17
-43	0.158	0.116	0.76	0.82	0.21
-44	0.177	0.052	0.86	0.92	0.10
-45	0.181	0.086	0.81	0.86	0.15
-46	0.206	0.052	0.87	0.92	0.09
-47	0.201	0.077	0.84	0.89	0.13
-48	0.102	0.068	0.82	0.86	0.15
-49	0.102	0.106	0.77	0.82	0.20
-50	0.102	0.134	0.74	0.79	0.23
-51	0.131	0.135	0.73	0.77	0.24
-52	0.050	0.0	0.94	0.93	0.0
-53	0.176	0.0	0.93	0.93	0.0
-54	0.201	0.0	0.94	0.93	0.0

Figure 1

NEW PIPING CONNECTION DIAGRAM FOR COLD FLOW FLUID DYNAMICS UNIT

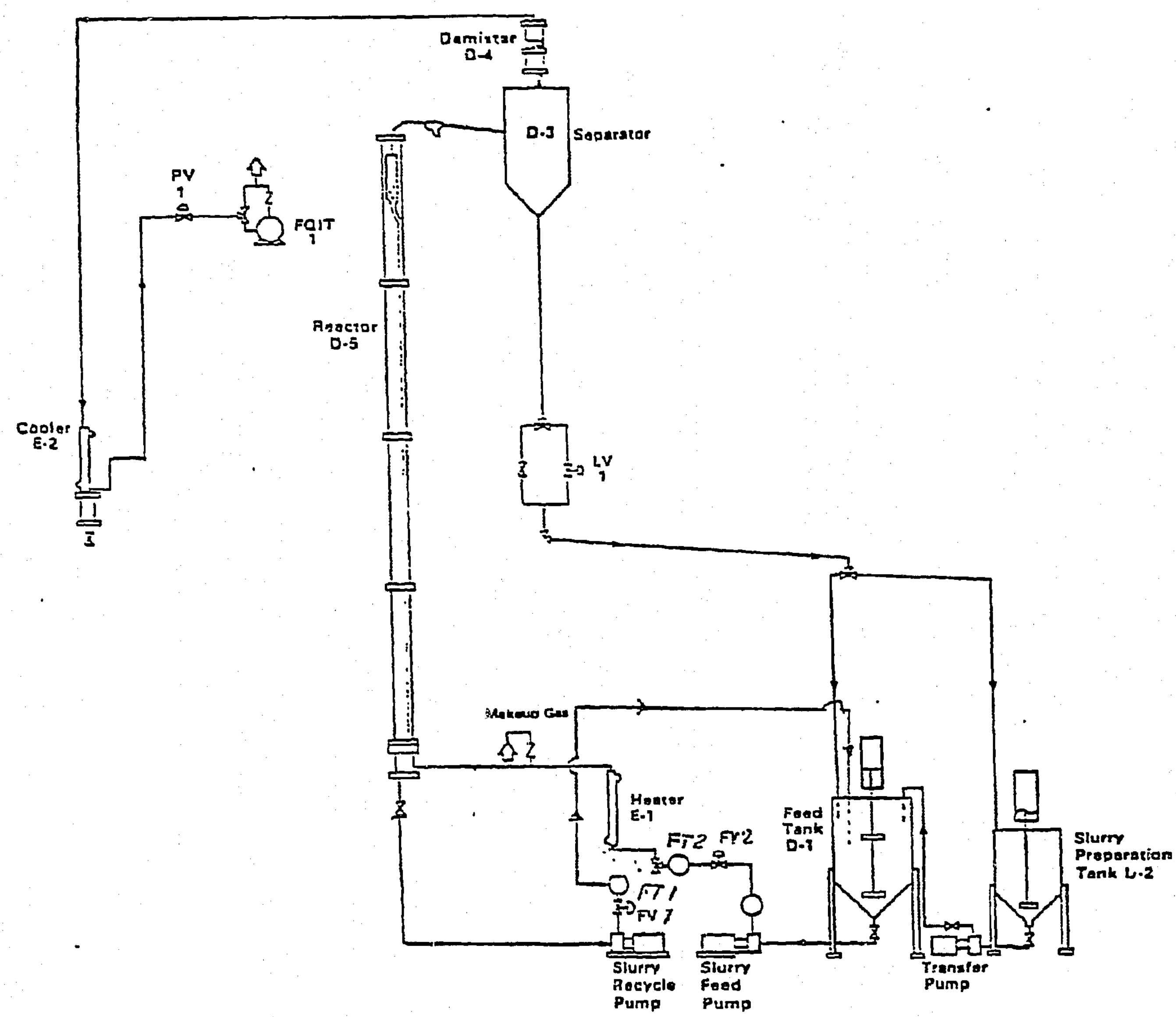

Figure 2

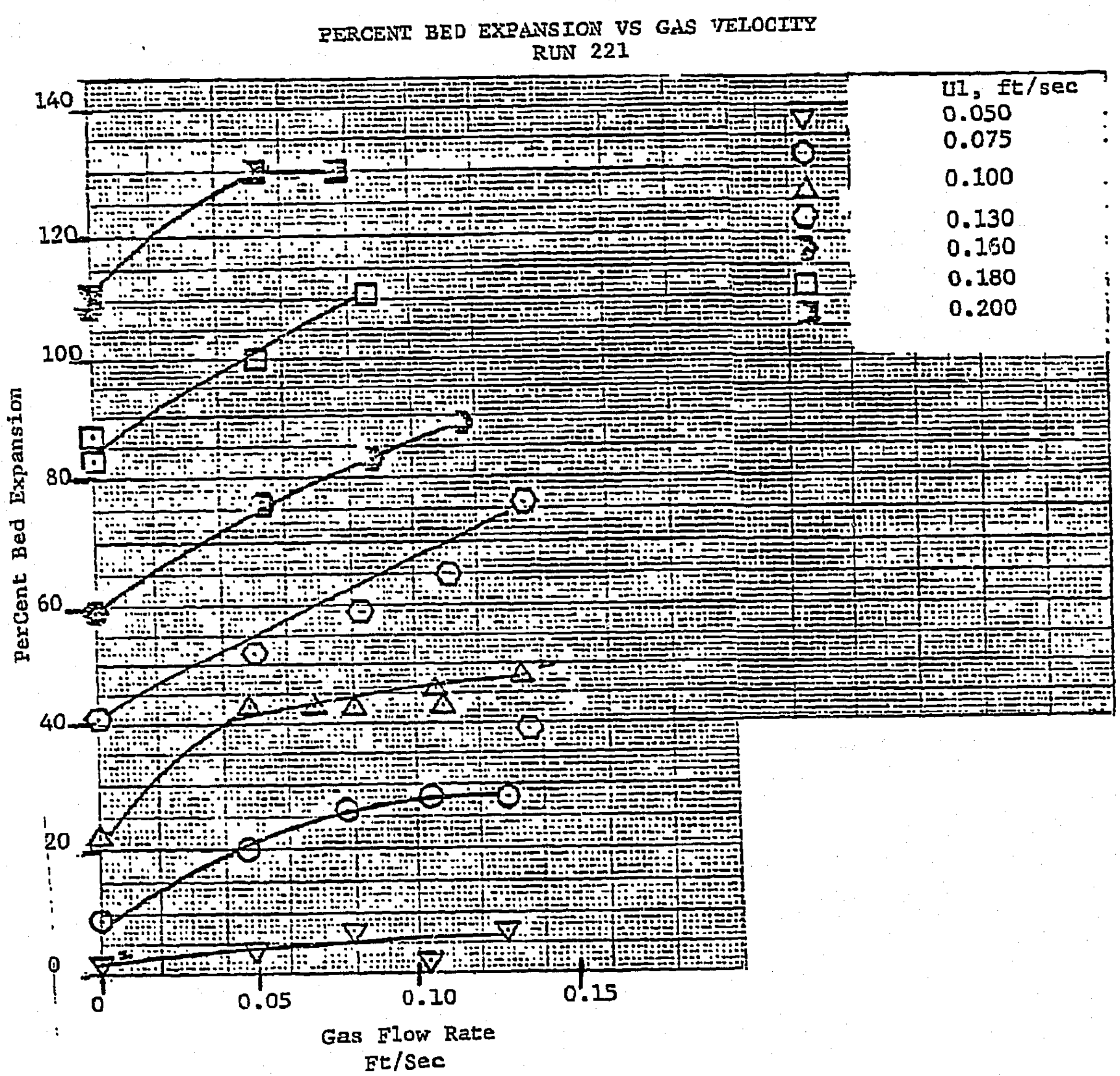

PERCENT BED EXPANSION VS GAS VELOCITY
RUN 221
Ul, ft/sec
0.050
0.075
0.100
0.130
0.160
0.180
0.200
140
120
100
80
60
40
20
0
PerCent Bed Expansion
0
0.05
0.10
0.15
Gas Flow Rate
Ft/Sec

Figure 3
DRIFT FLUX VS GAS HOLDUP
RUN 221

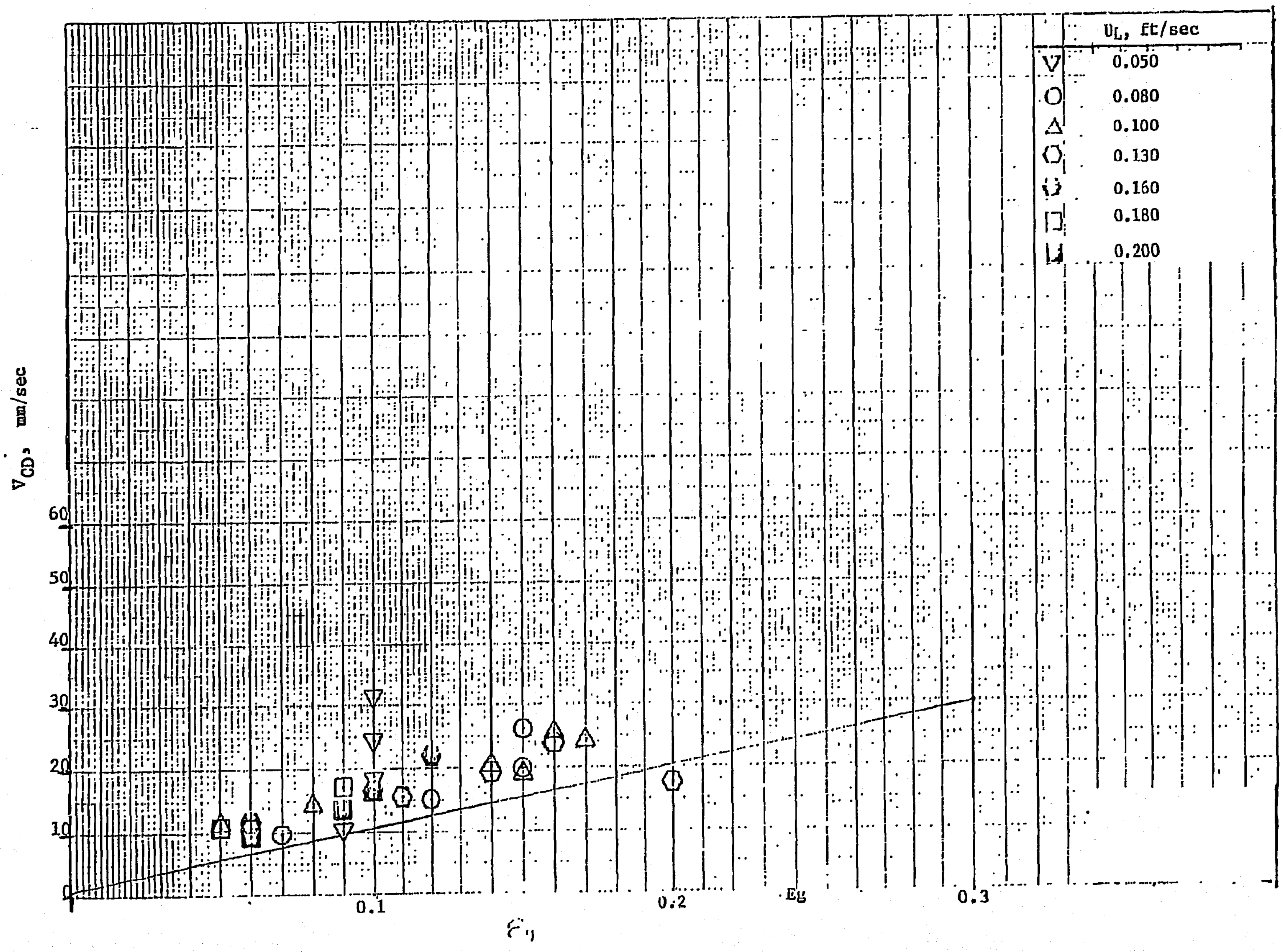

Figure 4

DRIFT FLUX COMPARISON: RUN 221 VS RUN 204

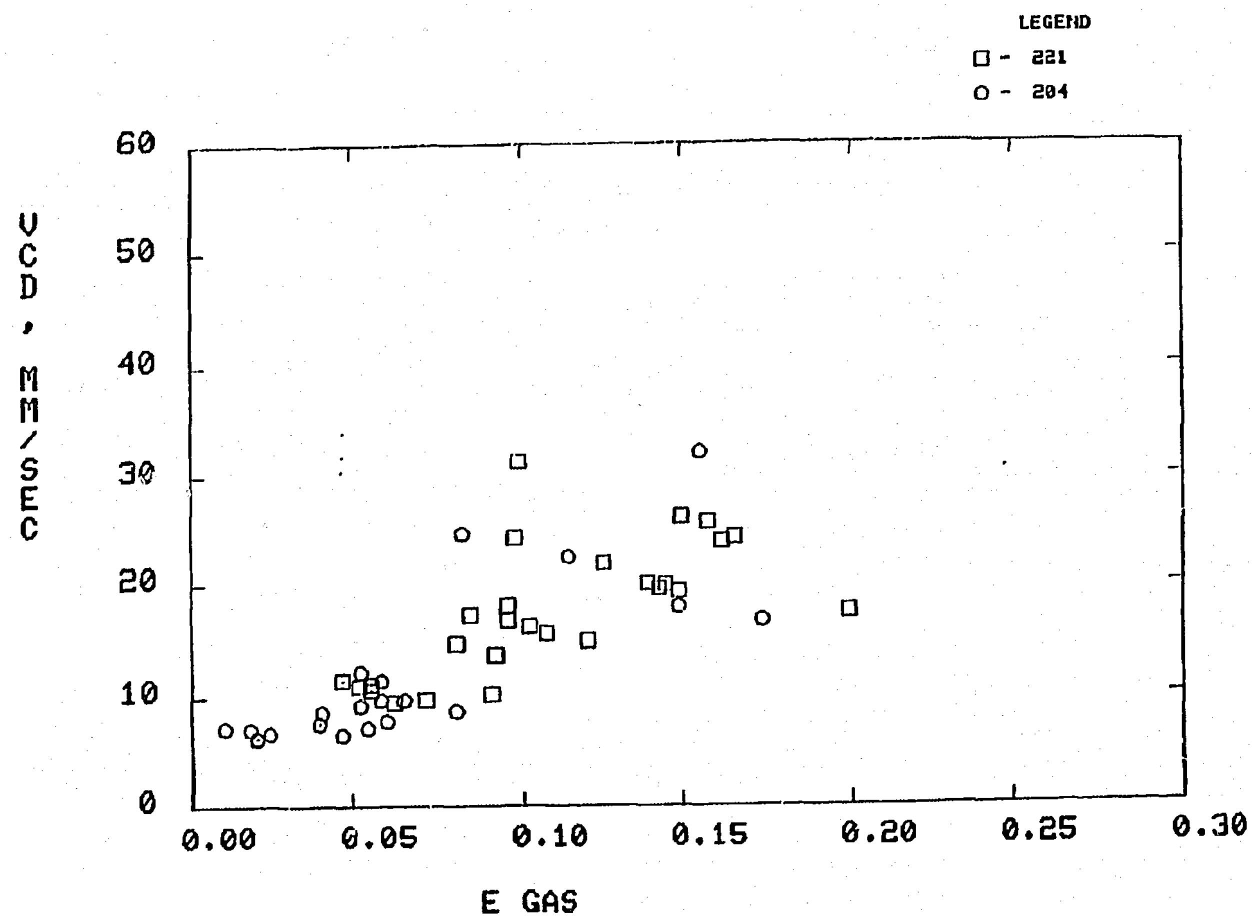

APPENDIX A

NORTHWESTERN UNIVERSITY MONTHLY PROGRESS REPORTS

MONTHLY (JULY 1981) PROGRESS REPORT ON AMOCO DOE CONTRACT

"ON H-COAL FLUID DYNAMICS"

1. Light Beam Probe

In last month's report we stated our hope of using a single mode optical fiber to transmit the light into the input probe. We received 15 meters of the fiber from ITT and used it in a test set-up. The fiber worked very well. We have ordered some positioning equipment and lenses (for focusing the laser into the fiber). After they are installed it will be much easier to operate the light beam probe.

2. Three Inch Diameter Column

The supplies necessary for constructing the small column have now either arrived or are expected very soon. Also, the shop has the work orders for the inlet and outlet sections, along with the spool pieces. Thus, the small column should be ready for use by about the end of August.

3. Holography

Attached are two photographs taken at different planes of focus from a hologram. We took 16 such pictures to traverse the 6" test section. The mean diameter of the bubbles is about 2.3 mm. The resolution is satisfactory to make accurate measurements. Bubbles in focus in one photograph are not in focus in the other photograph. We are now taking holograms at higher flow rates to determine the limit of its applicability.

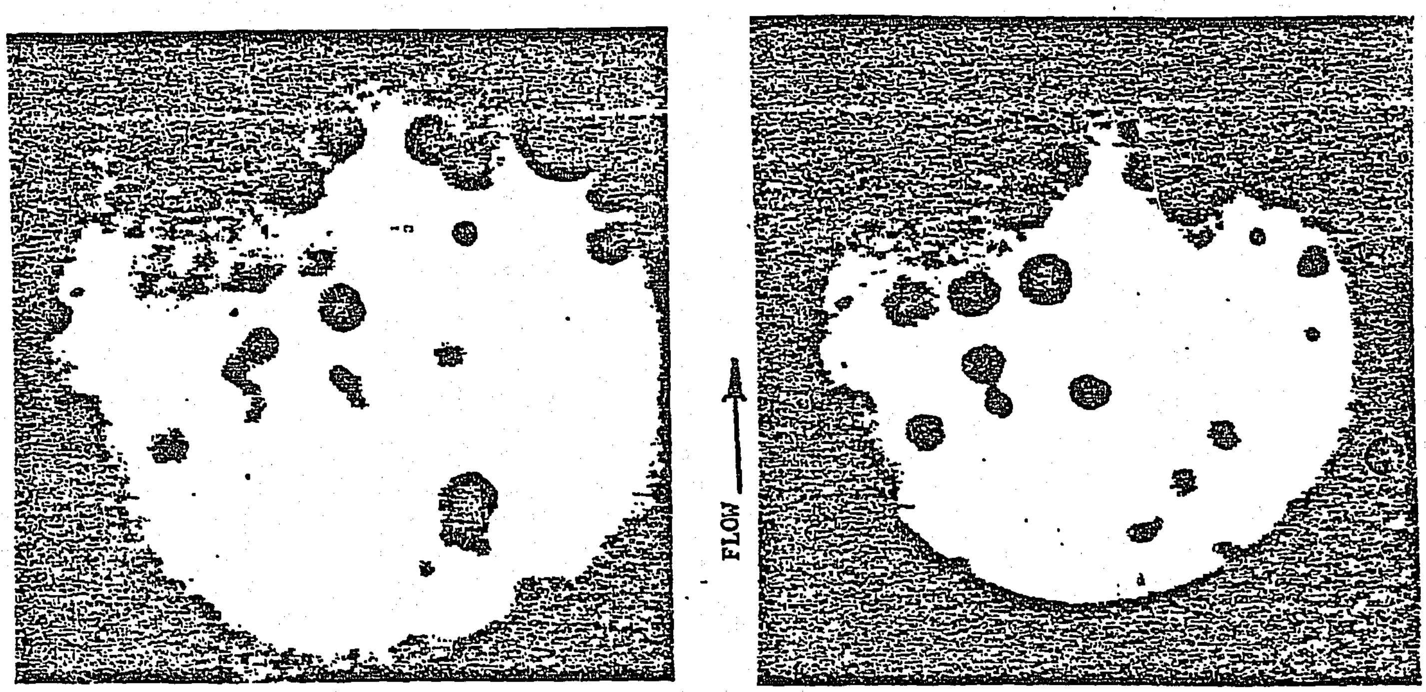

Scale 1" = 76.5 mm

Liquid Flow rate = 0.62 ft^3/ min.; Gas Flow = 0.01 lb/min.

MONTHLY (AUGUST 1981) PROGRESS REPORT ON AMOCO DOE CONTRACT

"ON H-COAL FLUID DYNAMICS"

I. Pressure Drop Measurement and Holography

Measurements were made of the fluidized bed height for various liquid flowrates in order to determine the average liquid void fraction within the fluidized bed. The percent bed expansion was calculated and plotted versus the liquid flowrate. (See attached Table 1 and Figure 1.) The superficial liquid velocity and the volume fractions of each phase, solid and liquid, were also found. A copy of these results were forwarded to Joseph Leung of Amoco's research center in Naperville at his request.

Data has also been taken as an attempt to determine average volume fractions of a three-phase system having both liquid and gas travelling through the bed. This is being done by measuring the pressure drop between spool pieces using a Validyne pressure transducer. The output from the transducer is connected to the analog-to-digital converter of the Mechanical Engineering Department's PDP 11/44 Computer. By taking a large number of pressure readings over a period of time, we are able to determine the mean pressure drop of the steady-state system. It is hoped that such measurements will be a quick way to determine the volume fractions of each phase for different operating conditions. These measurements can later be compared to similar results obtained by the other research methods being developed for this project. To date, one quarter of the measurements needed to complete this portion of the project have been taken and analyzed. It is hoped that this effort will be completed within the next two weeks.

The laser holography research has been temporarily halted while new lenses used to collect and focus the laser light on to the holographic plate have been ordered. The lens system currently in use has a very long focal distance, with some of the images being focused in the same plane as the holographic plate. By testing other lens arrangements using a computer simulation developed, it was found that a lens with a longer focal length was required. When implemented, this new lens arrangement should allow for better image formation over an improved focal length.

Also added to the laser holography set-up was a photography reticle attached to the end of the light pipe used to input the laser light to the test section. The reticle is an etched glass disk with a 20 mm graduated scale. This should aid in size calibrations along with determining the the amount of optical distortion.

II. Light Beam Probe

A considerable amount of work was put into making the light beam probe utilizing a single-mode optical fiber operational. That has been accomplished and it is now a relatively simple matter to re-position the probes anywhere in the column and quickly align them.

The two primary difficulties which had to be overcome were:

1. Elimination of undesired cladding modes of light propagation in the optical fiber. These modes are stripped off by bathing a section of the fiber in an index matching fluid. See Figure 2.
2. Converting the highly divergent light obtained from the exit end of the optical fiber into a collimated beam of the proper diameter propagating along the axis of the input probe. The optics are shown in Figure 2, and that assembly slides into the body of the input probe. The design of the tip portion of the probe is shown in Figure 3.

III. Small Column Construction

Some of the necessary materials and equipment took longer than expected to arrive, but all major items are now in. The shop is currently making the necessary column sections and will next put together the holding tank.

IV. Impedance Probe

As mentioned before, the output signal from the probe can be transformed into a binary sequence with the help of either a single threshold or a double threshold. Two trigger circuits have been set up to achieve the job. But the difference of the two trigger levels, which are built in the double-threshold circuit, can not be adjusted. The setting of the threshold is therefore quite restricted. Hence a computer program has to be developed in order to increase the flexibility of trigger-setting. Such a program has been constructed, and the thresholds can be set easily by the user.

Local void fractions have been measured at different threshold levels and gas flow rates. The results are shown in the diagrams attached. So far, the liquid flow rate is kept constant, and the bed is not fluidized. Figs. 4 - 7 show how the void fraction changes with the threshold at various gas flow rates. It can be clearly seen that the higher the difference of the two trigger levels is, the smaller the void fraction can be obtained. Therefore the void fraction determined at single threshold has the largest value. The phenomenon is more pronounced for higher gas flow rate.

Figs. 8 - 11 show how the void fraction changes with the gas flow rate. From those figures, the void fraction varies with the gas flow rate. However, it is not so obvious for the two curves corresponding to gas flow rate 0.0892, and 0.1319 ft^3/min.

Also, from those figures, it is noted that the distribution of bubbles is not symmetric at all times. There may be some channels in the packing bed.

Table 1

BED EXPANSION WITH LIQUID FLOW

LIQUID FLOWRATE (FT^3/MIN)	PERCENT BED EXPANSION	SUPERFICIAL LIQ. VELOCITY (FT/MIN)	VOLUME FRACTION (SOLID)	VOID FRACTION (LIQUID)
0.3081	9.09	4.4245	0.6301	0.3699
0.4794	9.09	6.8845	0.6301	0.3699
0.6189	9.09	8.8878	0.6301	0.3699
0.7802	10.91	10.9006	0.6198	0.3802
0.9404	16.82	12.1365	0.5884	0.4116
1.0954	22.73	13.2274	0.5601	0.4399
1.2503	27.27	14.4413	0.5401	0.4599
1.4020	34.55	15.2268	0.5109	0.4891
2.5477	93.64	20.9794	0.3550	0.6450
2.7060	104.09	21.6741	0.3368	0.6632
3.0220	127.27	23.0115	0.3024	0.6976
3.1800	140.00	23.6717	0.2864	0.7136
2.3960	83.64	20.3412	0.3743	0.6257
2.2445	73.64	19.7364	0.3957	0.6041
2.0715	65.45	18.8260	0.4155	0.5845
1.8985	57.27	17.9158	0.4371	0.5629
1.7260	50.00	16.9223	0.4582	0.5418
1.5530	41.82	16.0091	0.4847	0.5153
1.4020	32.73	15.4478	0.5179	0.4821

TOTAL VOLUME OF PACKING = 0.29664 FT^3
BED HEIGHT, (NO LIQUID FLOW), = 2.2917 FT, (TIGHTLY PACKED BED).
AT 0.00% BED EXPANSION, THE SOLID VOLUME FRACTION = 0.6876
TEMPERATURE = 78°F.

BED EXPANSION WITH LIQUID FLOW

TEMPERATURE = 78°F

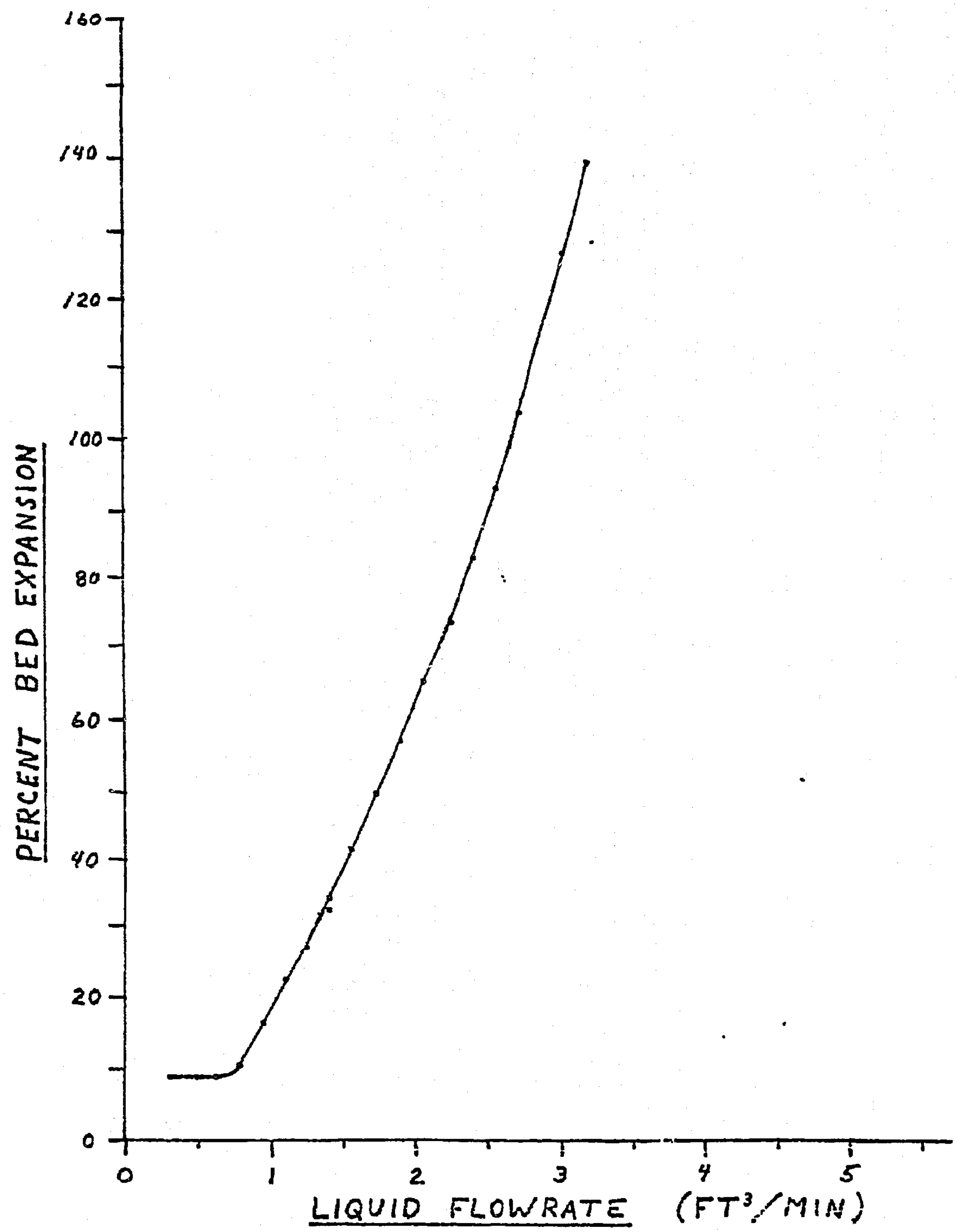

Figure 1

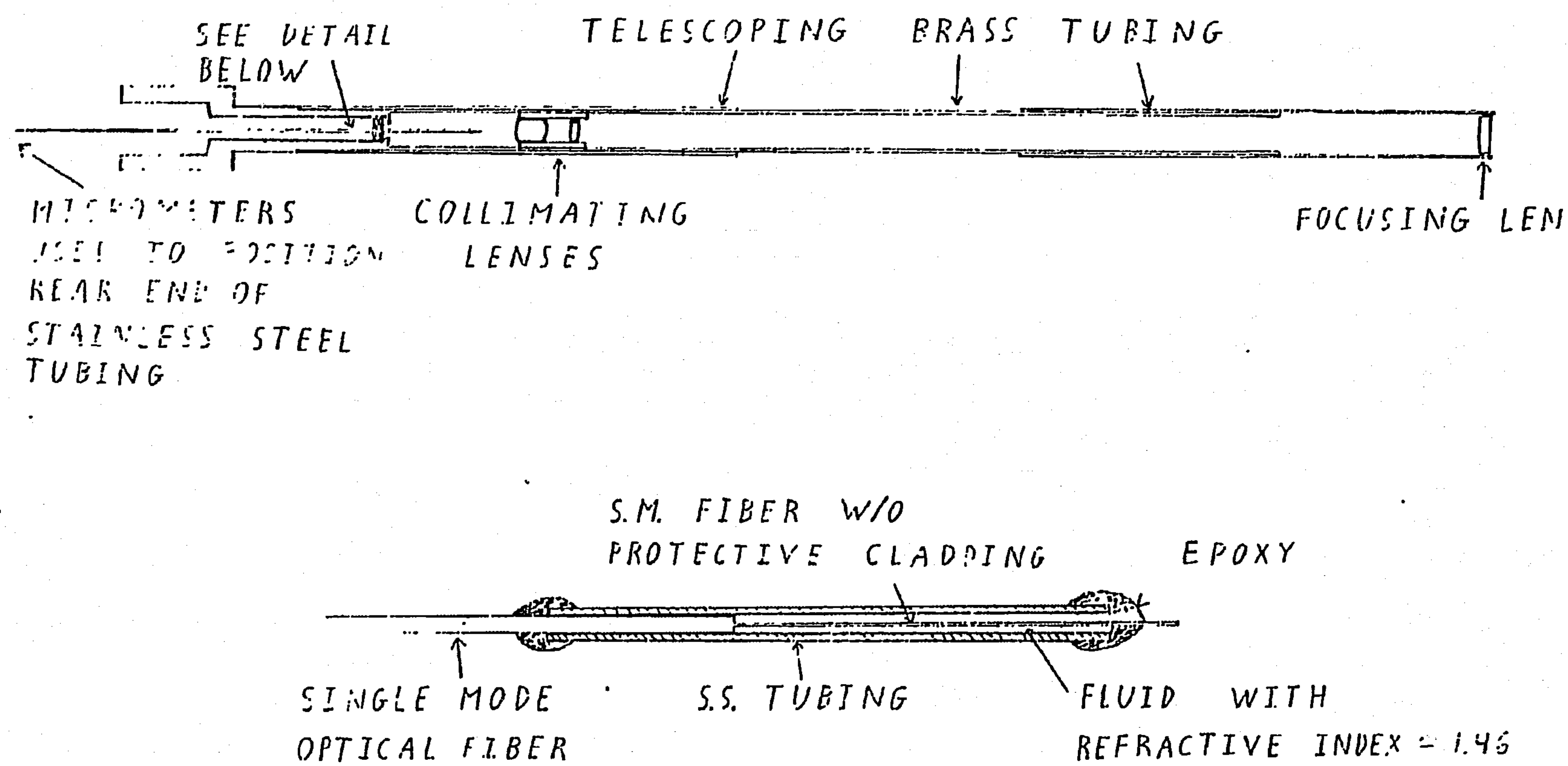

Fig 2 OPTICAL ARRANGEMENT FOR INPUT PROBE

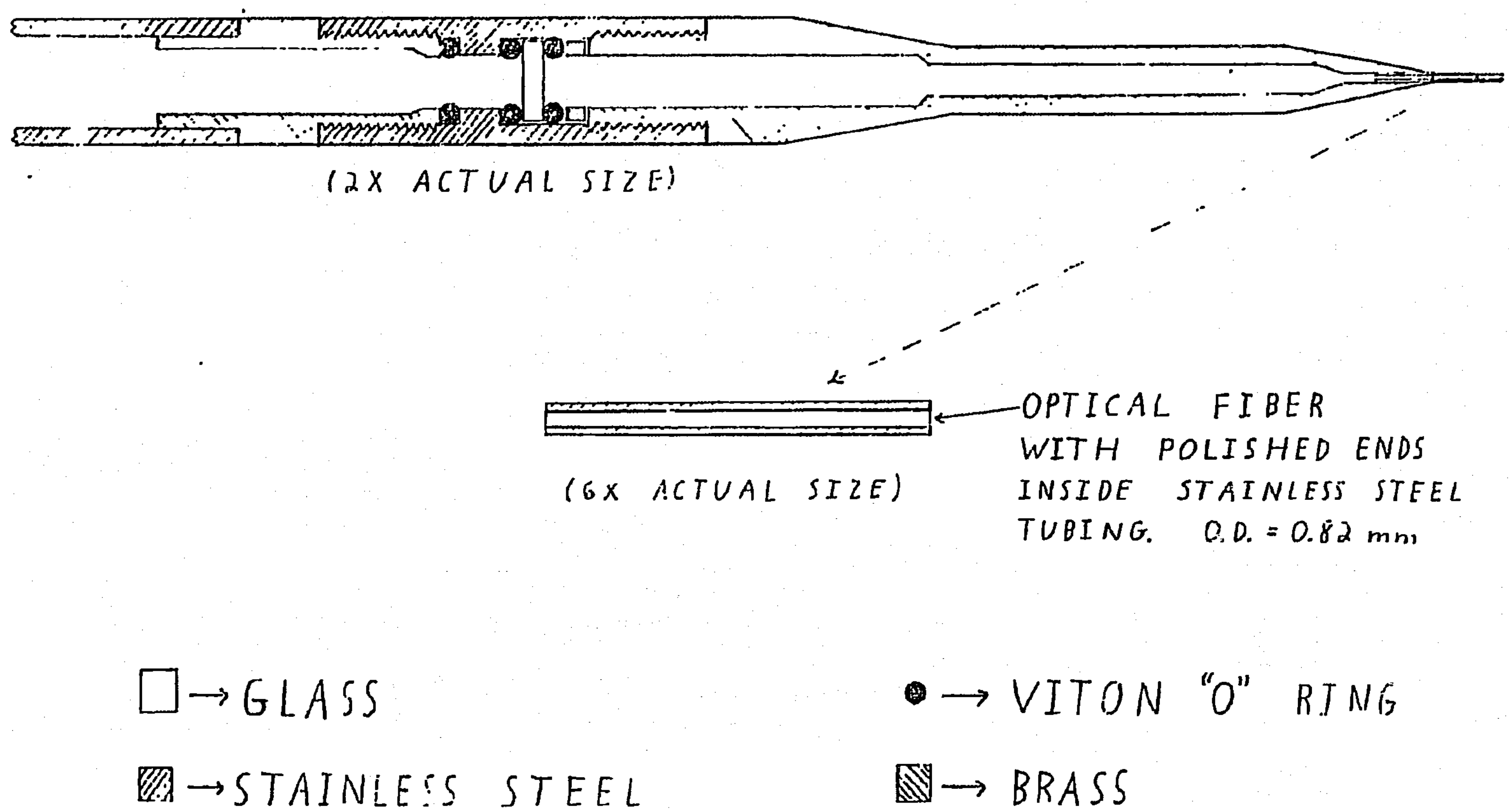

CROSS-SECTIONAL VIEW OF LIGHT-BEAM PROBE TIP

Fig. 3

Above bed

Fig 4:

Liquid Flow Rate : 0.31 ft^3/min

Gas Flow Rate : 0.0575 ft^3/min

Thresholds.

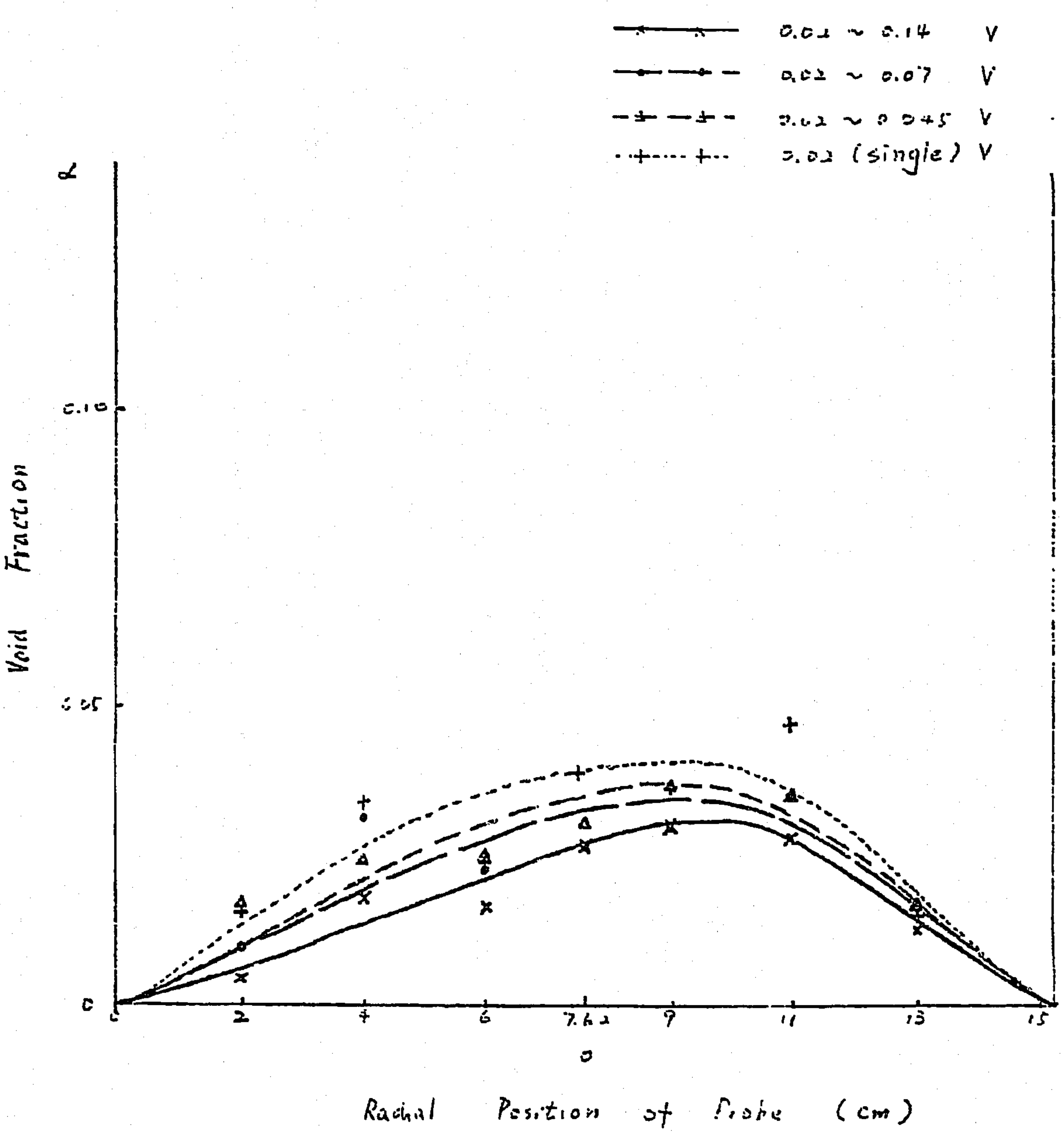

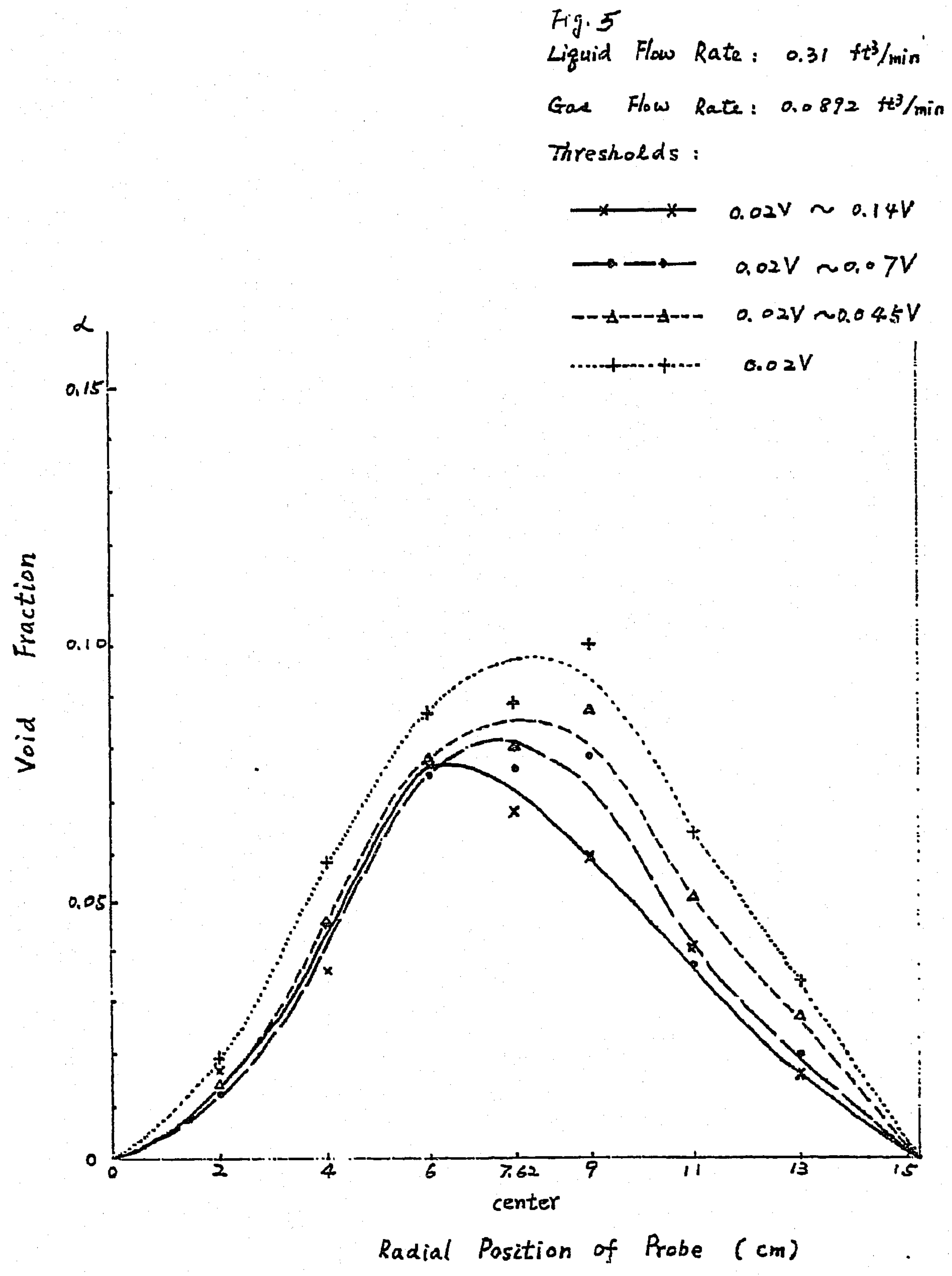
Fig. 5
Liquid Flow Rate: 0.31 ft³/min
Gas Flow Rate: 0.0892 ft³/min
Thresholds:
0.02V ~ 0.14V
0.02V ~ 0.07V
0.02V ~ 0.045V
0.02V
α
Void Fraction
0.15
0.10
0.05
0
0
2
4
6
7.62
9
11
13
15
center
Radial Position of Probe (cm)

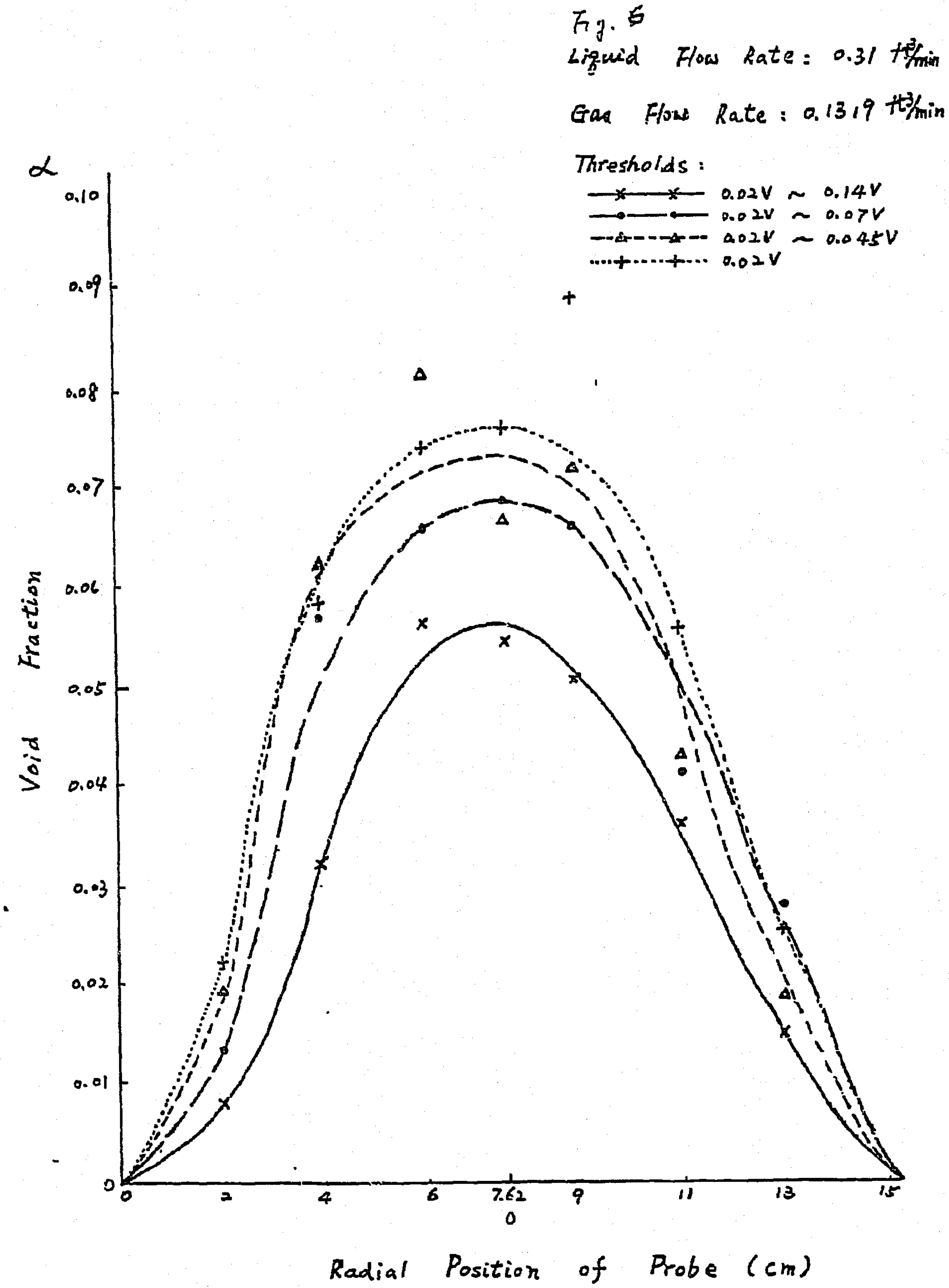
Fig. 5
Liquid Flow Rate: 0.31 ft³/min
Gas Flow Rate: 0.1319 ft³/min
Thresholds:
0.02V ~ 0.14V
0.02V ~ 0.07V
0.02V ~ 0.045V
0.02V
α
Void Fraction
0.10
0.09
0.08
0.07
0.06
0.05
0.04
0.03
0.02
0.01
0
0
2
4
6
7.62
0
9
11
13
15
Radial Position of Probe (cm)

Fig. 7

Liquid Flow Rate : 0.31 ft³/min

Gas Flow Rate : 0.1715 ft³/min

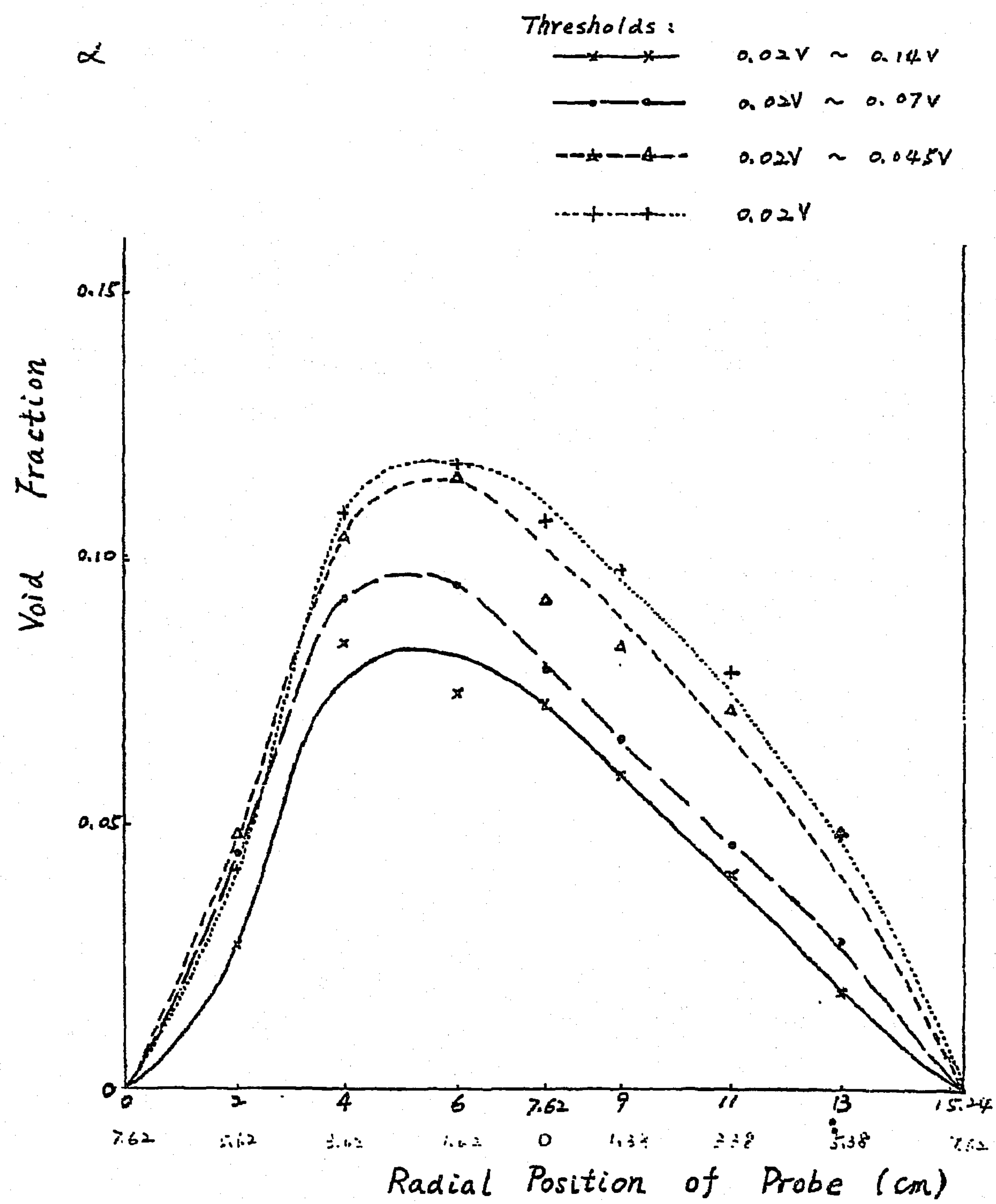

Fig. 8

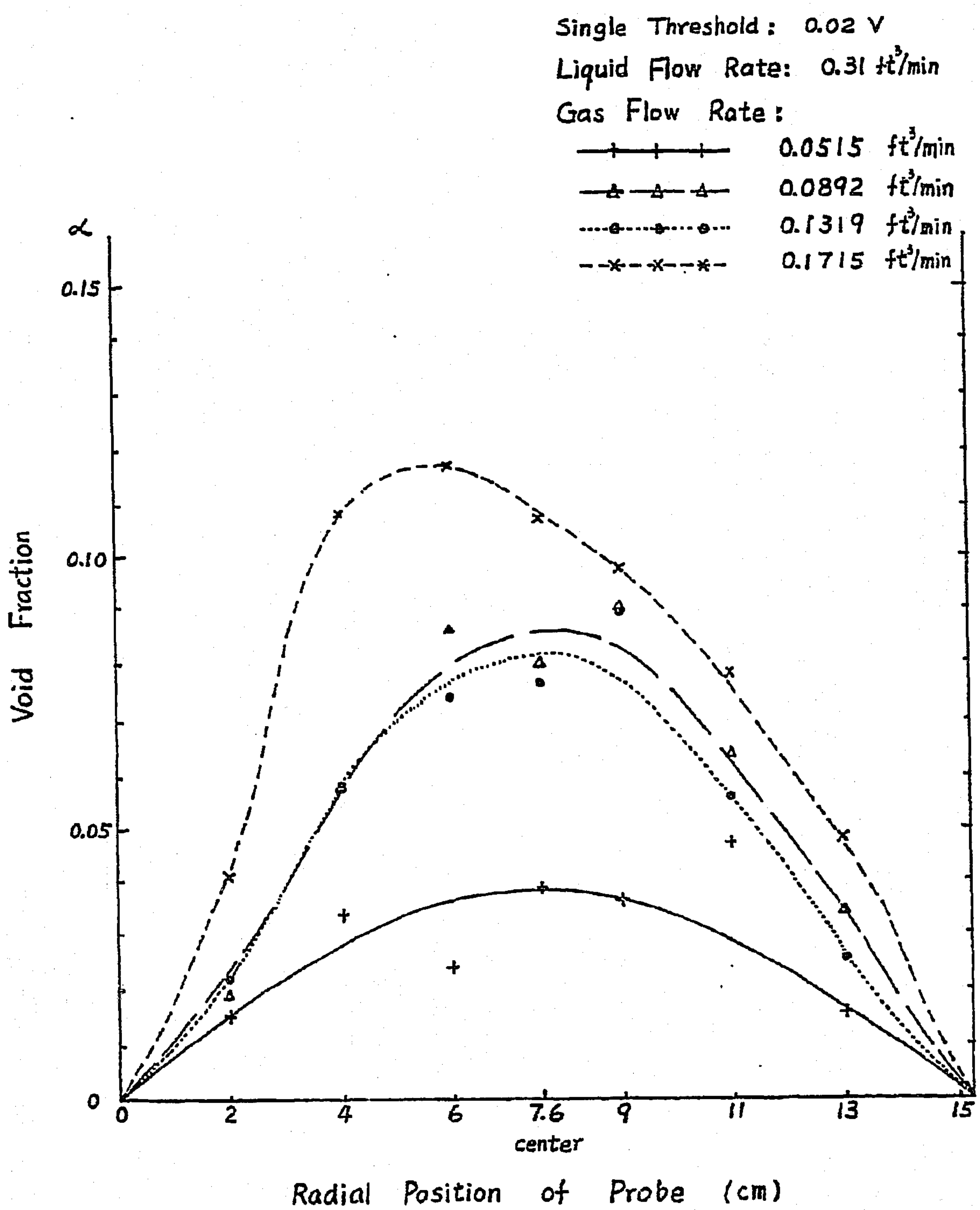

Single Threshold : 0.02 V
Liquid Flow Rate: 0.31 ft³/min
Gas Flow Rate :
0.0515 ft³/min
0.0892 ft³/min
0.1319 ft³/min
0.1715 ft³/min
α
0.15
0.10
0.05
0
Void Fraction
0
2
4
6
7.6
9
11
13
15
center
Radial Position of Probe (cm)

Fig. 9

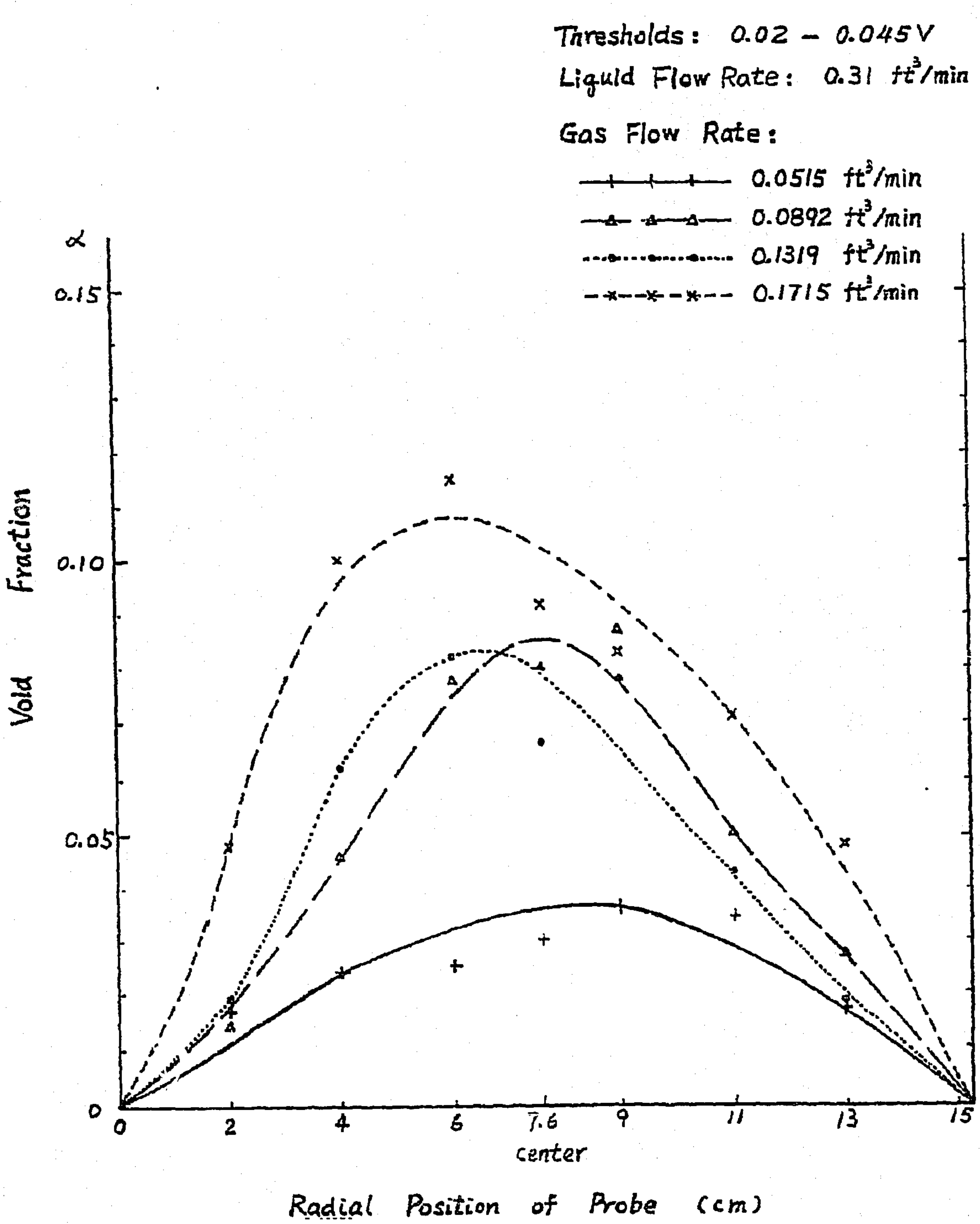

Thresholds: 0.02 – 0.045V
Liquid Flow Rate: 0.31 ft³/min
Gas Flow Rate:
0.0515 ft³/min
0.0892 ft³/min
0.1319 ft³/min
0.1715 ft³/min
α
0.15
0.10
0.05
0
Void Fraction
0
2
4
6
7.6
center
9
11
13
15
Radial Position of Probe (cm)

Fig. 10

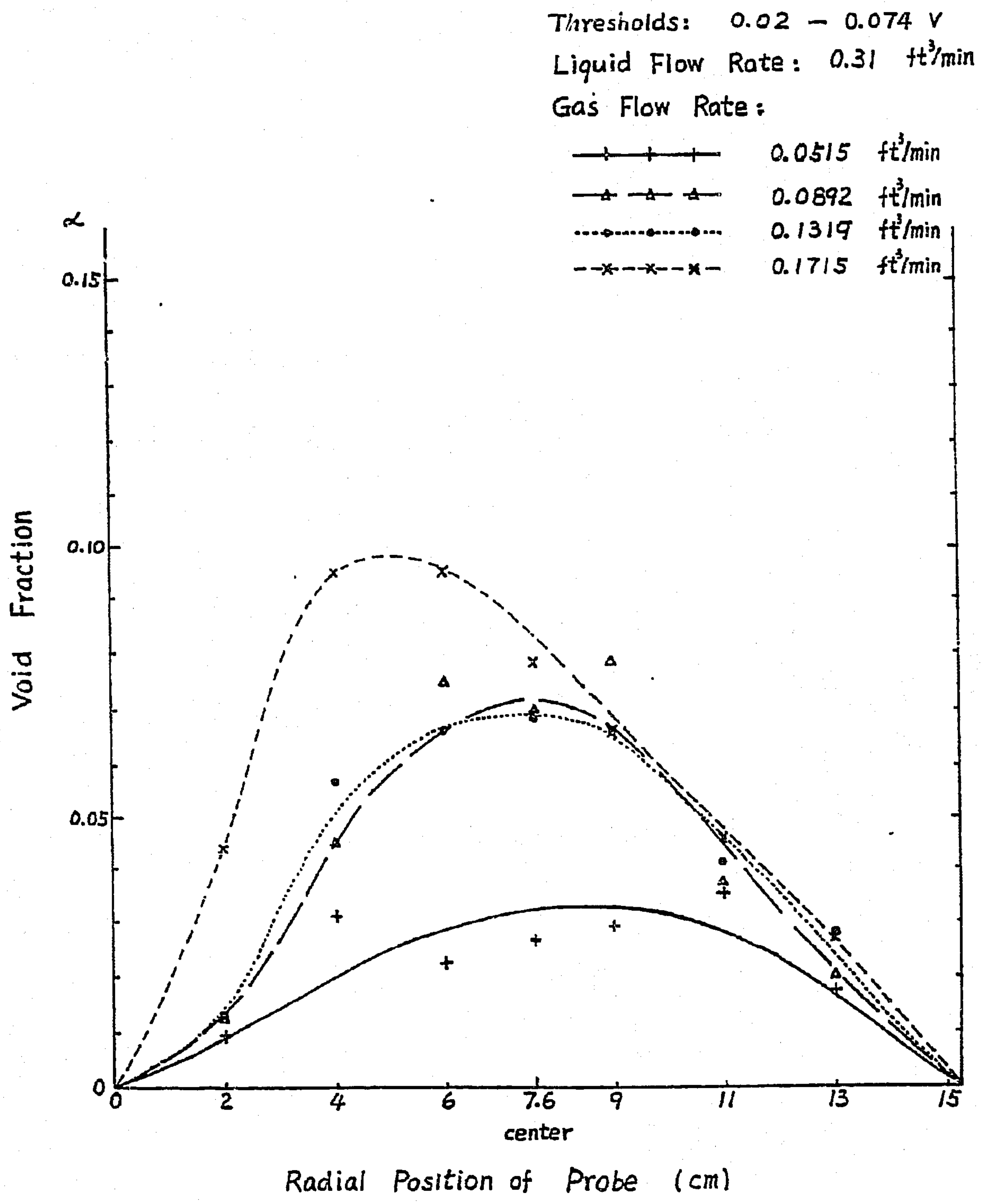
Thresholds: 0.02 – 0.074 V
Liquid Flow Rate: 0.31 ft³/min
Gas Flow Rate:
0.0515 ft³/min
0.0892 ft³/min
0.1319 ft³/min
0.1715 ft³/min
α
0.15
0.10
0.05
0
Void Fraction
0
2
4
6
7.6
9
11
13
15
center
Radial Position of Probe (cm)

Fig #1

Thresholds : 0.02 ~ 0.14 V

Liquid Flow Rate · 0.31 ft^3/min

Gas Flow Rate :

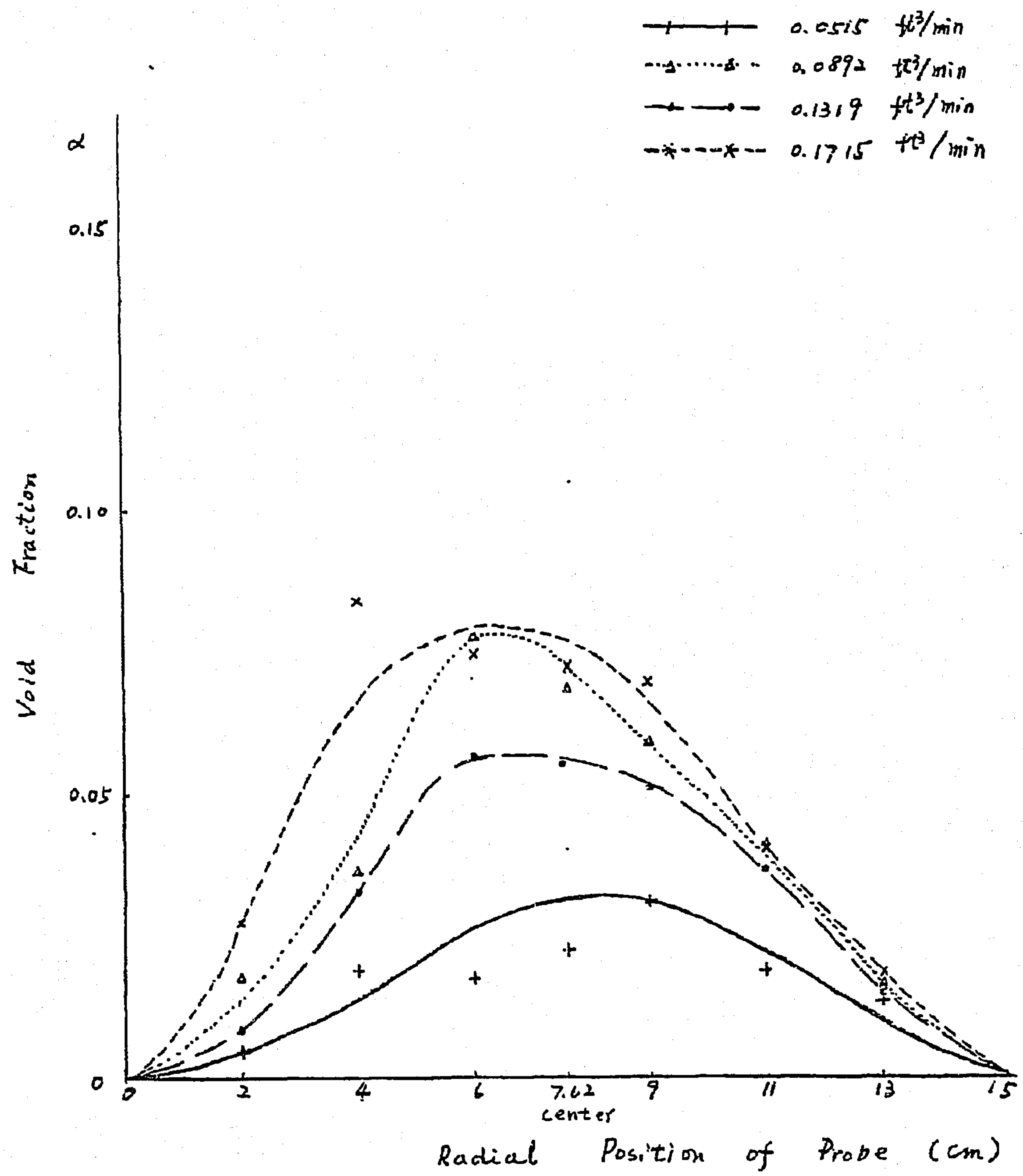

MONTHLY (SEPTEMBER 1981) PROGRESS REPORT ON AMOCO DOE CONTRACT

"ON H-COAL FLUID DYNAMICS"

Work on the light beam probe portion of this project for the past month has focused on determining the best way to analyze data produced by small bubbles (0.05 mm to about 1. mm diameter) which only partially block the light beam. Based upon data from a small sample (eleven) of such partial blockages, it appears as though it will be possible to determine the size and velocity of individual bubbles which generate such data.

Our next steps in the development of the method are to:

1. Write the computer programs for the collection of large samples os data, followed of course by data taking and analysis.
2. Check the accuracy of the method using glass beads and latex spheres in the above stated size range. These are currently being ordered.

In addition, a description of the technique will be written up soon and made available to AMOCO.

APPENDIX B

LIQUID MIXING IN THE H-COAL SYSTEM: LITERATURE SEARCH

APPENDIX B

LIQUID MIXING IN THE H-COAL SYSTEM: LITERATURE SEARCH

Introduction

The H-Coal reactor is a three phase fluidized bed. In the cold flow unit used at AMOCO to model the pilot plant, the catalyst bed is fluidized by a kerosene and coal char slurry phase and nitrogen gas. An understanding of the mixing phenomena within the fluidized bed is essential to model the H-Coal reactor. Mixing data will be combined with other hydrodynamic data (ie. bed expansion) and kinetics to ultimately complete the H-Coal process model.

AMOCO's contract tasks include characterizing the gas and liquid phase mixing using the cold flow unit. Gas phase mixing experiments were completed in Naperville under the first H Coal contract. (1) Argon-41 was employed as a radioactive tracer, and the system was modeled using the number of stirred tanks in series approach. Liquid phase mixing experiments will be performed under the current contract. While radioactive tracers could be used, disposal of large quantities of low level radioactive liquid wastes would be a major problem. Elimination of the waste proposal problem provides the incentive for examining other experimental techniques. Possible experimental methods were identified and flow models used in characterizing liquid mixing were reviewed in the literature search. The slope and methods used in the literature search are discussed in Appendix C. A knowledge of reactor engineering and residence time distribution models is assumed.

Liquid Phase Mixing Experiments

A number of tracers and techniques have been used to obtain residence time distribution functions for chemical reactors. In this particular case the interest is in obtaining an RTD for the liquid phase of the gas-liquid solid system under non-reacting conditions. Some basic requirements must be met by any tracer experiment:

- The tracer compound must be miscible and have similar physical properties to the fluid stream
- The tracer compound should be accurately detectable in small concentrations
- The concentration of the tracer must be easily monitored and the detector response should be linear
- The tracer compound should not be absorbed on solids in the system
- The tracer compound should be chemically inert

These criteria will affect the choice of tracers for H-Coal, and a brief discussion is included in the discussion section.

Among recent liquid mixing experiments in three phase fluidized beds is work done by Ying, et. al. (7) at Air Products and Chemicals, Inc. The SRC-I process was modeled using an air/water/sand mixture, and the mixing performance of the liquid phase was followed using a conductivity tracer.

Roadcap, et.al. (8) at Oak Ridge National Labs studied liquid mixing in three phase bioreactors. The experimental method employed used a flouroscein dye as a tracer, and the tracer concentration measurements were taken in a sampling leg. The data was reduced by several methods of analysis, and a correlation between the Peclet number and the flow parameters was made.

Examples of experimental techniques prior to 1980 are reviewed in several books and review articles. Three phase experiments are discussed in Shah's text (2A). A table of commonly used tracers is included, broken down by the components of the three phase system.

Wen and Fan (3) divided liquid phase experiments into catagories by tracer method. Four classes were indexed: conductivity salts, color and uv dyes, radioactive tracers, and titrations. Forty five papers are included, eight of them dealing with fluidized beds.

Shah, Stiegel and Sharma (1) give a more extensive review of experimental work, indexed by reaction system. Twenty-eight examples of liquid phase tracers from the literature are given, with three citations for work in three-phase fluidized beds, but no additional tracer techniques are presented. Other review articles covering the earlier development of tracer methods and mixing models include Ostergaard (5) and Bischoff (6).

A summary of liquid phase mixing experiments from fluidized beds is included in Table B-I.

Input Functions and Mixing Models

Five input tracer functions have been used by investigators to study the mixing behavior of liquid phases in reactors. The two best known and most widely used are step and pulse concentration functions, but others are possible. The results are fitted to a dispersion model, which ordinarily is a one parameter model like the n-CSTR or Peclet number models. Two, three, and four parameter models have been used in more complicated cases, (i.e. segregated flow in reactors).

Levenspiel (9) or Carberry (10) offer an introductory treatment of the simplest cases involving pulse and step inputs, and present the mathematics of the one-parameter models under conditions of perfect tracer inputs.

A more useful technique for analyzing pulse input tracer data is provided by the analysis of moments method first used by Ostergaard and Michelson (11). The method of moments is the most commonly used analytical technique for obtaining an axial Peclet number and was used by both Ying, et al. (7) and Roadcap, et al. (8).

Steady state, oscillatory (sinusoidal), and random tracer input functions are complicated to analyze. Special mathematical transfer functions have been used and are reviewed by Mecklenburgh and Hartland (12). The treatment of random tracer injection by Laguerre functions is covered by Anderssen and White (13). While the mathematics allow for any input function, they are unecessarily complicated for most experimental work.

Application to H-Coal

Despite the vast prior literature, application of a mixing model to characterize the liquid phase of the H-Coal reactor has been hampered by the difficulty of finding a suitable experimental tracer system.

If the H-Coal reactor is assumed to be well-mixed radially, a one-parameter model can characterize the liquid mixing if recycle is ignored. This method was used by Ying et al. (7) and Roadcap et. al. (8). If recycle is not neglected, the two parameter model used by Vasalos et. al (1) to model the H-Coal gas phase mixing can be applied. In all three of these studies the tracer input was pulsed with data analyzed by the moments method of Ostergaard and Michelsen (11, 7, 8) or by trial and error (1).

Conductivity Salts

While conductivity salts are normally used in aqueous liquid systems, additives are available that increase the conductivity of petroleum fuels in low concentrations. These additives are miscible organic salts and are detectable in the ppm range. Conductivity is a linear function of the additive concentration, since kerosene and kerosene/coal slurries are non-conductive. There are several problems with conductivity salts: a conductivity probe is an invasive technique which may cause flow disruptions; the invasive probe must operate in an environment of fines, catalyst pellets, and gas bubbles; and the conductivity additives are organic and may adsorb onto the catalyst or fines.

UV and Visible Dyes

Organic soluble dyes are available from a number of sources, and have been used extensively in studying mixing of clear liquids. Dyes offer the experimental advantage that the detector is outside the reactor and does not disrupt the flow. The dye method requires the use of a transparent system, and is therefore incompatible with coal char fines used in the H-Coal fluid dynamics studies.

Radioactive Tracers

Use of radioisotope tracers is an attractive experimental technique, because it combines the non-invasive detection of a dye experiment with the ability to use the gas/slurry/catalyst system. Radioactive Argon gas was previously used to model the H-Coal dispersion (1).

A fifth method, magnetic flux was used by Lytle, et.al. (14) to study the residence time of particles in a coal hydrogenation reactor. Each of these five methods involves a tradeoff among the previously mentioned criterm. For a good tracer system a particular problem arises because the liquid phase for the H-Coal study is kerosene, whereas all the previous studies in Table B-1 used water.

Conclusions

1. Liquid mixing in flow reactors is well described in the literature. Models of varying complexity are available. Wen and Fan (3) is recommended as the most complete recent treatise.

p p

REFERENCES - APPENDIX B

(1) I. A. Vasalos, E. M. Bild, D. F. Tatterson, C. C. Wallin "H-Coal Fluid Dynamics Topical Report Part I: Literature Search" Prepared under D.O.E. Contract EF-77-C-01-2588. Report FE-2588-6 Published May, 1978

(2) Y. T. Shah Gas-Solid Liquid Reactor Design, McGraw Hill, New York, 1979

(3) C. Y. Wen, L. T. Fan Models For Flow Systems and Chemical Reactors, Marcel Dekker, New York, 1975

(4) Y. T. Shah, J. Stiegel, M.M. Sharma, AIChE J. v 24, no 3 p. 369, 1978

(5) K. Ostergaard "Gas Liquid Particle Operations in Chemical Reaction Engineering" Advance in Chemical Engineering v. 7 Academic Press, New York (1968).

(6) K.B. Bischoff Ind. Eng Chem. v 58, n. 11, p. 18, 1966.

(7) D. Ying, R. Sivasubramanian, E. N. Givens "Gas Slurry Flow in Coal Liquifaction Processes" Air Products & Chemicals-January, May, August, and December 1980.

(8) S. Roadcap, R. A. Trevino - Lozano, S. Znaimer "Residence - Time Distribution Studies in Fluidized-Bed Bioreactors," ORNL/MIT - 319, March 1981

(9) O. Levenspiel Chemical Reaction Engineering, 2 ed. John Wiley & Sons, New York, 1972

(10) J. J. Carberry Chemical and Catalytic Reaction Engineering, McGraw Hill, New York, 1976

(11) K. Ostergaard and M. L. Michelsen Canadian J. Chem. Eng., v47, p107, 1969

(12) J. C. Mecklenburgh and S. Hartland, The Theory of Backmixing, Wiley Interscience, New York, 1975

(13) A. S. Anderssen and E. T. White, Canadian Journal of Chemical Engineering, v.47, p.288, 1969

(14) Lylte, J.M. Jr. "A Kinetic Study of the Liquifaction by Catalytic Hydrogenation of Various Utah Coals." Thesis. University of Utah, 1979

TABLE B-1

SUMMARY OF LIQUID MIXING EXPERIMENTS IN FLUIDIZED BEDS

System			Tracer	Input	Reference
Liquid	Gas	Solid			
H_2O		Sand	$NaNO_3$	Step	B1
H_2O		Glass lead beads	$NaNO_3$	Step	B2
H_2O		Glass, steel beads	Fluorescein	Sinusoid or Pulse	B3
H_2O		Glass bead	KCl	Step	B4
H_2O		Benzoic acid	Benzoic acid	Steady state	B5, B6
H_2O		Sand	HCl	Steady state	B7
H_2O		Glass bead	Dye	Sinusoid	B8
H_2O		Glass, resin, steel	NaCl	Pulse	B9
H_2O		B napthol	B napthol	Steady state	B10
H_2O	air	Glass bead	NaCl (infrared)	---------	B11
H_2O	air	Glass bead	Br-82	---------	B12
H_2O	air	Glass	NaCl	---------	B13
H_2O	air	Sand	NaCl	Pulse	B14
H_2O	air	Coal	Fluoroscein	Pulse	B15

REFERENCES FOR TABLE B-1

B1 Bruinzeel, C., Roman, G. M., and Van Der Laan, E. Th., Third Congress of the European Federation of Chem. Eng., Olympia, London, June 20-29, 1962.

B2 Cairns, E. J., and Prausnitz, J. A., A.I.Ch.E. Journal, 6, 400 (1960).

B3 Chung, S. F., and Wen, C. Y., A.I.Ch.E. Journal, 14, 857 (1968).

B4 Kramers, H., and Alberda, G., Chem. Eng. Sci. 2, 173 (1953).

B5 Miller, E., M. S. Thesis, West Virginia University (1961).

B6 Wen, C. Y., Miller, E., and Fan, L. T., 140th ACS Meeting, Chicago, September 3-8, 1961.

B7 Muchi, I., Manuro, T., and Sasaki, T., Chem. Eng. (Japan), 25, 747 (1961).

B8 Nakanishi, K., Ph.D. Disertation, Toheku University, Sendi, Japan (1966).

B9 Shemilt, I. J., and Krishnaswamy, P. R., 16th Can. Chem. Eng. Conf., Windsor, Ontario, Oct. 16-19, 1966.

B10 Wakno, N., Oshima, T., and Yagi, S., Chem. Eng. (Japan), 22, 786 (1958).

B11 Hochman, J. M. and J. R. McCord. Chem Erg. Sci. vol 25. p97, 1970

B12 Michelsen, M. L. and K. Ostergaard Chem Eng J. vol 2, p 37, 1970

B13 Schugeri, K. Proceedings of an International Symposium on Fluidization, Netherland University Press, Amsterdam p. 782, 1967.

B14 D. Ying, R. Siuasubramanian, E. N. Givens "Gas Slurry Flow in Coal Liquifaction Processes" Air Products and Chemicals, January 1980.

B15 S. Roadcap, R. A. Trevino - Lozano, S. Znaimer Residence - Time Distribution Studies in Fluidized-Bed Bioreactors, ORNL/MIT-319, March 1981.

APPENDIX C

THE LITERATURE SEARCH - SCOPE AND METHODOLOGY

The subject matter covered by this search was defined as "Liquid phase mixing in three phase fluidized beds." The search was prepared to provide background in experimental techniques and data analysis for the liquid phase mixing experiments on the H-Coal Cold Flow Unit.

A computer search was conducted off the API and SDC International indices on key words such as axial dispersion, liquid mixing, three phase fluidization, radioactive tracers, residence time distributions, etc. Many citations were produced, with only a very limited number bearing directly on the proposed mixing experiments. Previous sources were then consulted, including the previous H-Coal literature search on the hydrodynamics of fluidized beds (1), and the chemical literature on residence time distributions in reactors.
(1) Vasalos, I. A.; Bild, E. M.; Tatterson, D. F.; Wallin, C. C. H-Coal Fluid Dynamics Topical Report Part1: Literature Search.

APPENDIX D

PDU LIQUID SLURRY DENSITY VS TEMPERATURE

Figure D-1

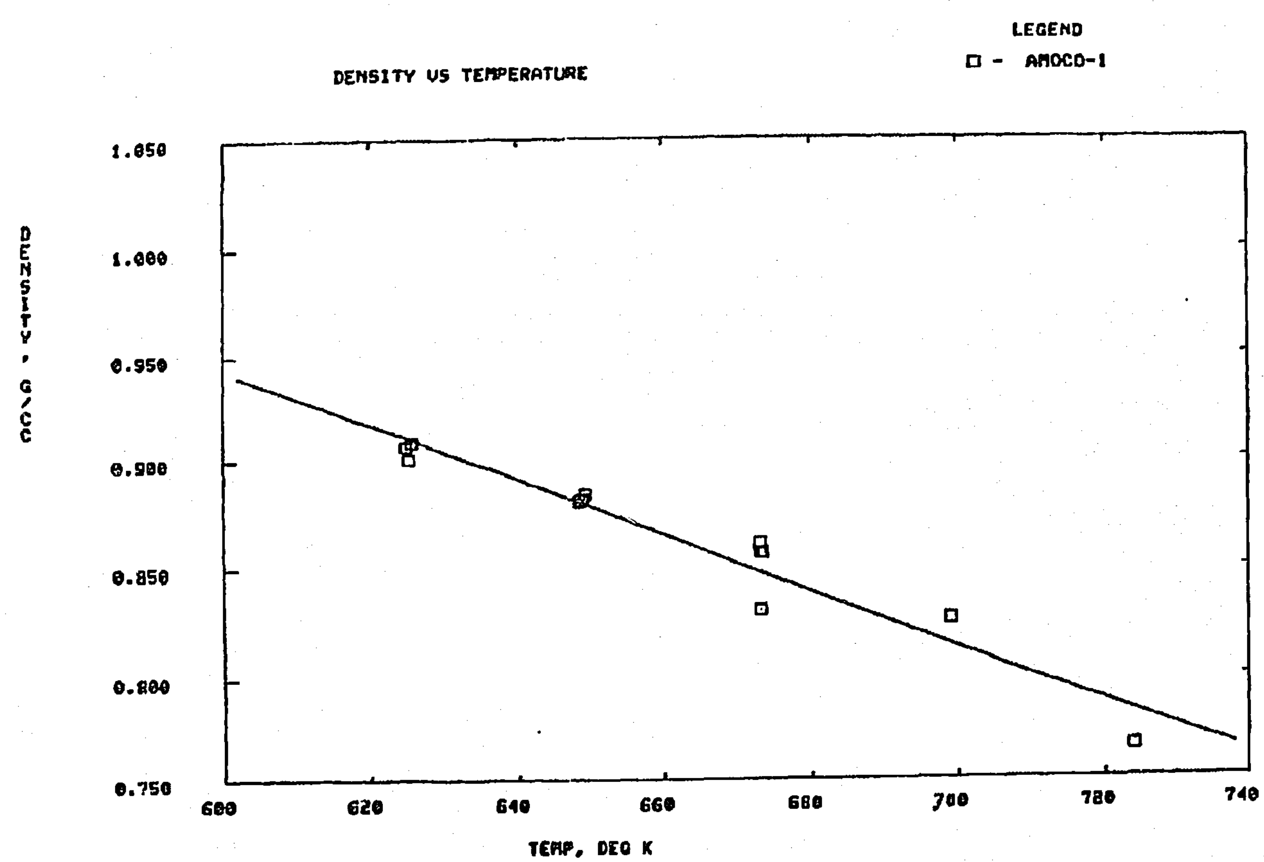

DENSITY VS TEMPERATURE
LEGEND
□ - AMOCO-1
DENSITY, G/CC
1.050
1.000
0.950
0.900
0.850
0.800
0.750
600
620
640
660
680
700
720
740
TEMP, DEG K

Figure D-2

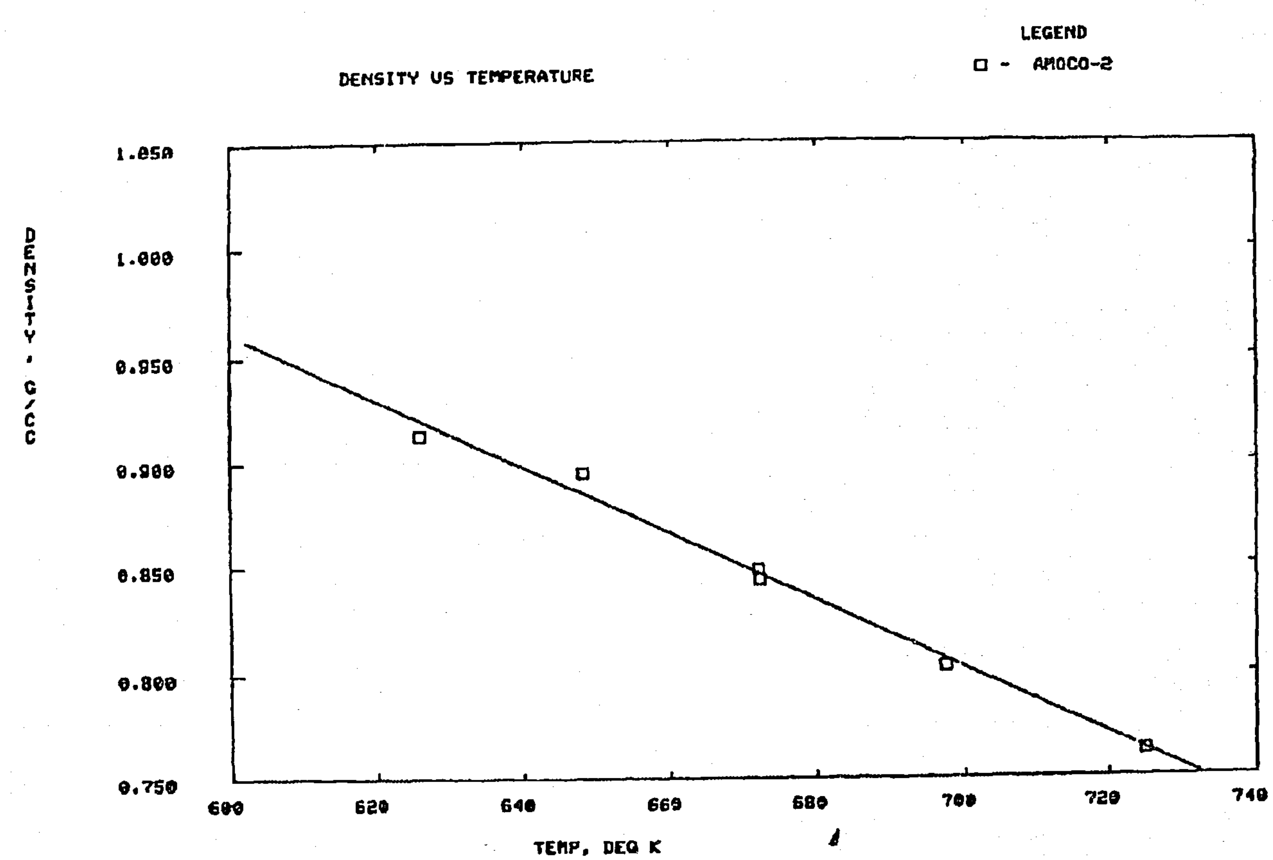
DENSITY VS TEMPERATURE
LEGEND
□ - AMOCO-2
DENSITY, G/CC
1.050
1.000
0.950
0.900
0.850
0.800
0.750
600
620
640
660
680
700
720
740
TEMP, DEG K

Figure D-3

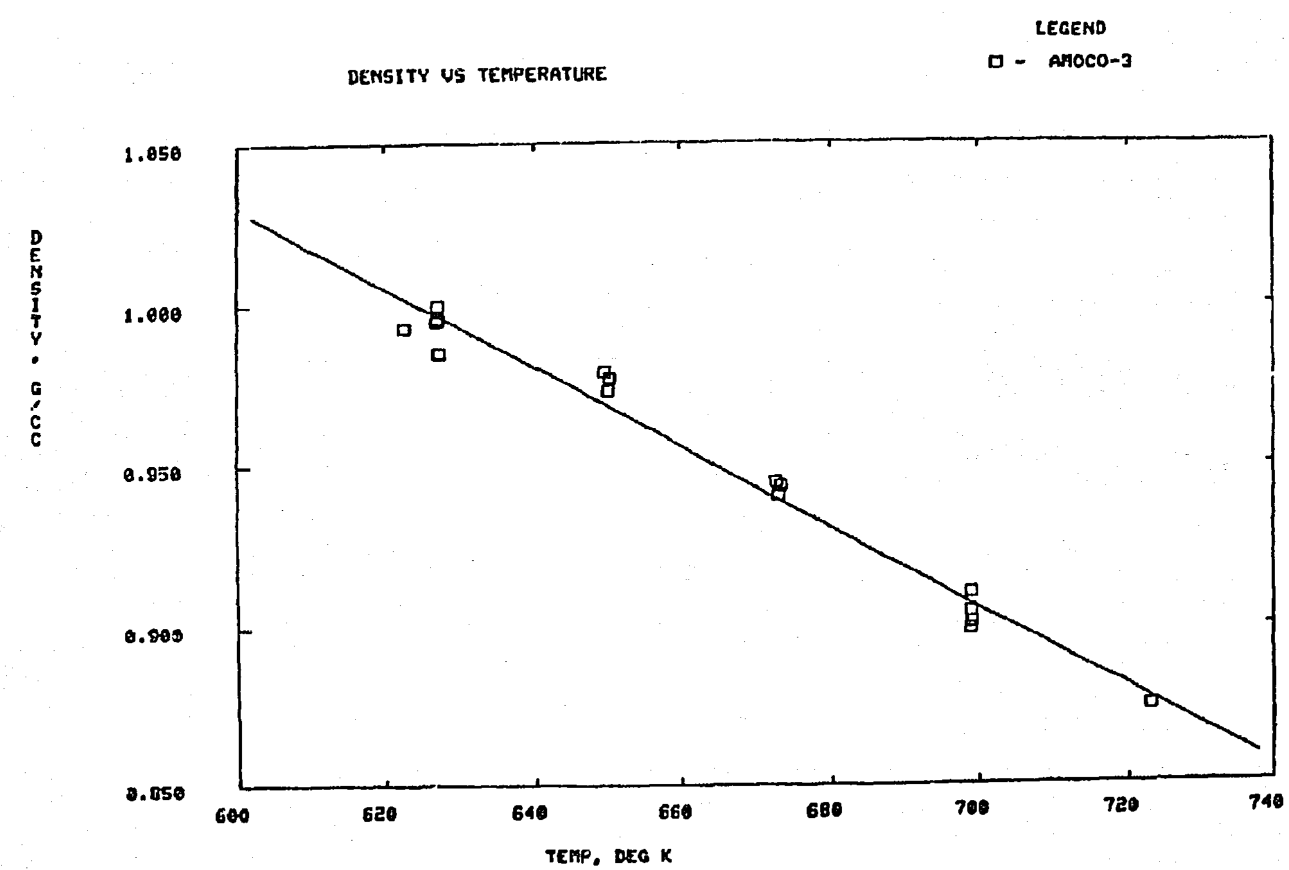

DENSITY VS TEMPERATURE
LEGEND
□ - AMOCO-3
DENSITY, G/CC
1.050
1.000
0.950
0.900
0.850
600
620
640
660
680
700
720
740
TEMP, DEG K

Figure D-4

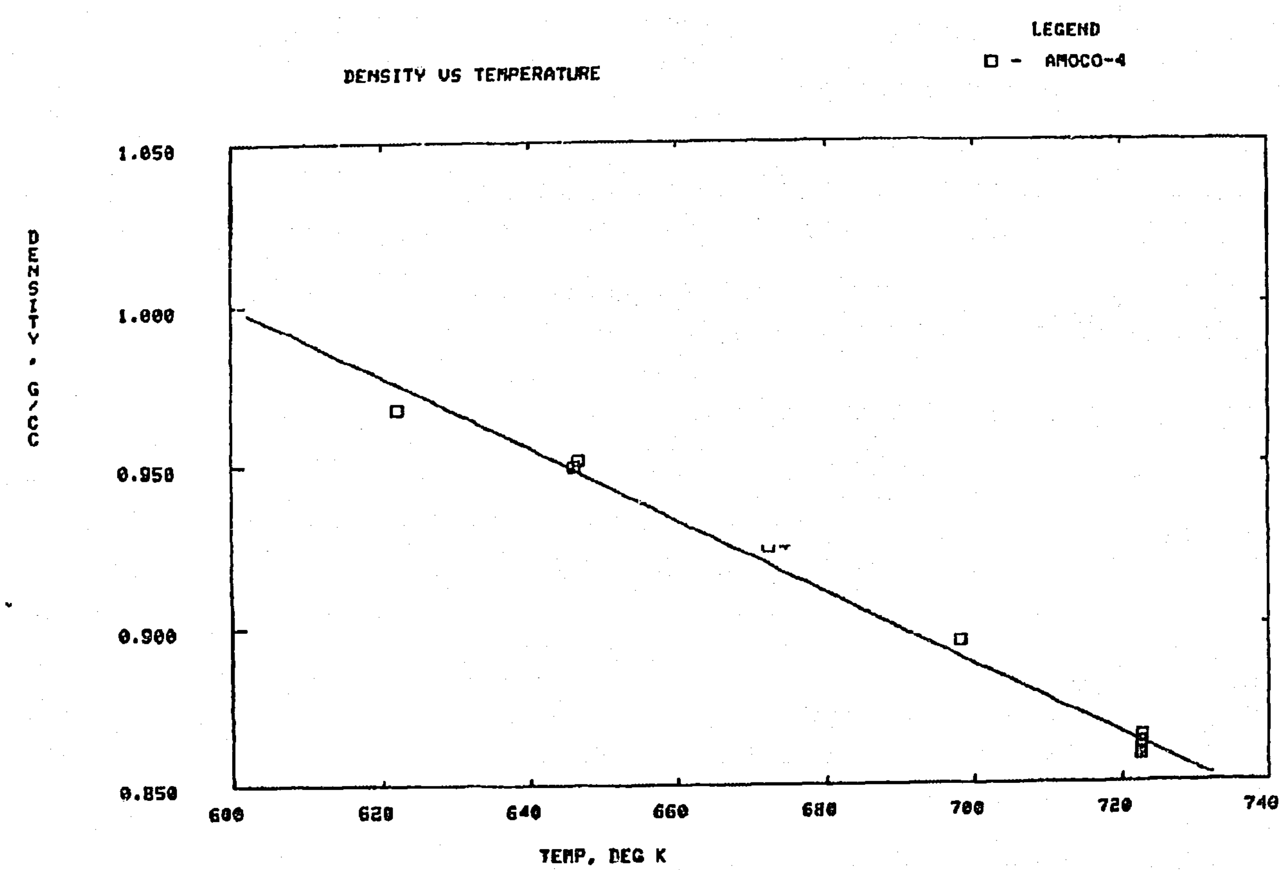
DENSITY VS TEMPERATURE
LEGEND
□ - AMOCO-4
DENSITY, G/CC
1.050
1.000
0.950
0.900
0.850
600
620
640
660
680
700
720
740
TEMP, DEG K

Figure D-5

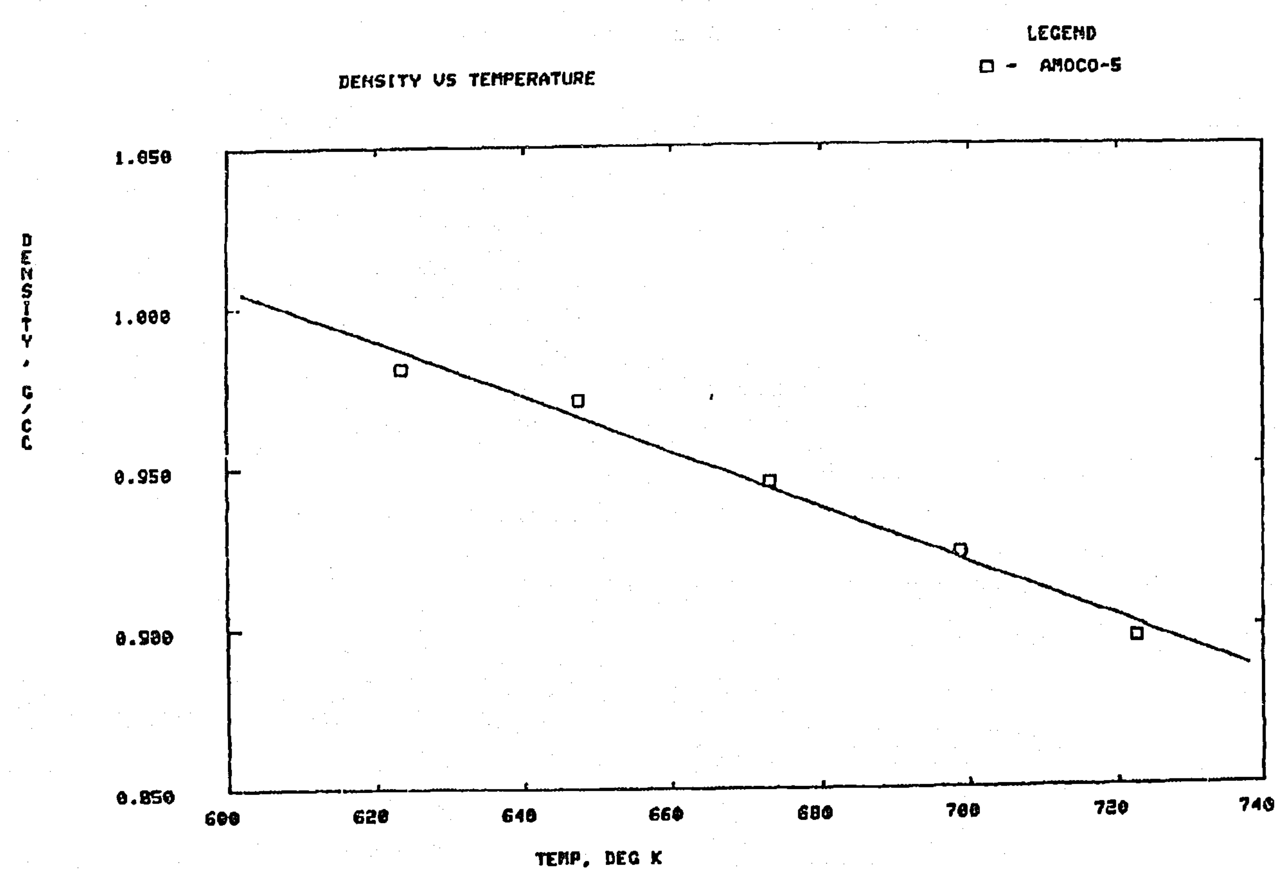

DENSITY VS TEMPERATURE
LEGEND
□ - AMOCO-5
DENSITY, G/CC
1.050
1.000
0.950
0.900
0.850
600
620
640
660
680
700
720
740
TEMP, DEG K

Figure D-6

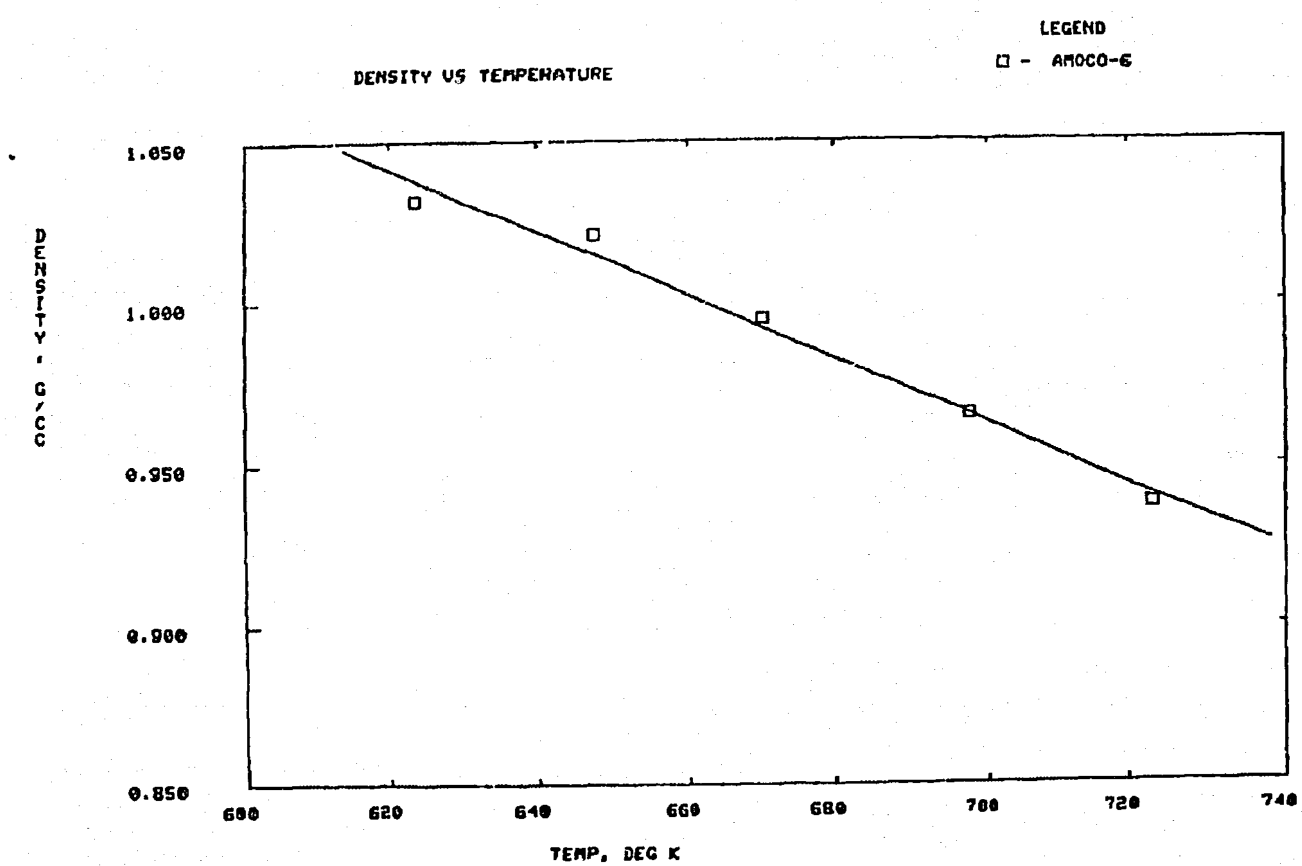
DENSITY VS TEMPERATURE
LEGEND
□ - AMOCO-6
DENSITY, G/CC
1.050
1.000
0.950
0.900
0.850
600
620
640
660
680
700
720
740
TEMP, DEG K

Figure D-7

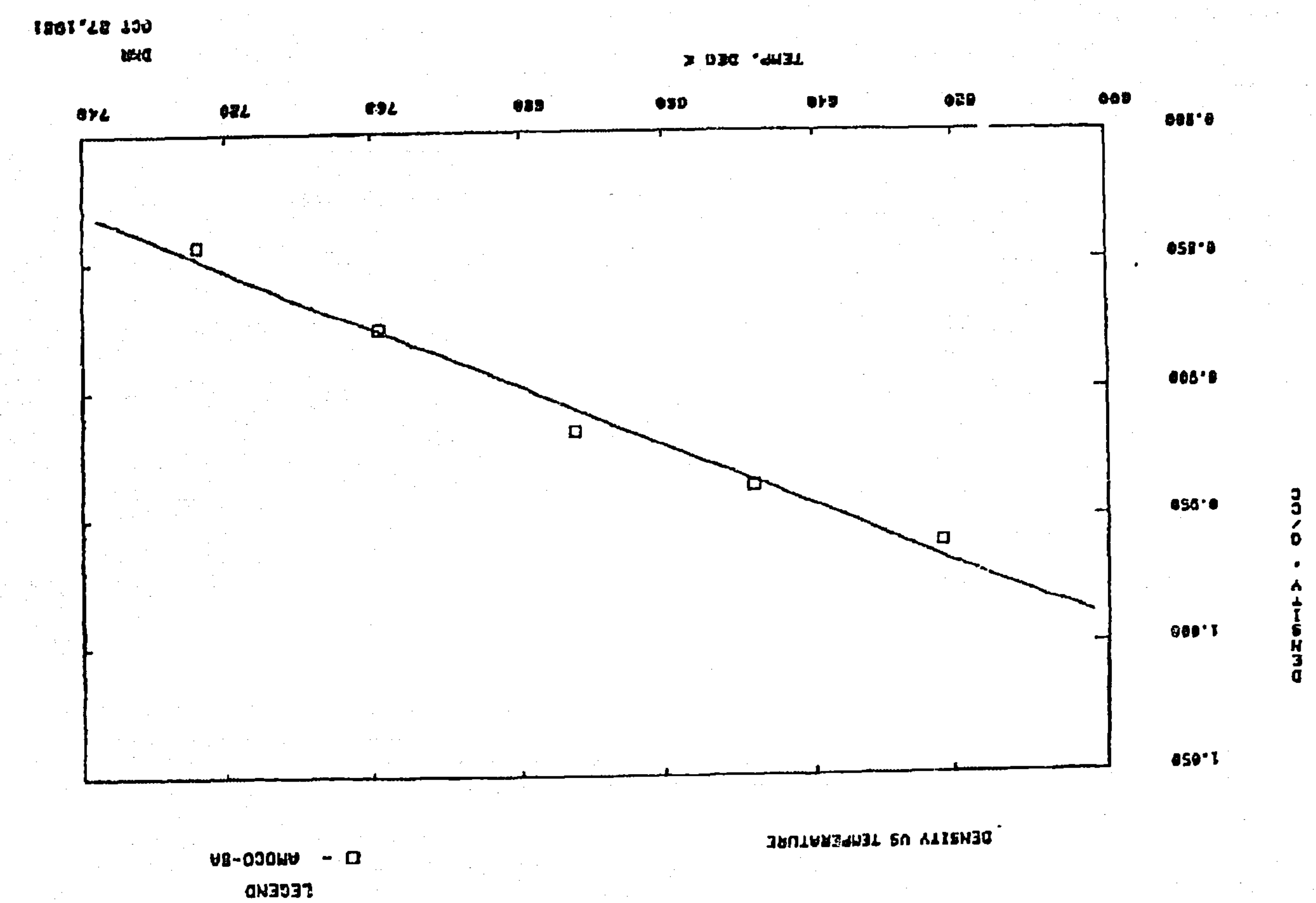

DENSITY VS TEMPERATURE
TEMP, DEG K
DENSITY, G/CC
0.800
0.850
0.900
0.950
1.000
1.050
LEGEND
□ - AMOCO-8A

Figure D-8

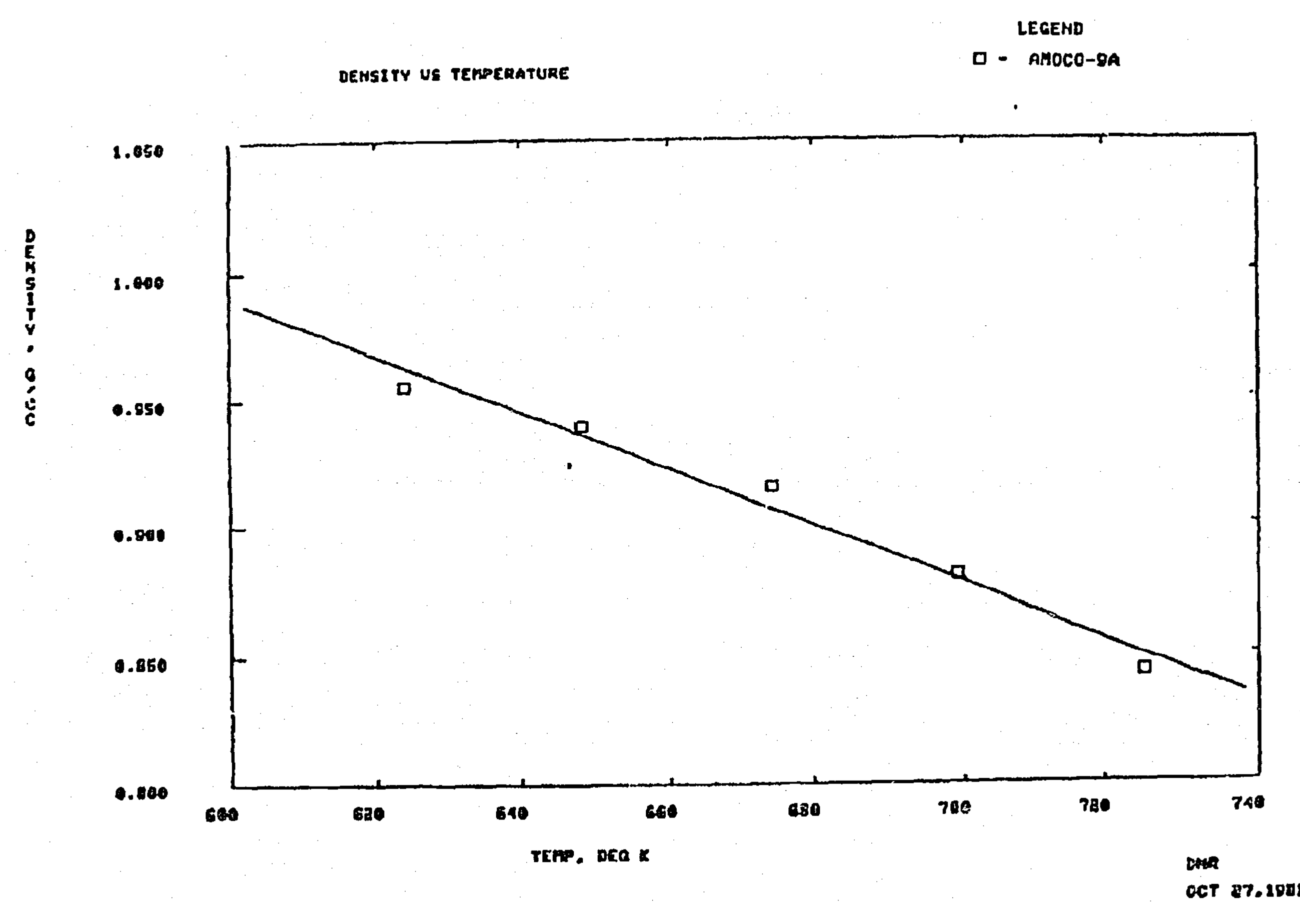

DENSITY VS TEMPERATURE
LEGEND
□ - AMOCO-9A
DENSITY, G/CC
1.050
1.000
0.950
0.900
0.850
0.800
600
620
640
660
680
700
720
740
TEMP, DEG K
DHR
OCT 27,1981

Figure D-9

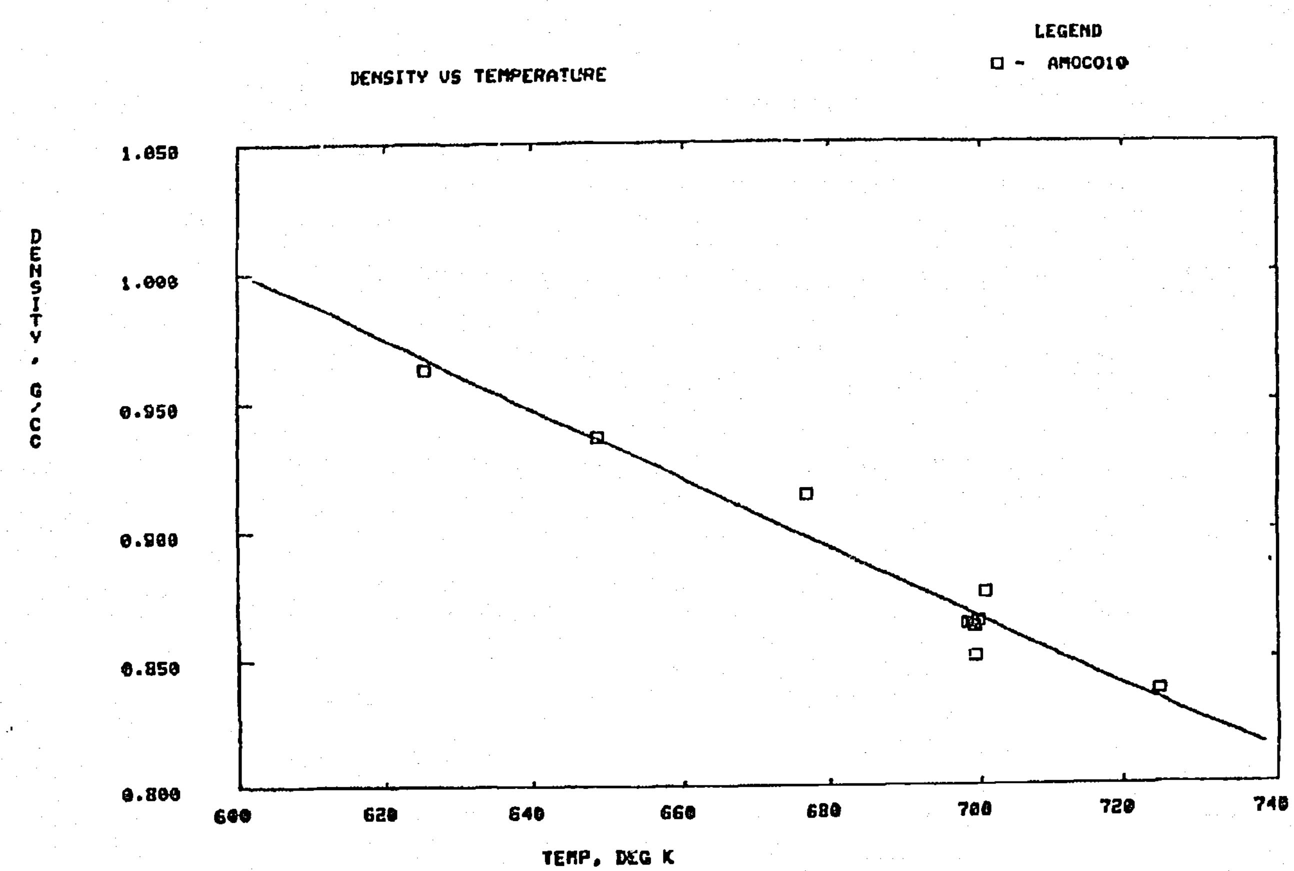
DENSITY VS TEMPERATURE
LEGEND
□ - AMOCO10
DENSITY, G/CC
1.050
1.000
0.950
0.900
0.850
0.800
600
620
640
660
680
700
720
740
TEMP, DEG K

Figure D-10

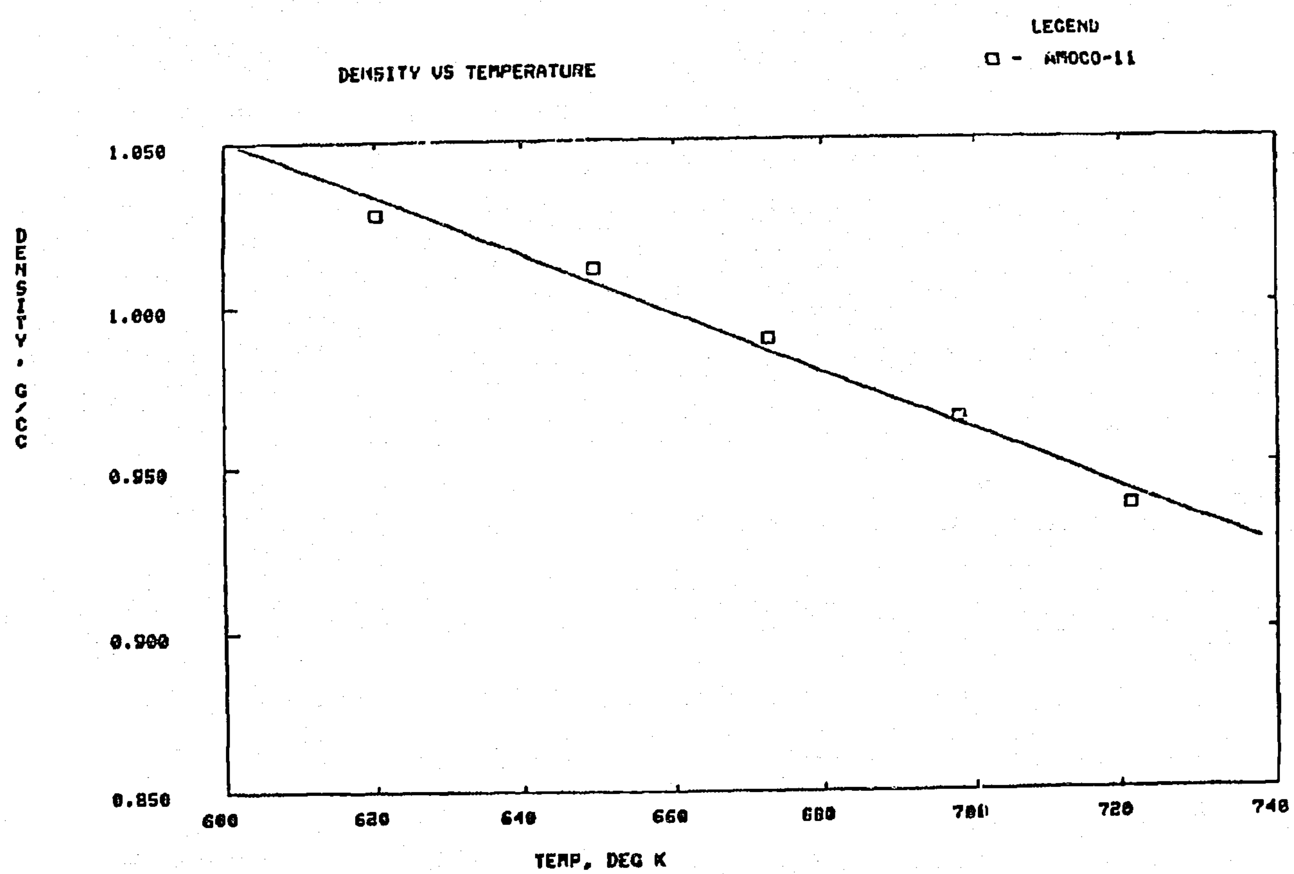
DENSITY VS TEMPERATURE
LEGEND
□ - AMOCO-11
1.050
1.000
0.950
0.900
0.850
DENSITY, G/CC
600
620
640
660
680
700
720
740
TEMP, DEG K

Figure D-11

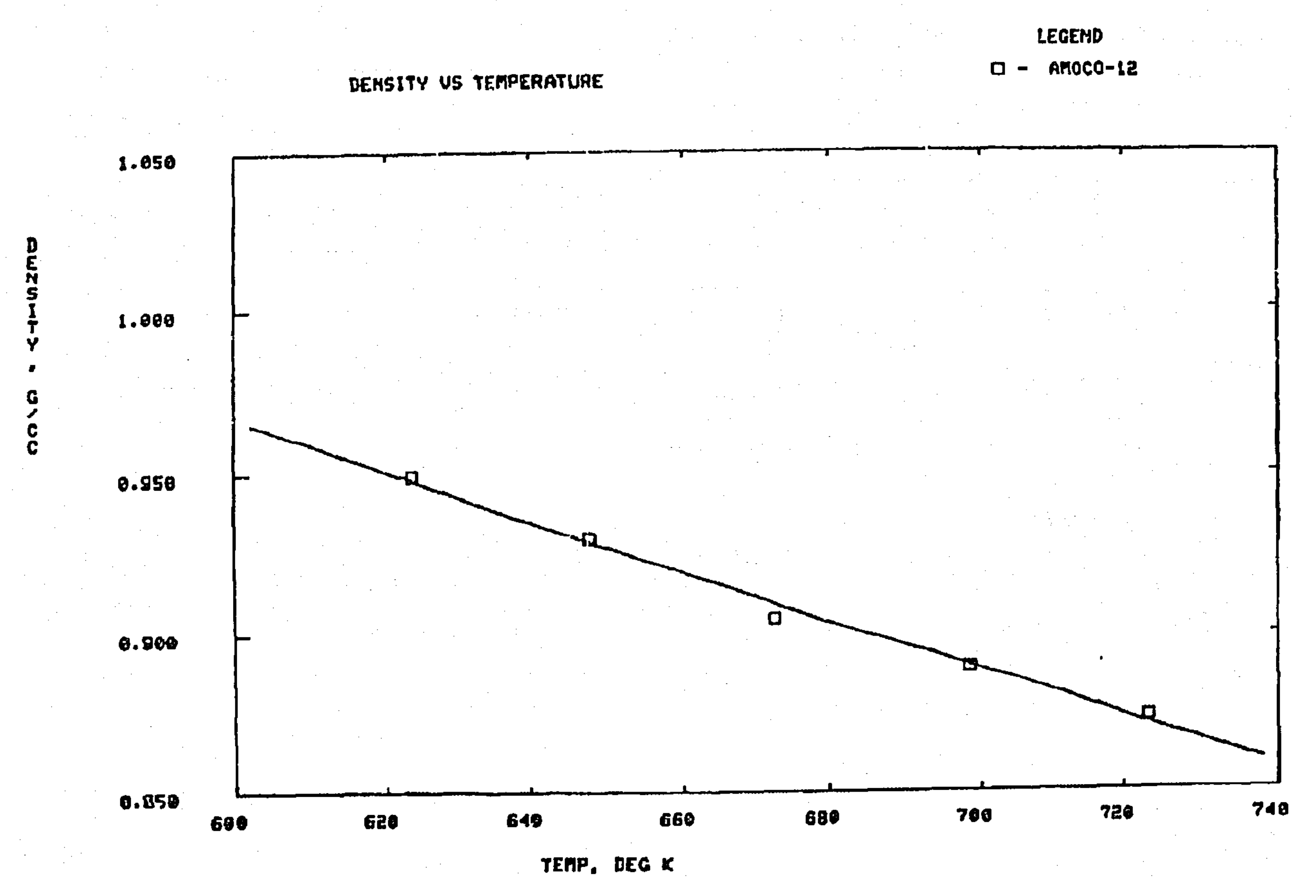
DENSITY VS TEMPERATURE
LEGEND
□ - AMOCO-12
DENSITY, G/CC
1.050
1.000
0.950
0.900
0.850
600
620
640
660
680
700
720
740
TEMP, DEG K

Figure D-12

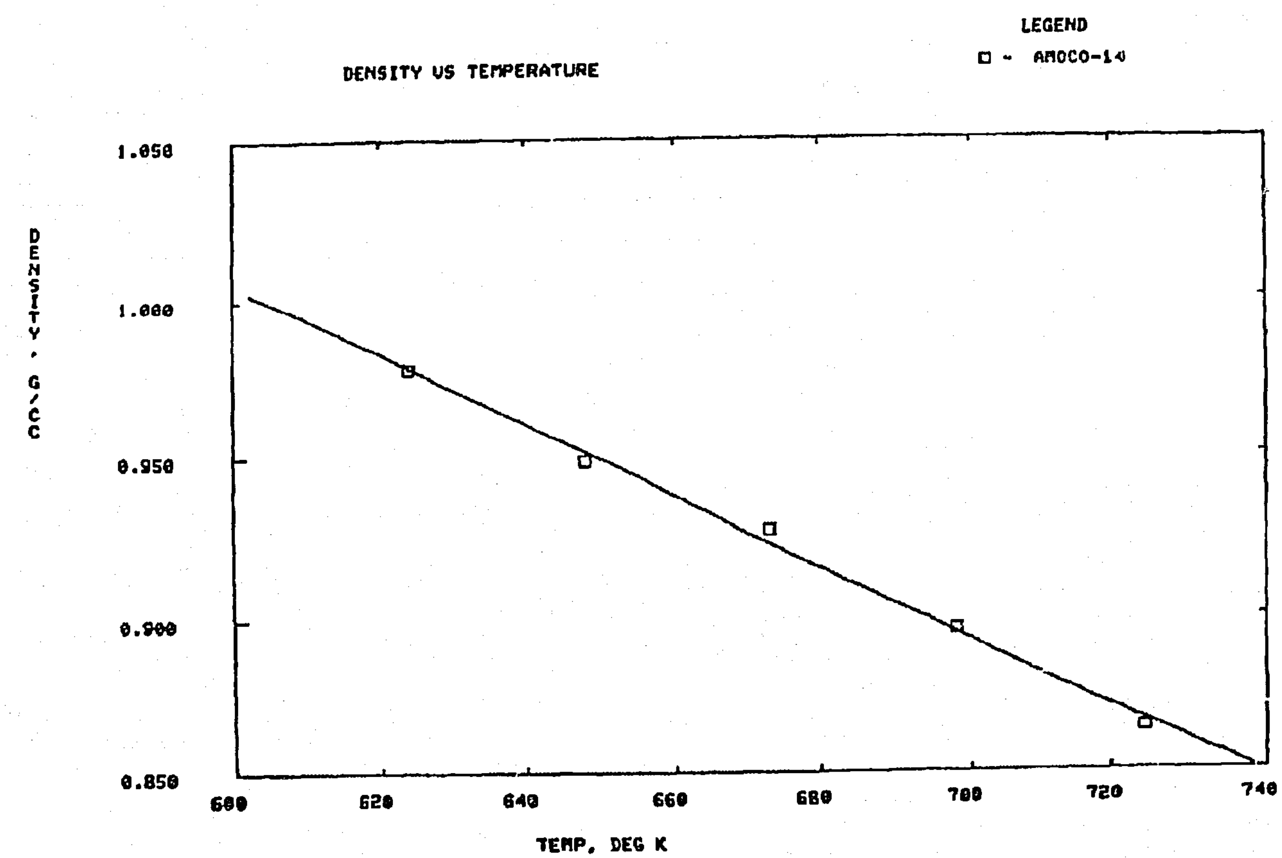
DENSITY VS TEMPERATURE
LEGEND
□ - AMOCO-14
DENSITY, G/CC
1.050
1.000
0.950
0.900
0.850
600
620
640
660
680
700
720
740
TEMP, DEG K

Figure D-13

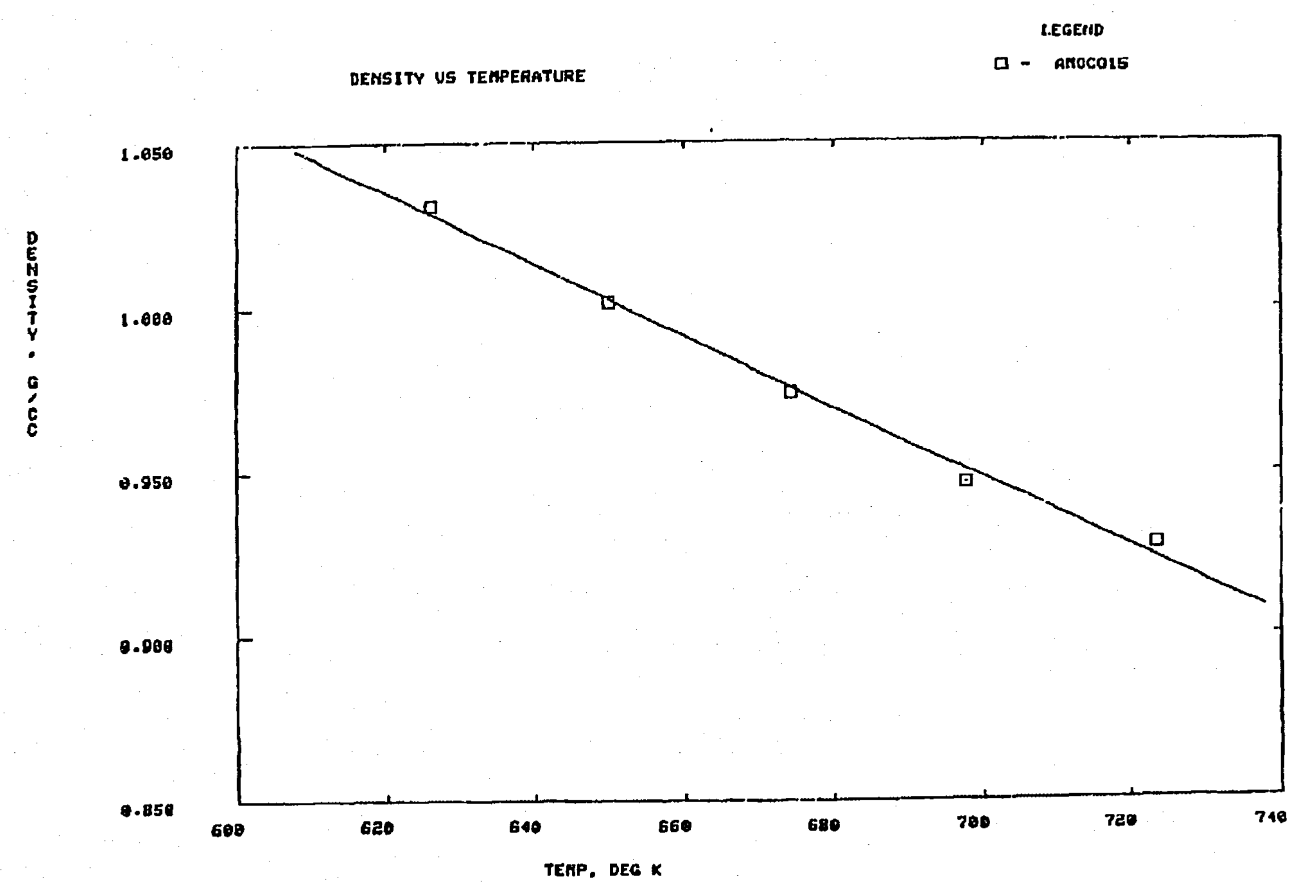
DENSITY VS TEMPERATURE
LEGEND
□ - AMOCO15
DENSITY, G/CC
1.050
1.000
0.950
0.900
0.850
600
620
640
660
680
700
720
740
TEMP, DEG K

Figure D-14

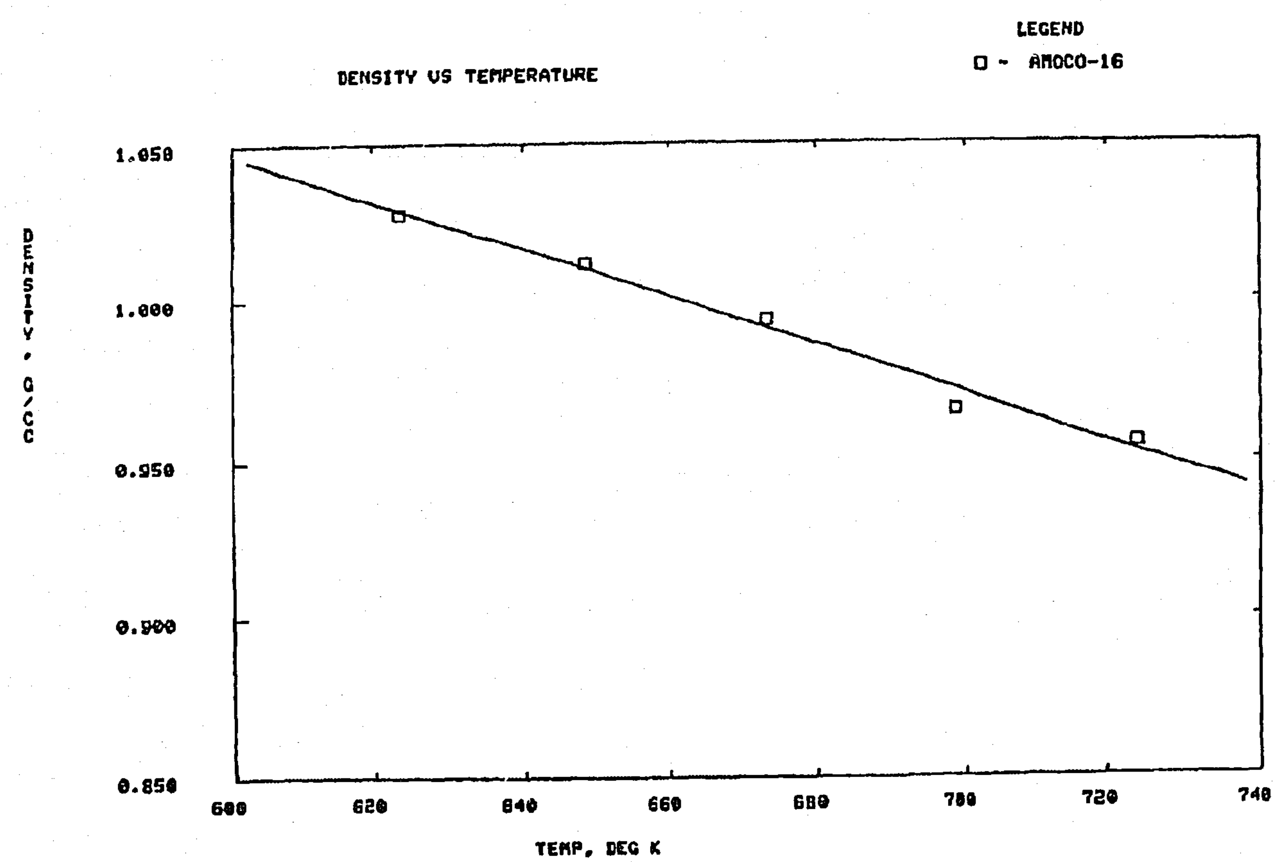
DENSITY VS TEMPERATURE
LEGEND
□ - AMOCO-16
DENSITY, G/CC
1.050
1.000
0.950
0.900
0.850
600
620
640
660
680
700
720
740
TEMP, DEG K

Figure E-1

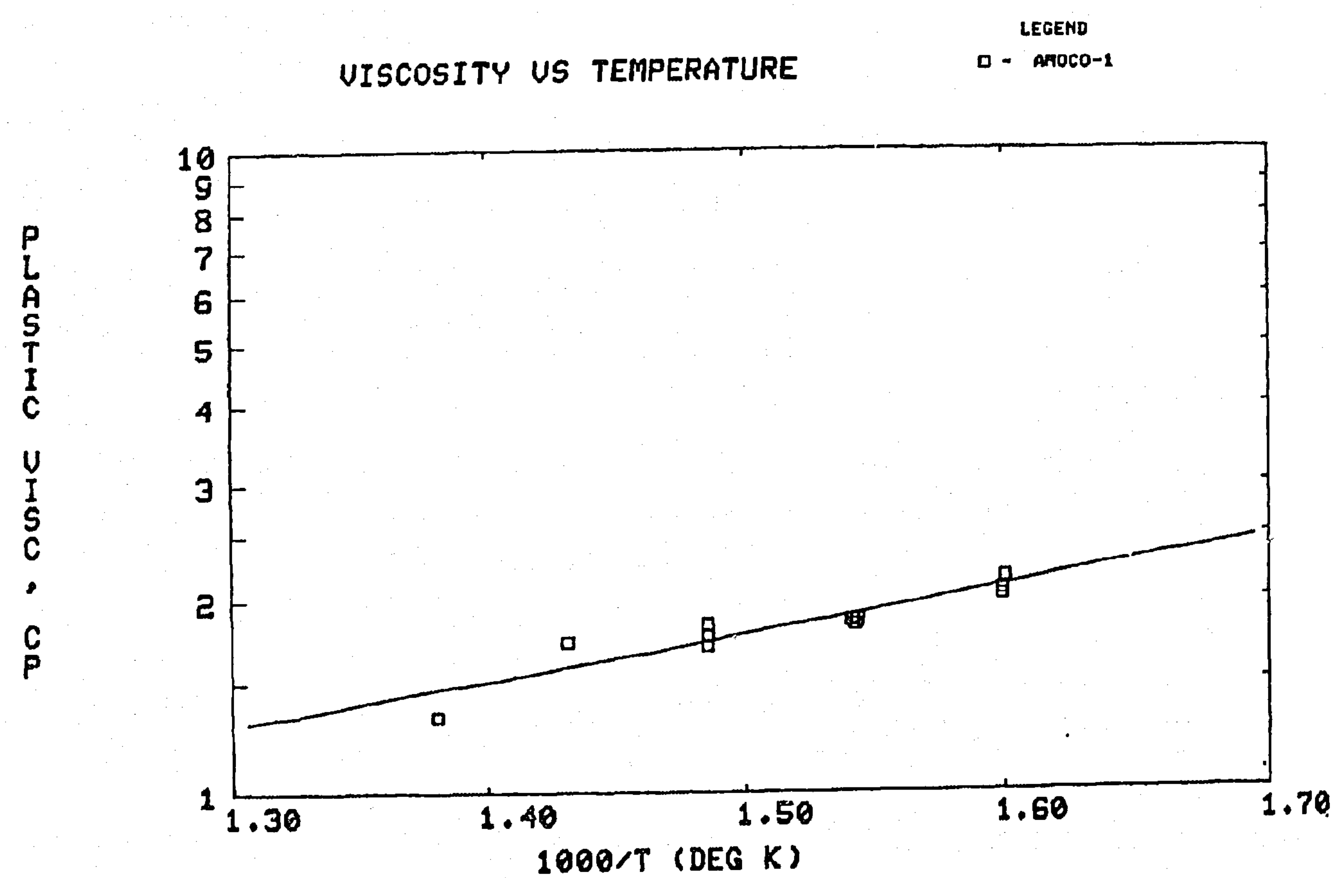
LEGEND
□ - AMOCO-1
VISCOSITY VS TEMPERATURE
PLASTIC VISC, CP
10
9
8
7
6
5
4
3
2
1
1.30
1.40
1.50
1.60
1.70
1000/T (DEG K)

Figure E-2

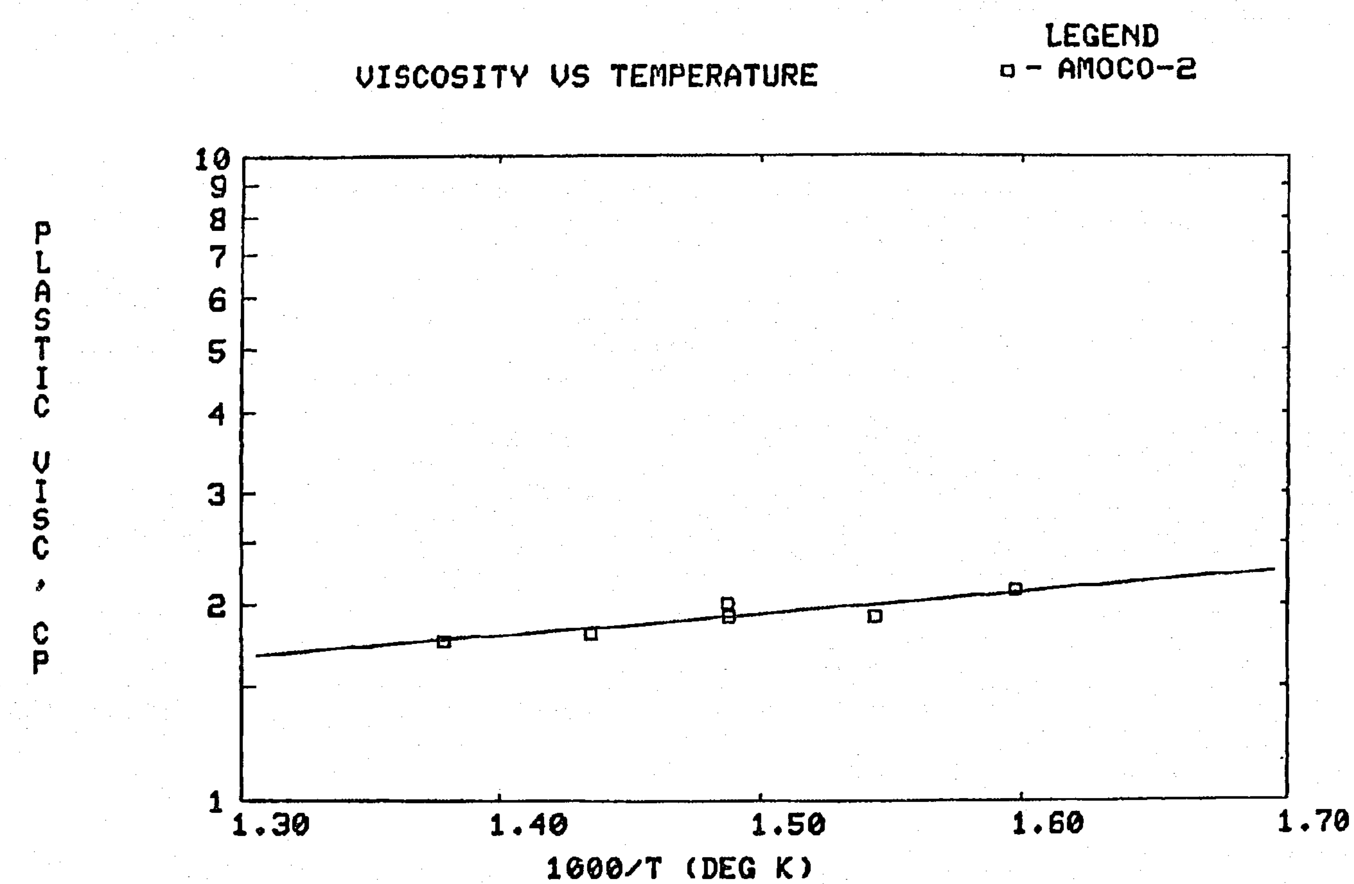
VISCOSITY VS TEMPERATURE
LEGEND
- AMOCO-2
PLASTIC VISC, CP
10
9
8
7
6
5
4
3
2
1
1.30
1.40
1.50
1.60
1.70
1000/T (DEG K)

Figure E-3

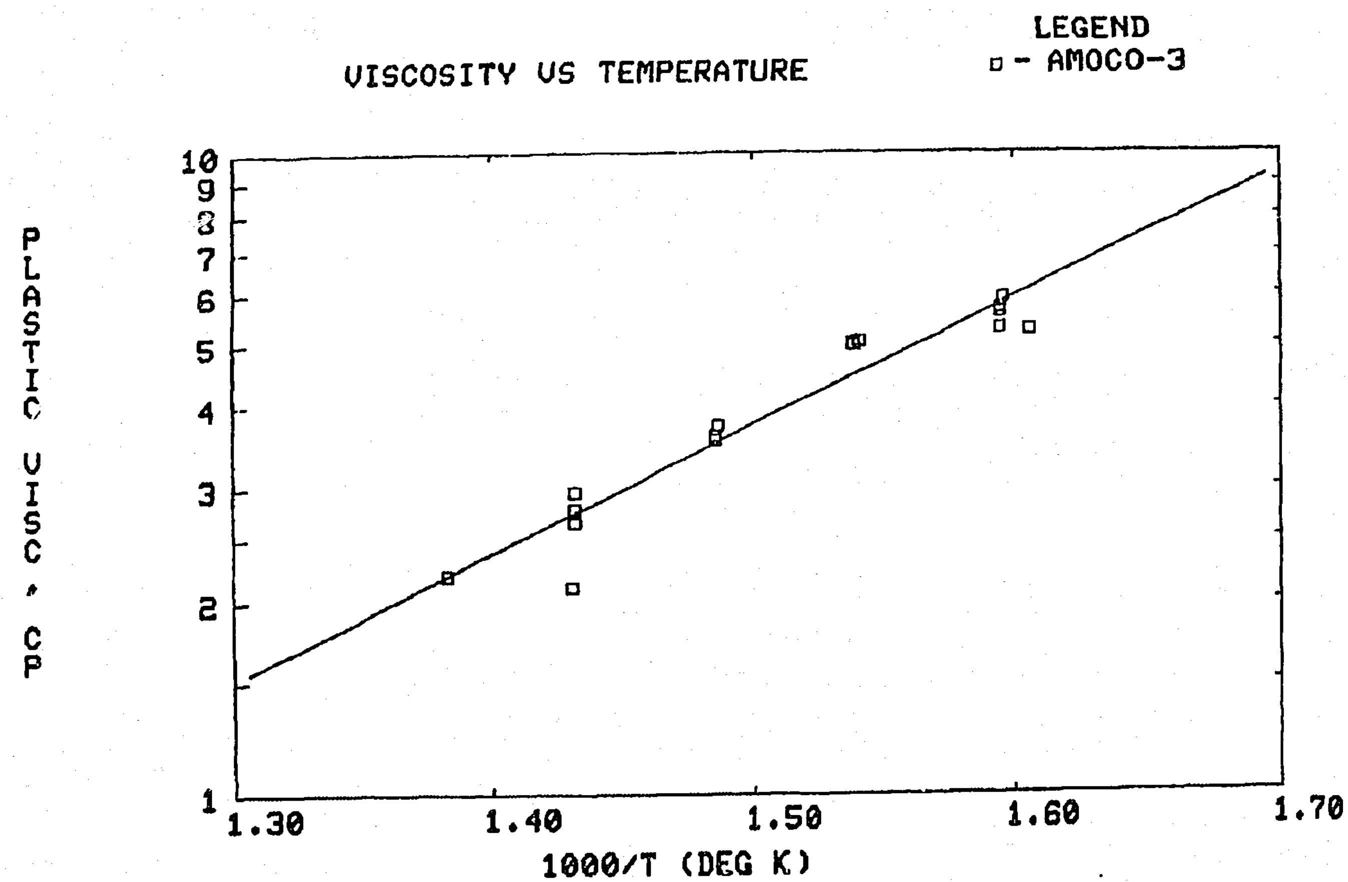
VISCOSITY VS TEMPERATURE
LEGEND
- AMOCO-3
PLASTIC VISC, CP
10
9
8
7
6
5
4
3
2
1
1.30
1.40
1.50
1.60
1.70
1000/T (DEG K)

Figure E-4

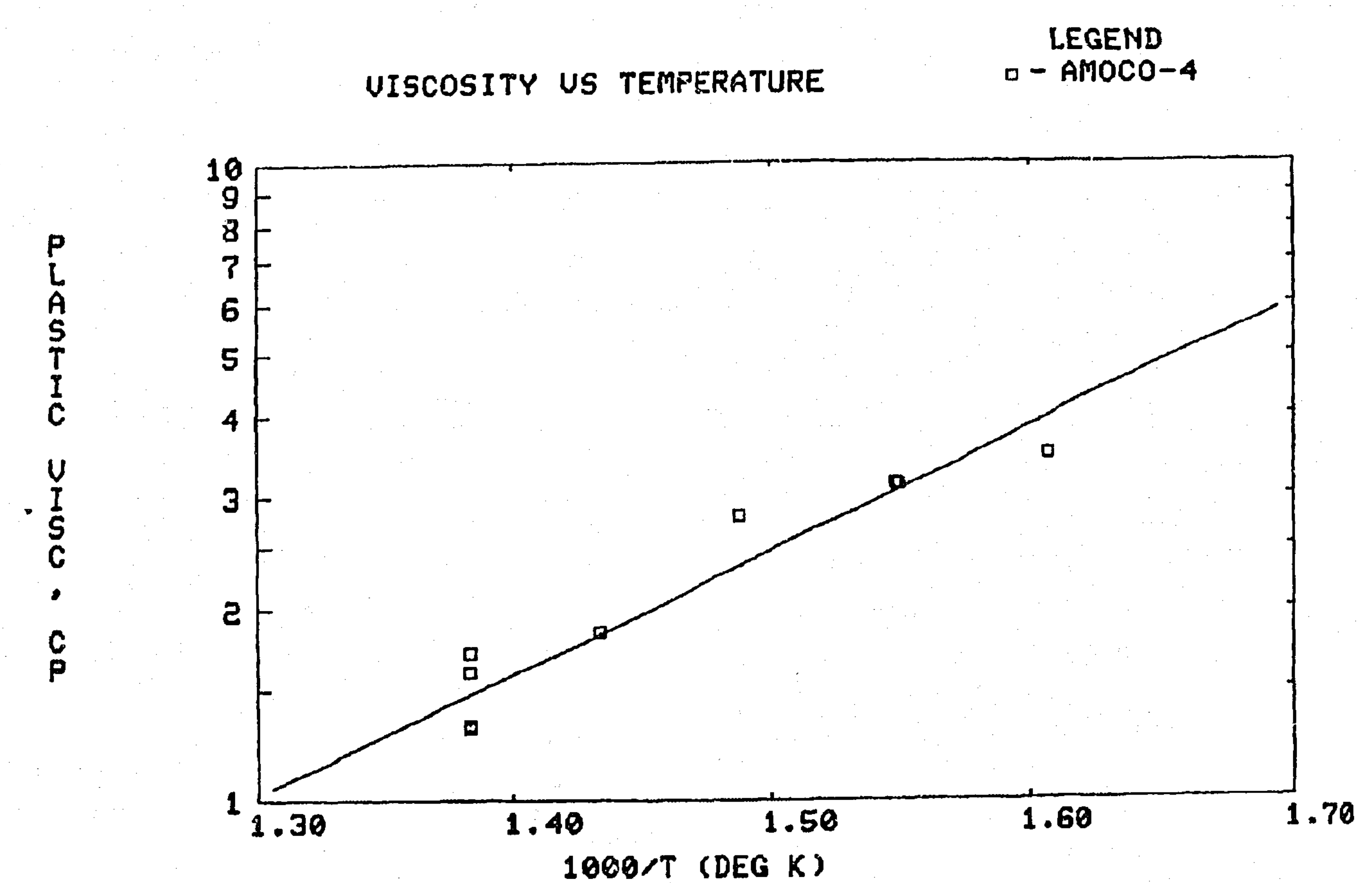
VISCOSITY VS TEMPERATURE
LEGEND
- AMOCO-4
PLASTIC VISC, CP
10
9
8
7
6
5
4
3
2
1
1.30
1.40
1.50
1.60
1.70
1000/T (DEG K)

Figure E-5

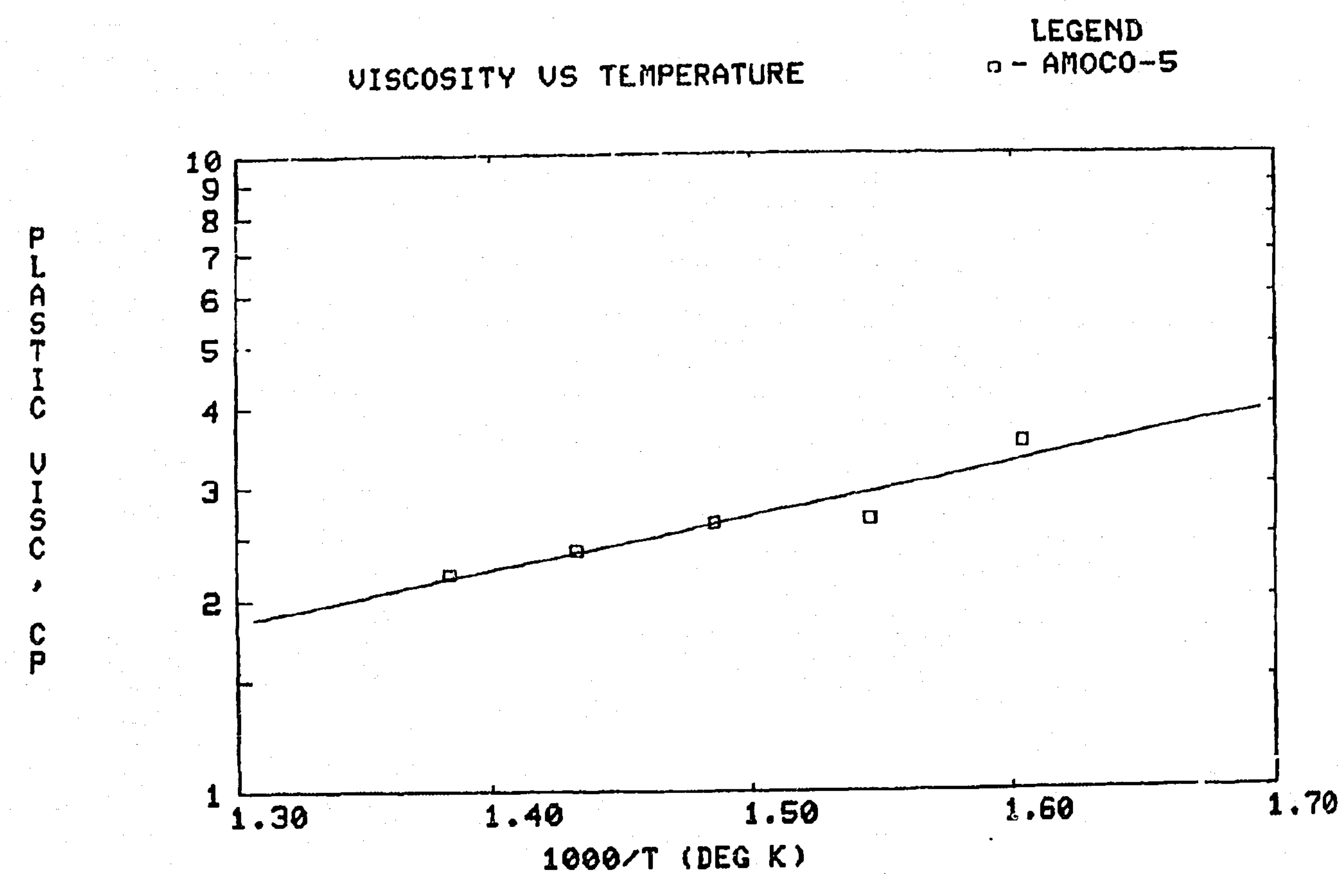
VISCOSITY VS TEMPERATURE
LEGEND
- AMOCO-5
PLASTIC VISC, CP
10
9
8
7
6
5
4
3
2
1
1.30
1.40
1.50
1.60
1.70
1000/T (DEG K)

Figure E-6

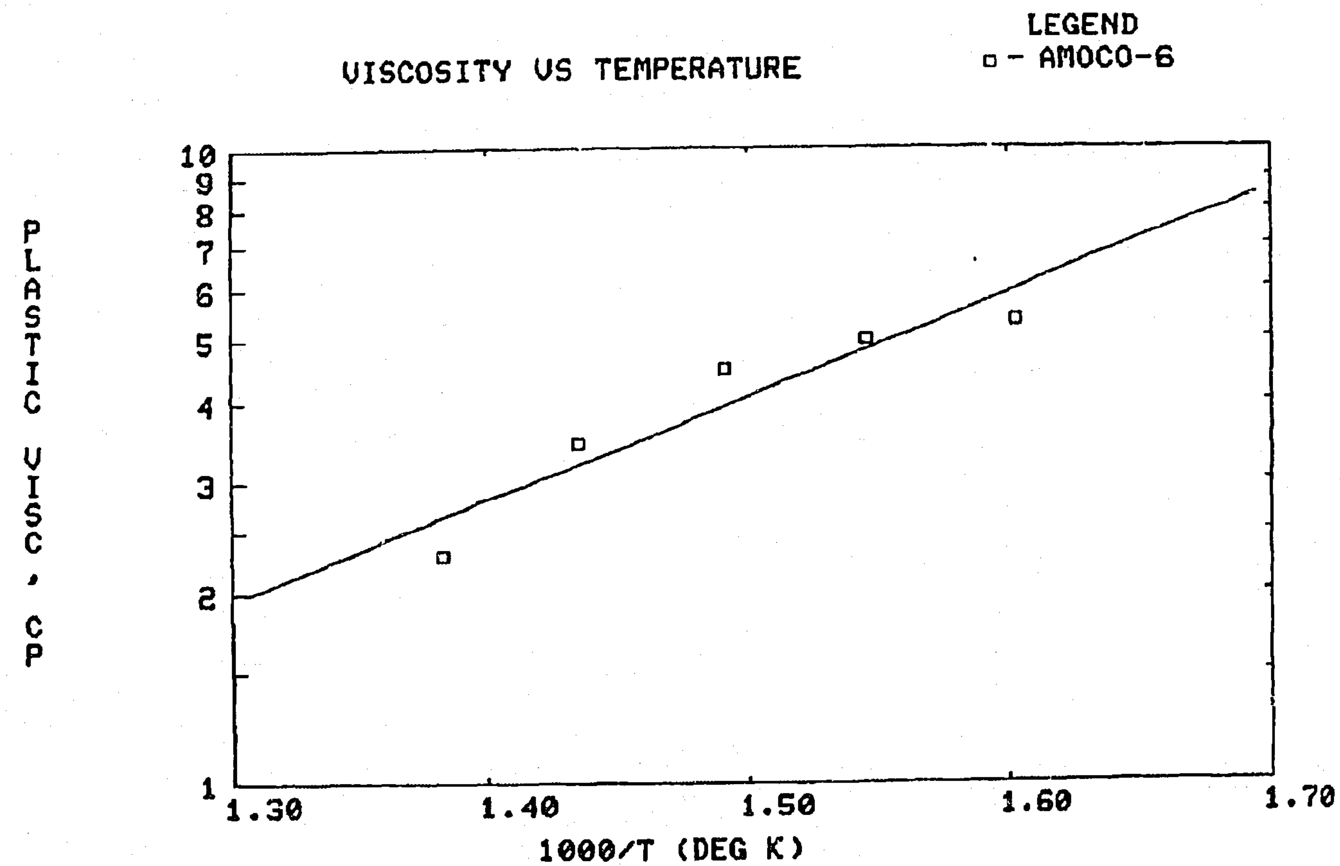
VISCOSITY VS TEMPERATURE
LEGEND
- AMOCO-6
PLASTIC VISC, CP
10
9
8
7
6
5
4
3
2
1
1.30
1.40
1.50
1.60
1.70
1000/T (DEG K)

Figure E-7

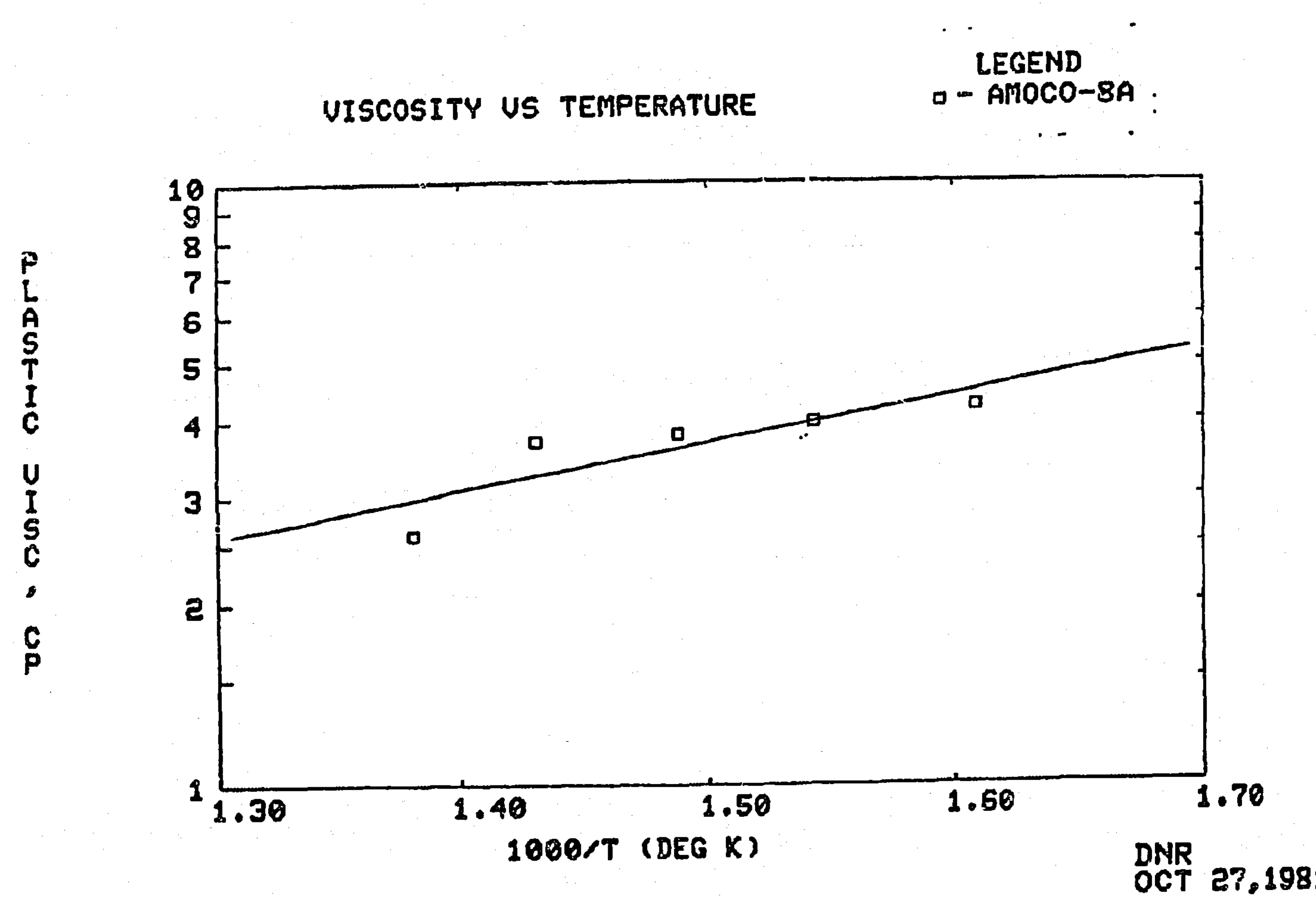
VISCOSITY VS TEMPERATURE
LEGEND
□ - AMOCO-8A
PLASTIC VISC, CP
10
9
8
7
6
5
4
3
2
1
1.30
1.40
1.50
1.60
1.70
1000/T (DEG K)
DNR
OCT 27,1981

Figure E-8

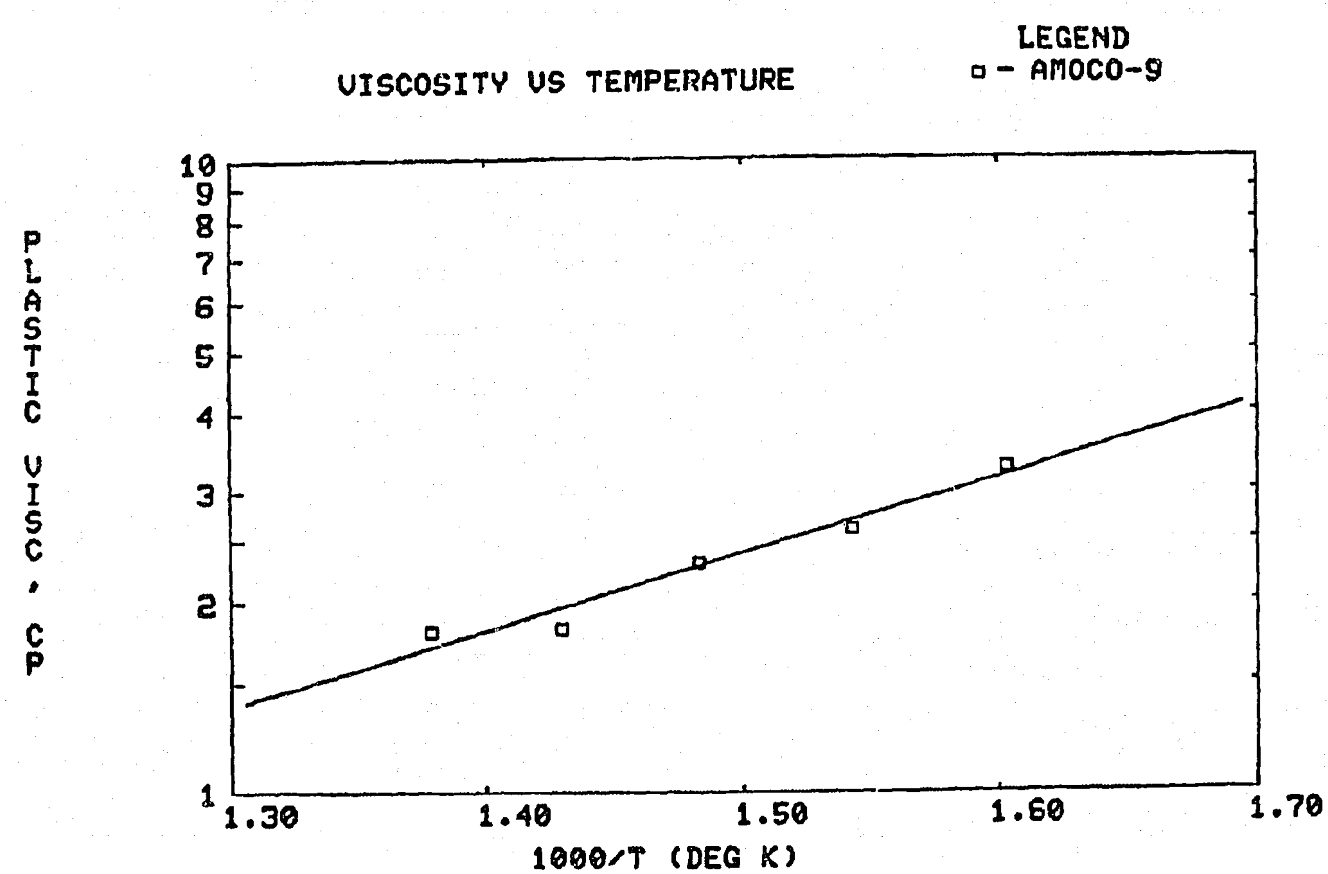
VISCOSITY VS TEMPERATURE
LEGEND
□ - AMOCO-9
PLASTIC VISC, CP
10
9
8
7
6
5
4
3
2
1
1.30
1.40
1.50
1.60
1.70
1000/T (DEG K)

Figure E-9

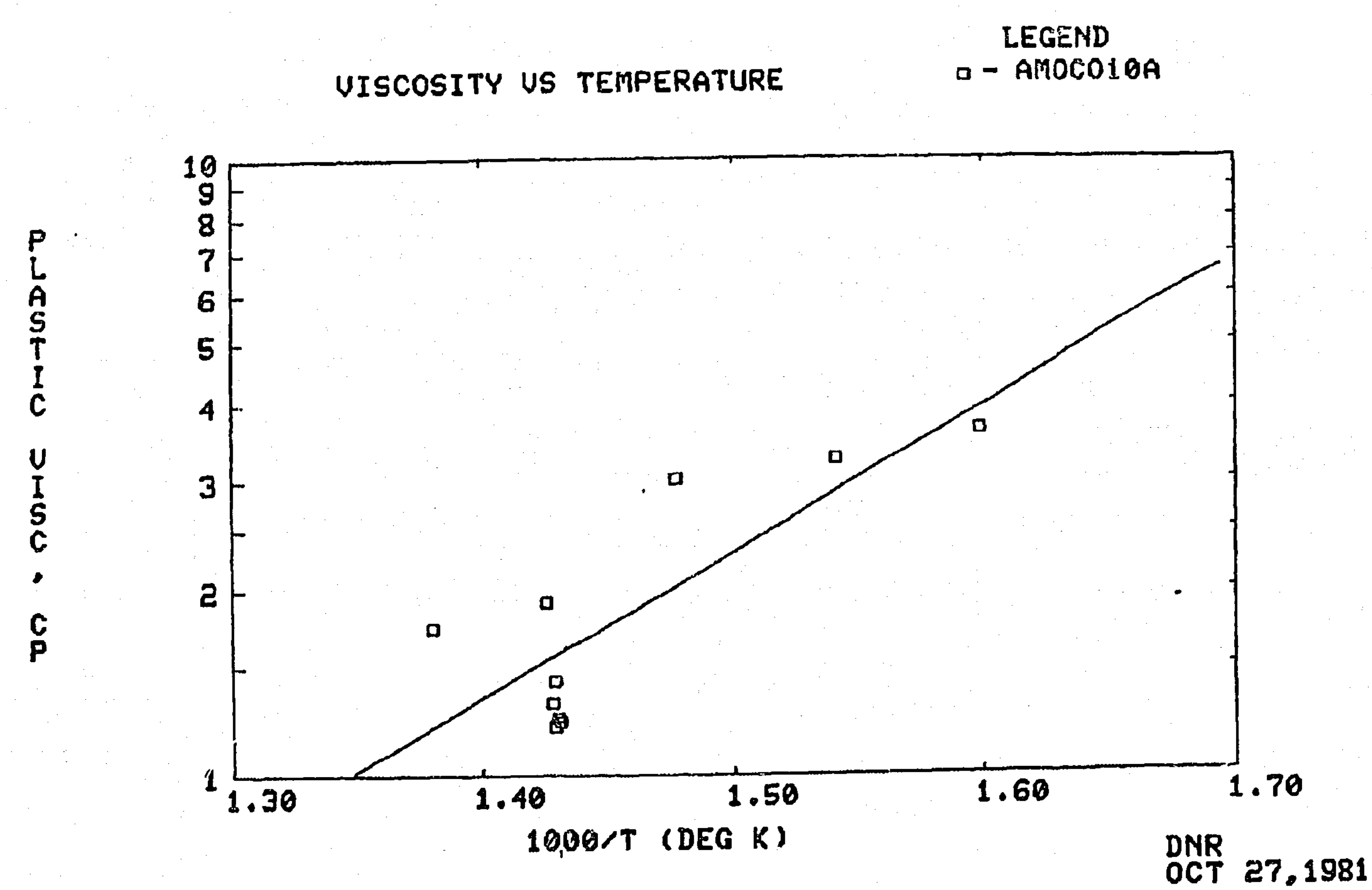

VISCOSITY VS TEMPERATURE
LEGEND
□ - AMOCO10A
PLASTIC VISC, CP
10
9
8
7
6
5
4
3
2
1
1.30
1.40
1.50
1.60
1.70
1000/T (DEG K)
DNR
OCT 27,1981

Figure E-10

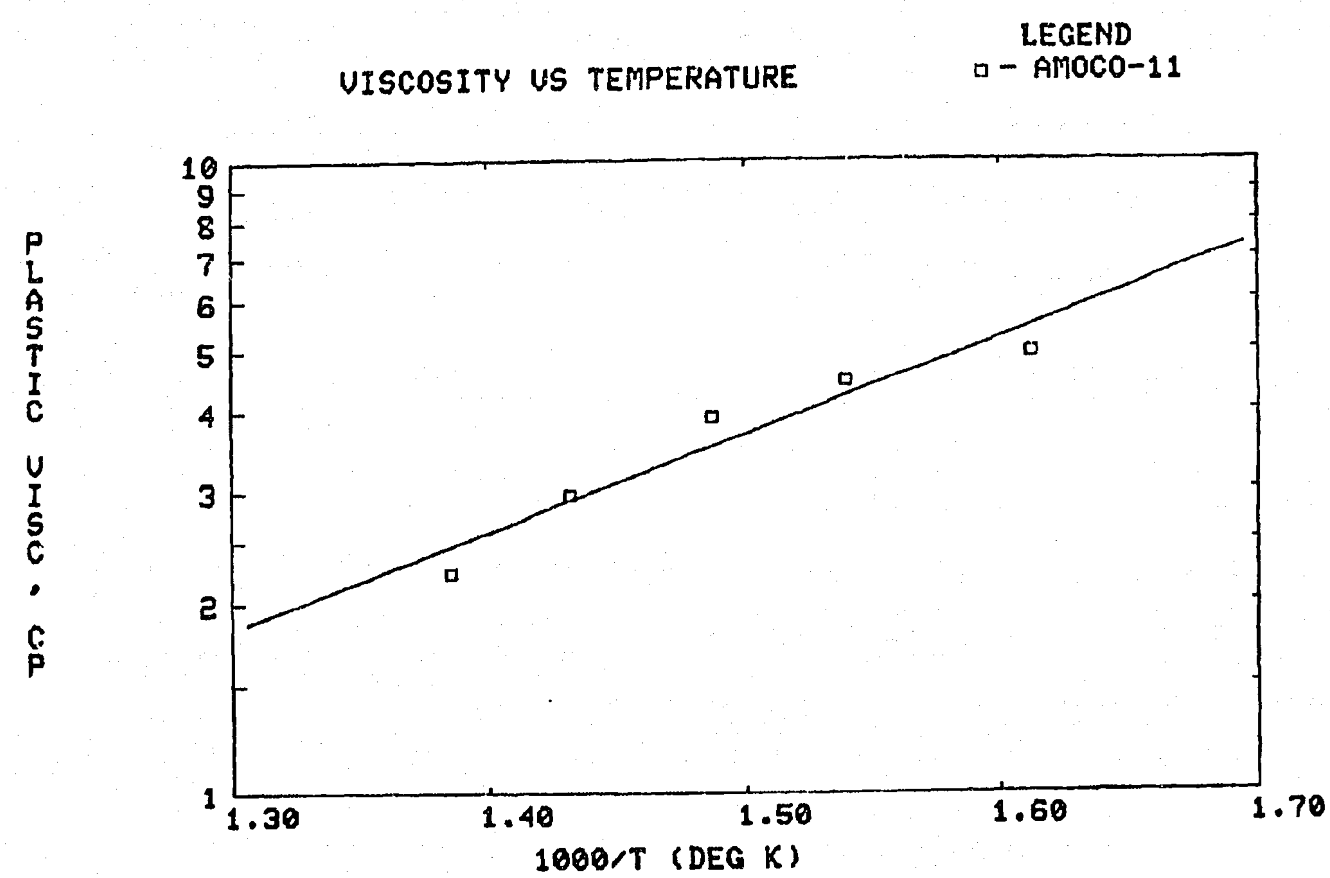
VISCOSITY VS TEMPERATURE
LEGEND
□ - AMOCO-11
PLASTIC VISC, CP
10
9
8
7
6
5
4
3
2
1
1.30
1.40
1.50
1.60
1.70
1000/T (DEG K)

Figure E-11

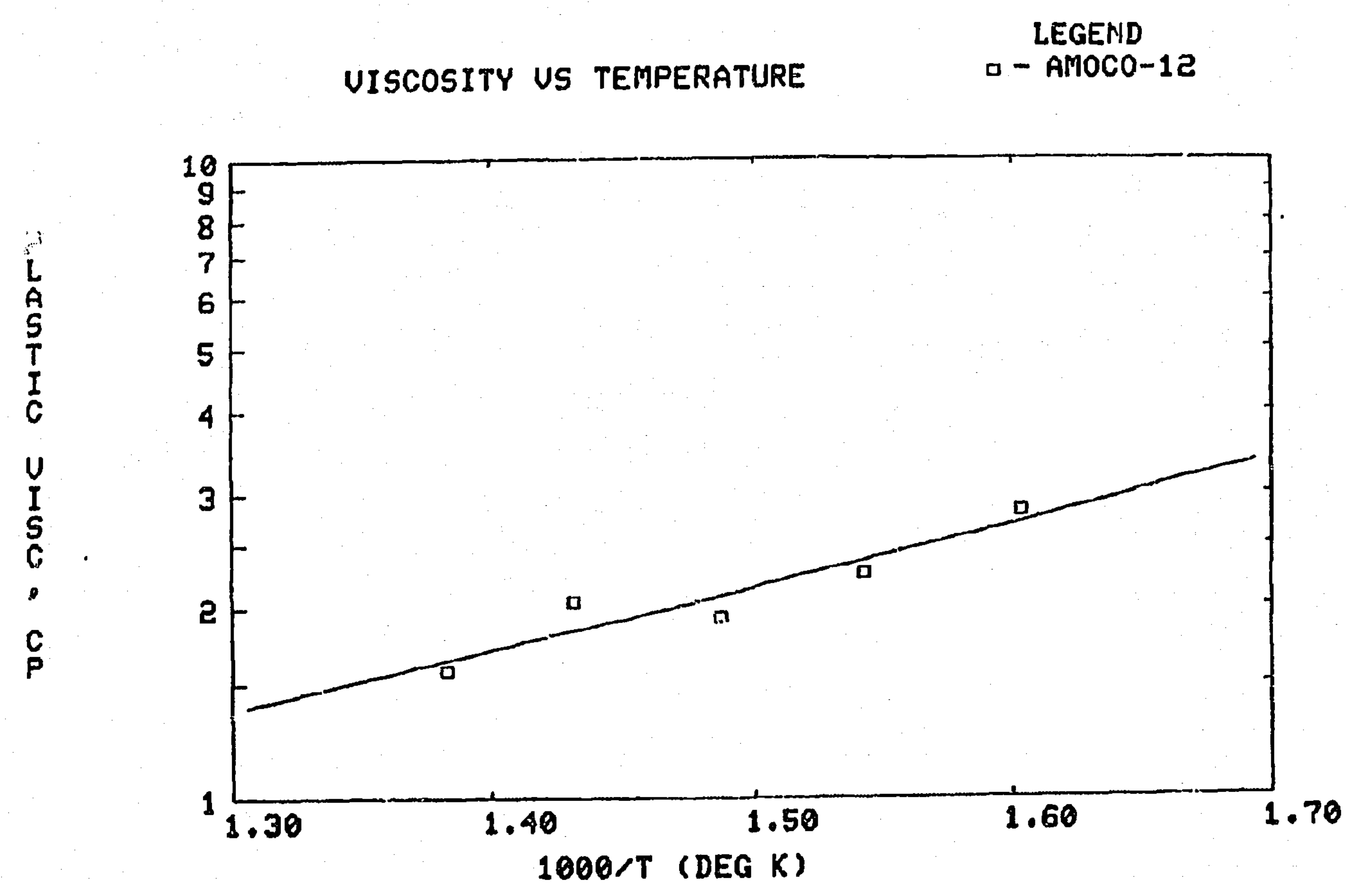
VISCOSITY VS TEMPERATURE
LEGEND
□ - AMOCO-12
PLASTIC VISC, CP
10
9
8
7
6
5
4
3
2
1
1.30
1.40
1.50
1.60
1.70
1000/T (DEG K)

Figure E12

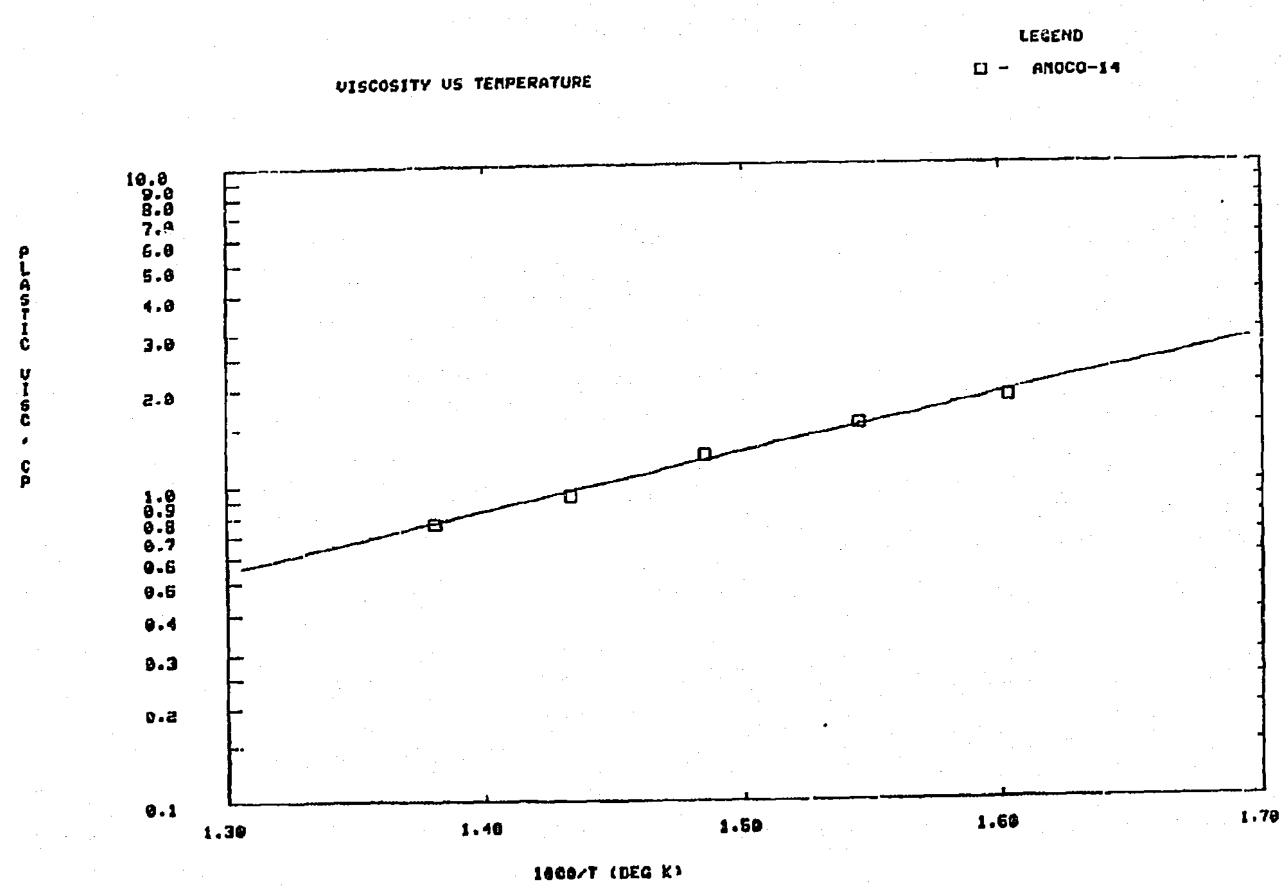
VISCOSITY VS TEMPERATURE
LEGEND
□ - AMOCO-14
PLASTIC VISC, CP
10.0
9.0
8.0
7.0
6.0
5.0
4.0
3.0
2.0
1.0
0.9
0.8
0.7
0.6
0.5
0.4
0.3
0.2
0.1
1.30
1.40
1.50
1.60
1.70
1000/T (DEG K)

Figure E-13

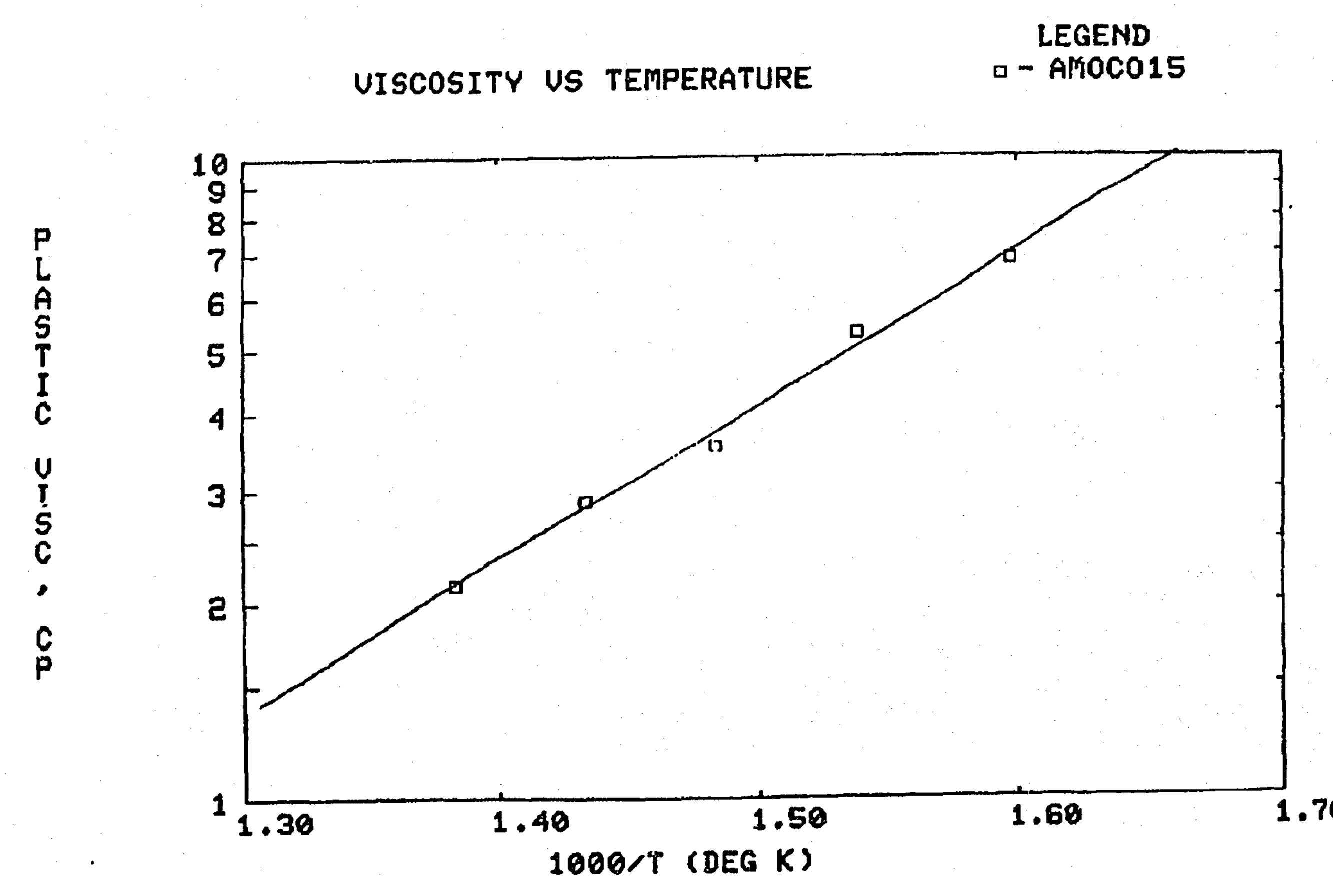

VISCOSITY VS TEMPERATURE
LEGEND
□ - AMOCO15
PLASTIC VISC, CP
10
9
8
7
6
5
4
3
2
1
1.30
1.40
1.50
1.60
1.70
1000/T (DEG K)

Figure E-14

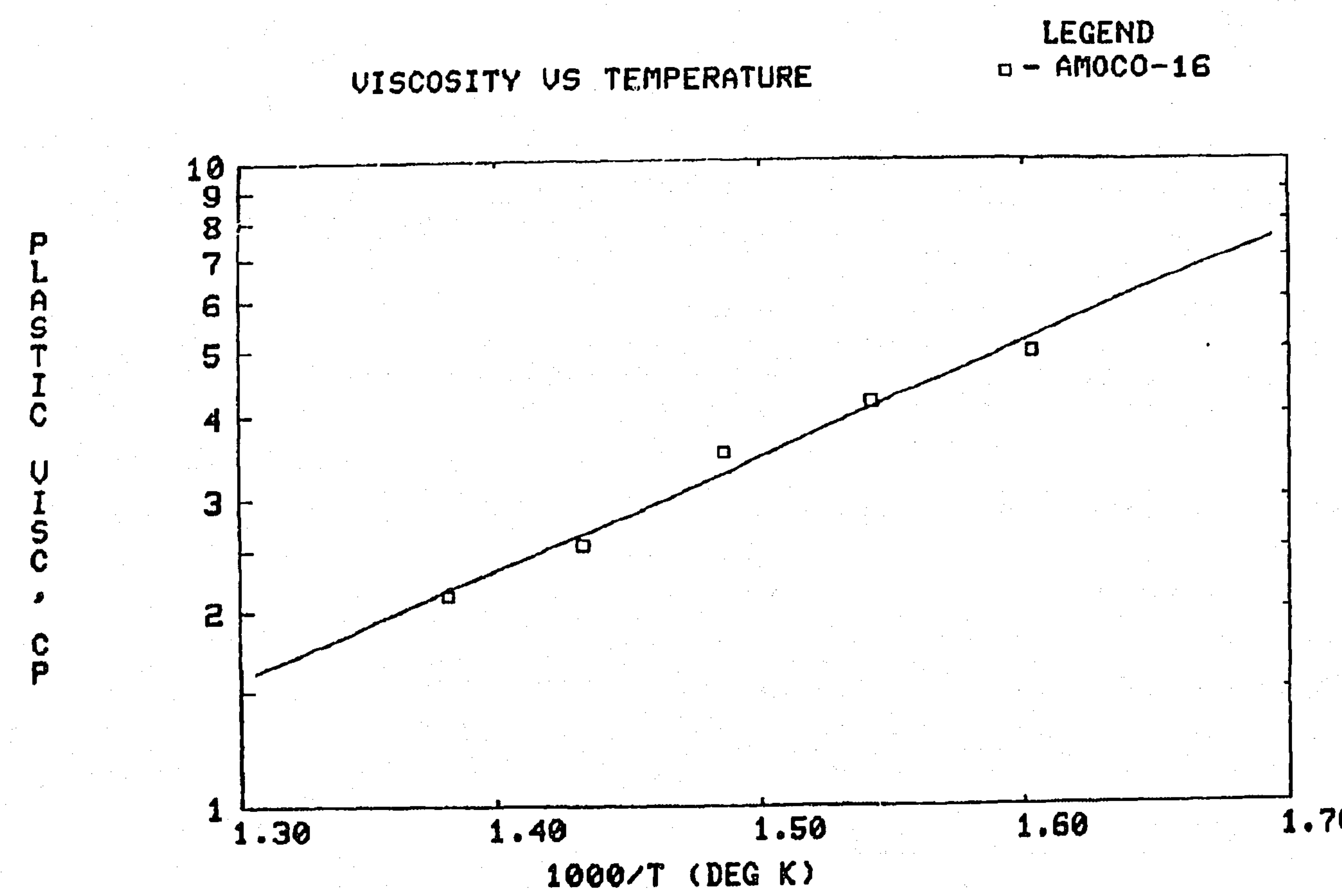

VISCOSITY VS TEMPERATURE
LEGEND
□ - AMOCO-16
PLASTIC VISC, CP
10
9
8
7
6
5
4
3
2
1
1.30
1.40
1.50
1.60
1.70
1000/T (DEG K)

Figure F-1

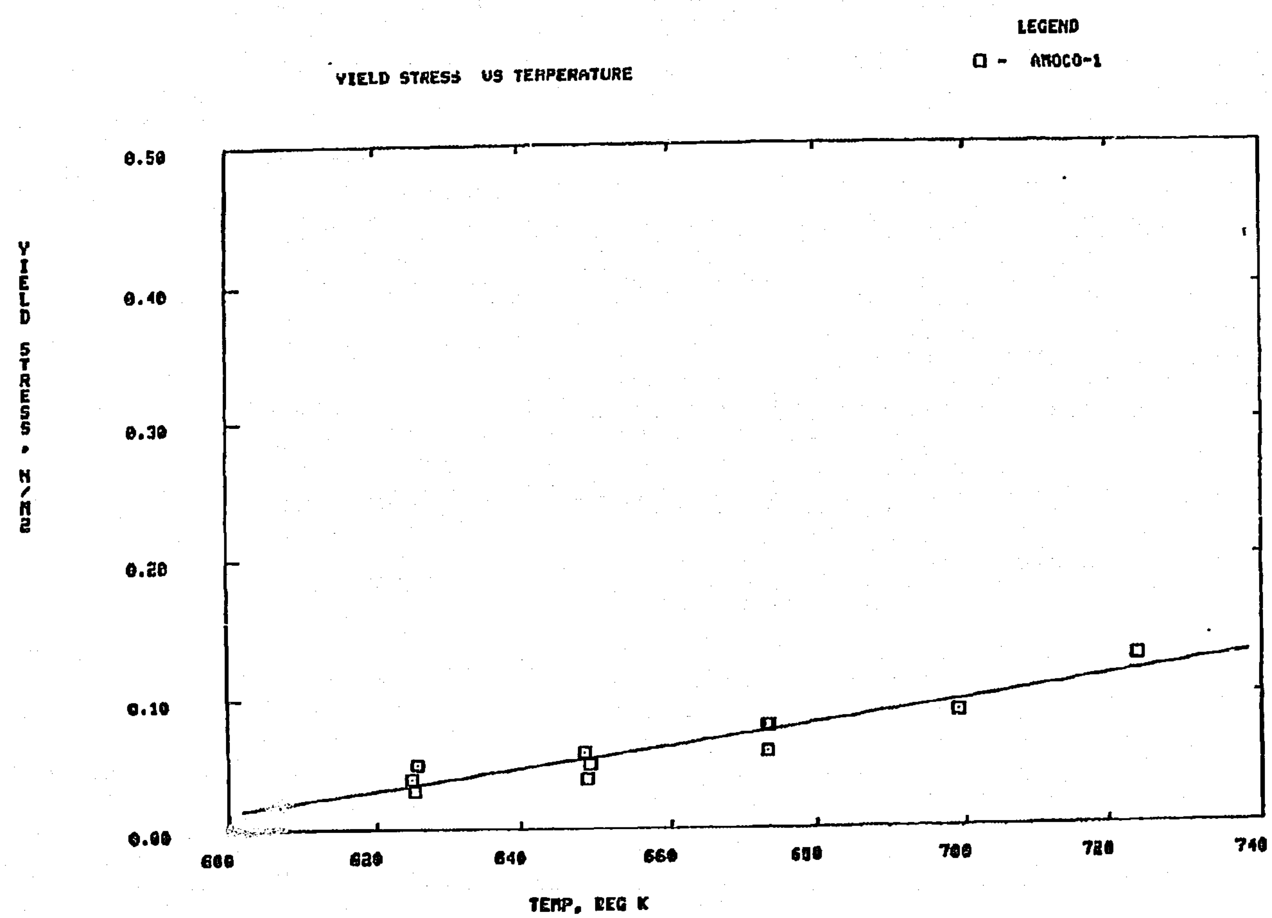
LEGEND
□ - AMOCO-1
YIELD STRESS VS TEMPERATURE
YIELD STRESS, N/M2
0.50
0.40
0.30
0.20
0.10
0.00
600
620
640
660
680
700
720
740
TEMP, DEG K

Figure F-2

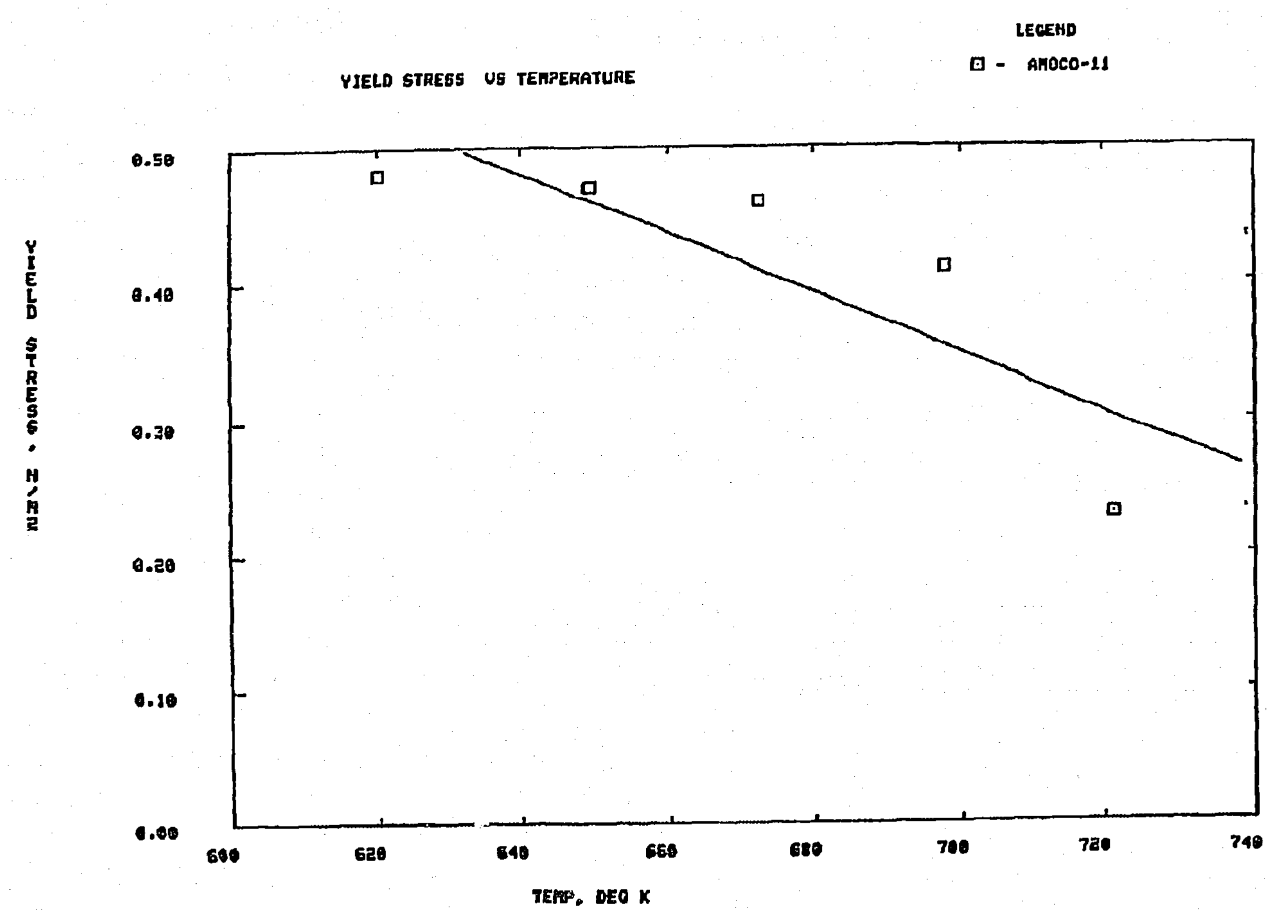
YIELD STRESS VS TEMPERATURE
LEGEND
- AMOCO-11
YIELD STRESS, N/M2
0.50
0.40
0.30
0.20
0.10
0.00
600
620
640
660
680
700
720
740
TEMP, DEG K

Figure F-3

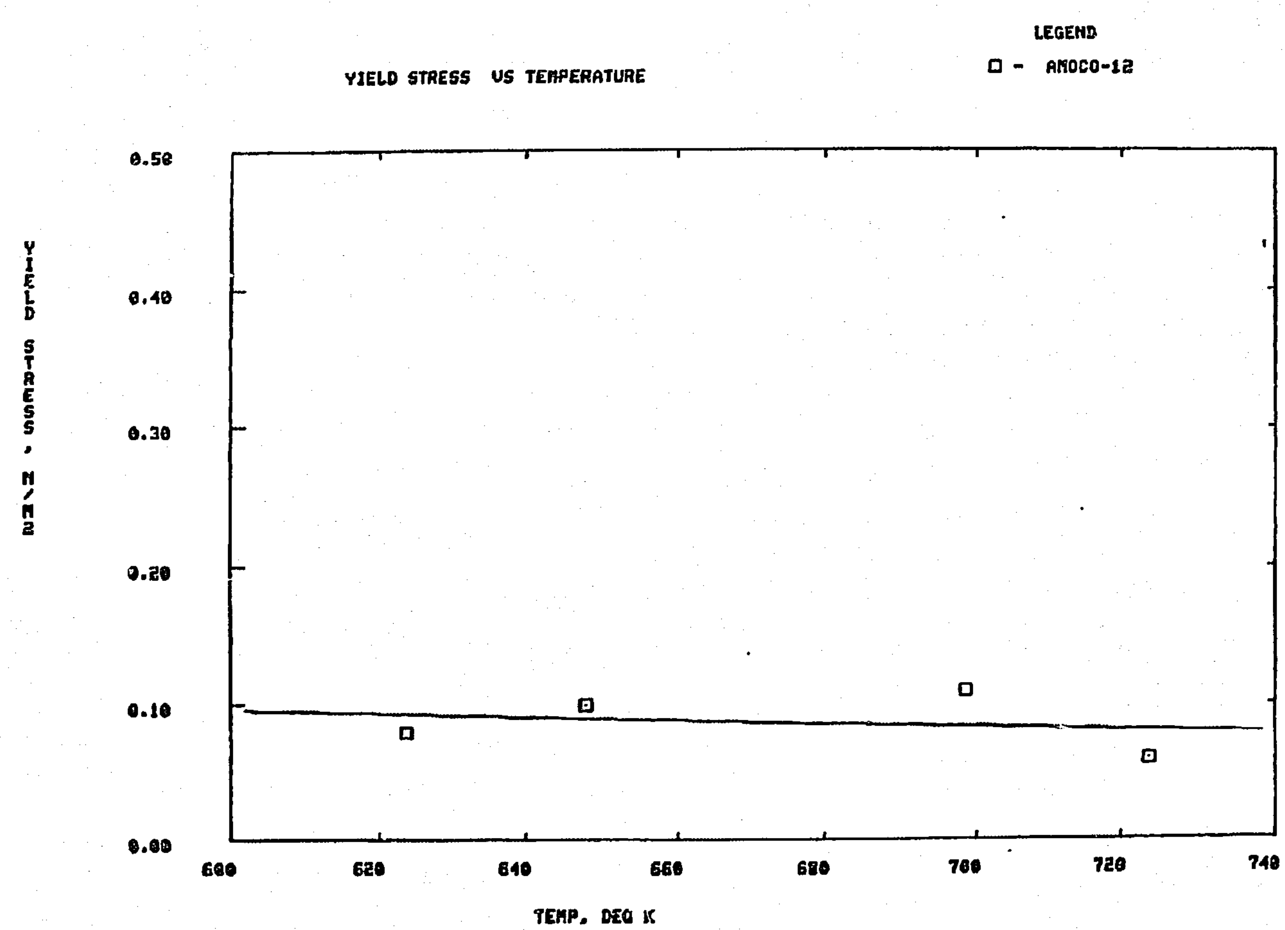
YIELD STRESS VS TEMPERATURE
LEGEND
□ - AMOCO-12
YIELD STRESS, N/M2
0.50
0.40
0.30
0.20
0.10
0.00
600
620
640
660
680
700
720
740
TEMP, DEG K

Figure F-4

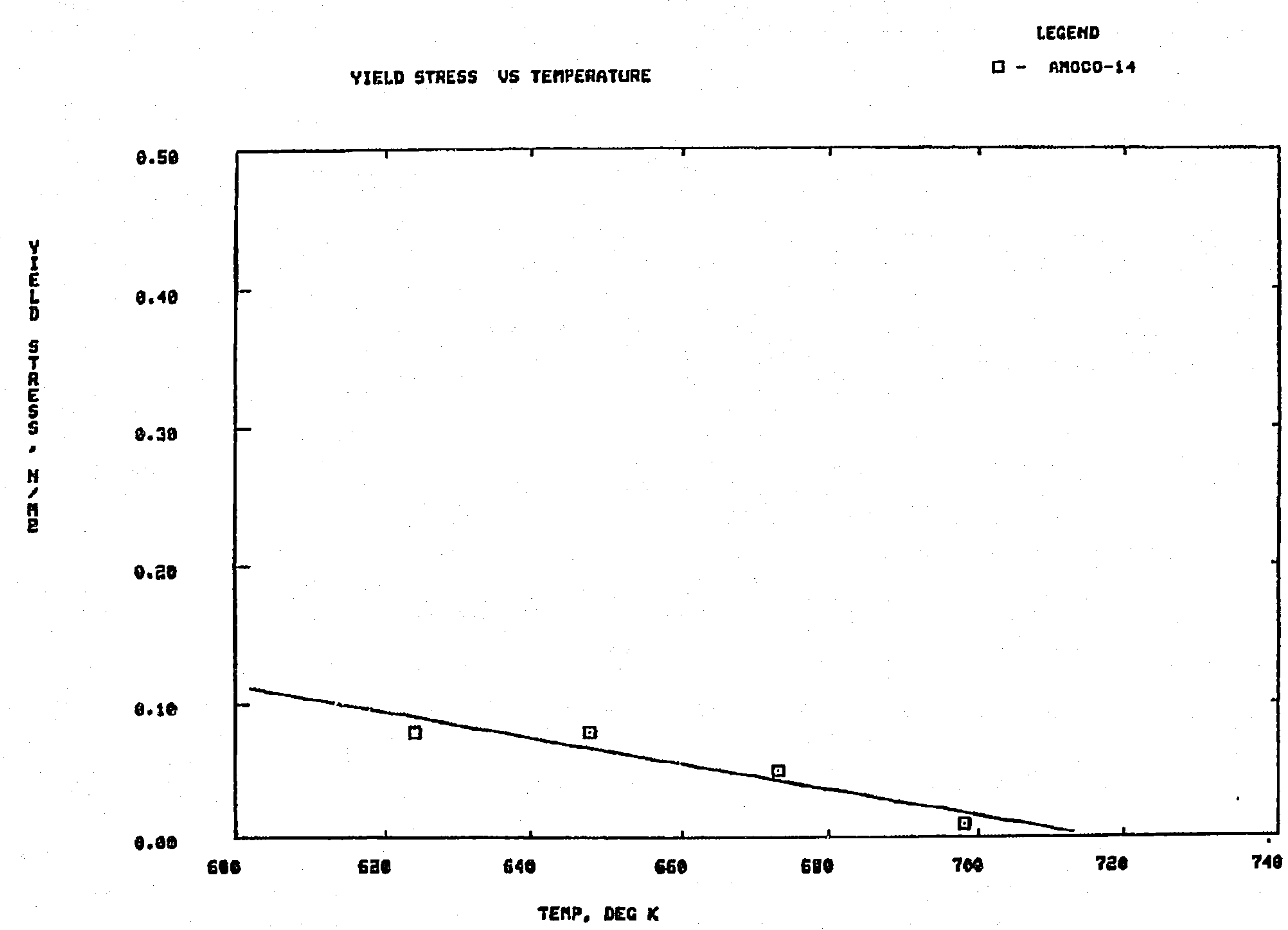

YIELD STRESS VS TEMPERATURE
LEGEND
□ - AMOCO-14
YIELD STRESS, N/M2
0.50
0.40
0.30
0.20
0.10
0.00
600
620
640
660
680
700
720
740
TEMP, DEG K

Figure F-5

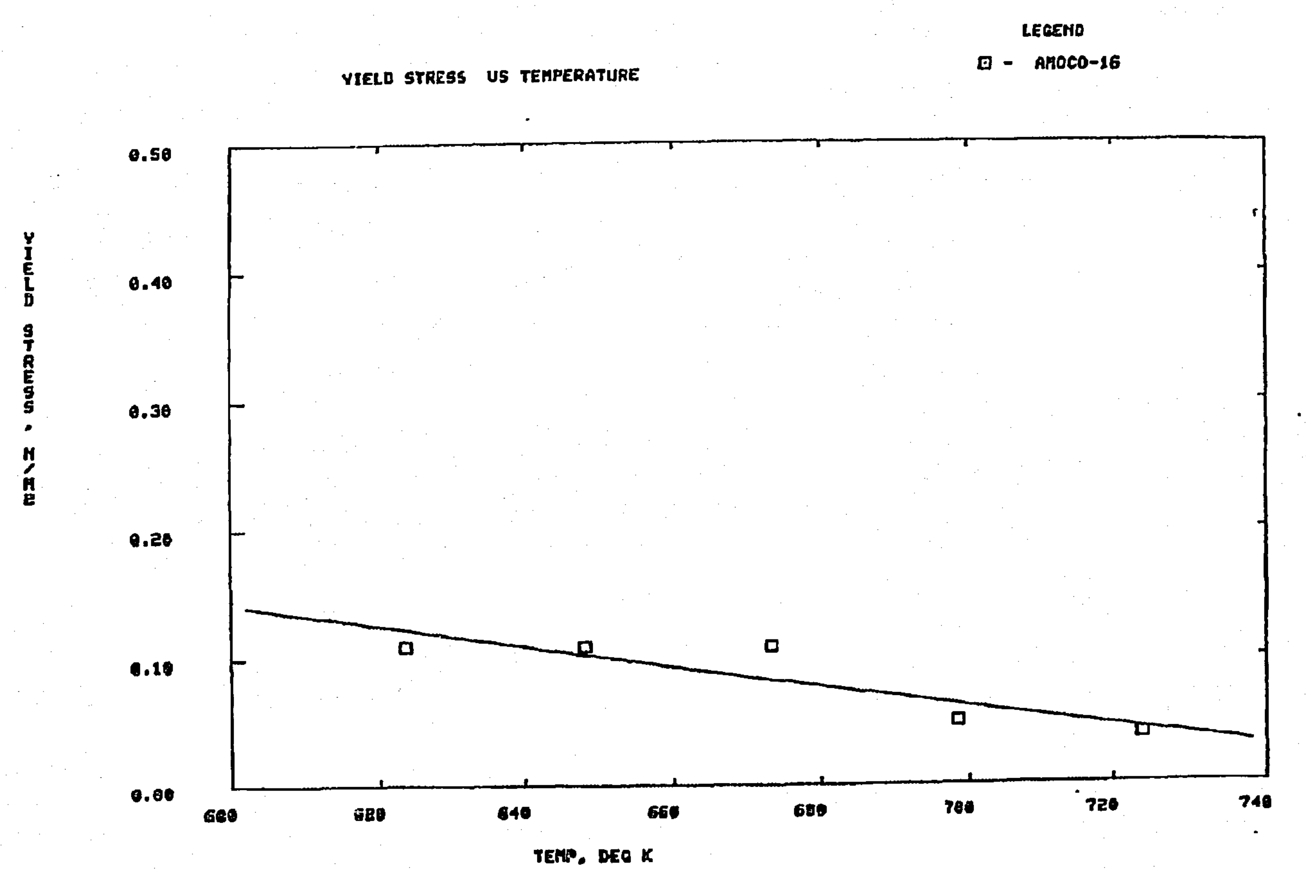
YIELD STRESS VS TEMPERATURE
LEGEND
□ - AMOCO-16
YIELD STRESS, N/M2
0.50
0.40
0.30
0.20
0.10
0.00
600
620
640
660
680
700
720
740
TEMP, DEG K

Figure F-6

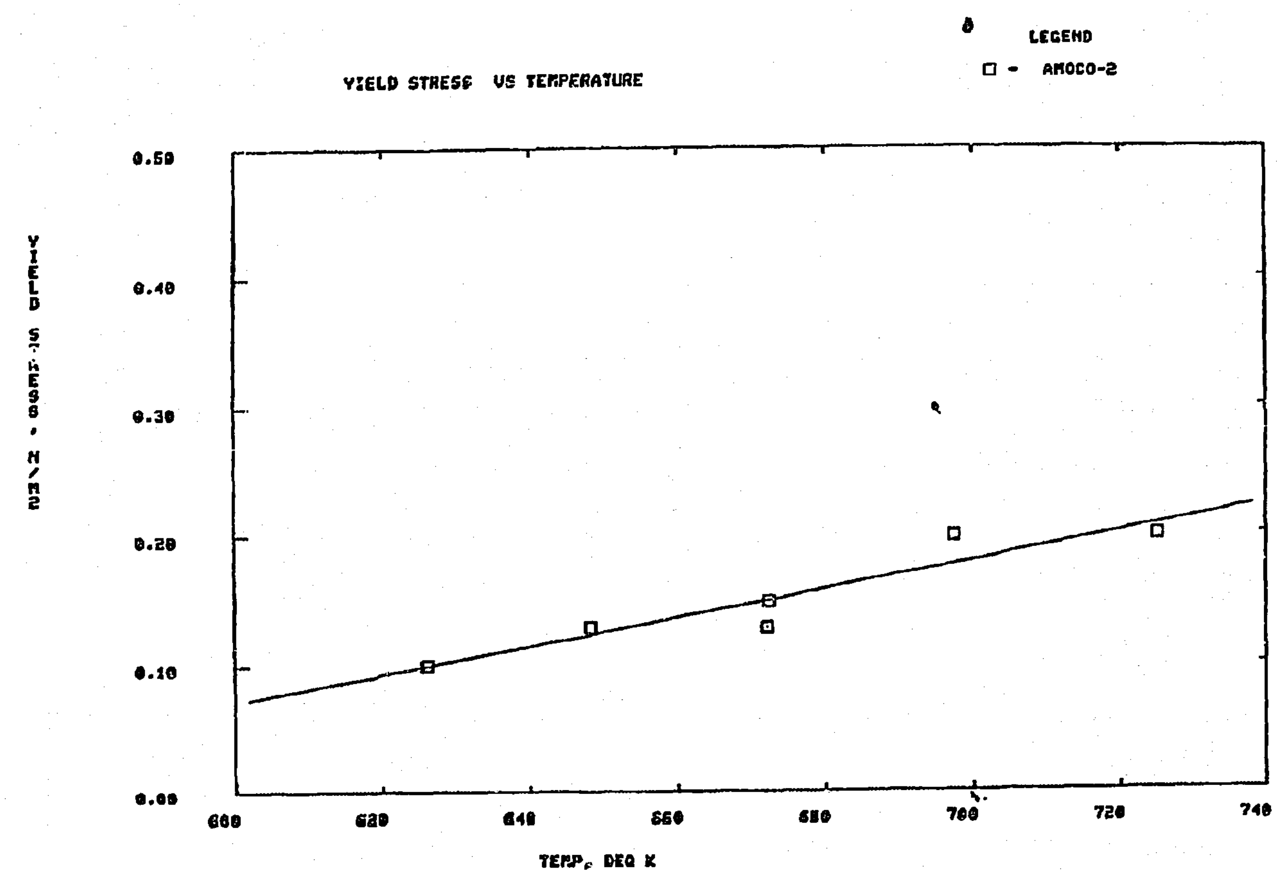

LEGEND
□ - AMOCO-2
YIELD STRESS VS TEMPERATURE
YIELD STRESS, N/M2
0.50
0.40
0.30
0.20
0.10
0.00
600
620
640
660
680
700
720
740
TEMP, DEG K

Figure F-7

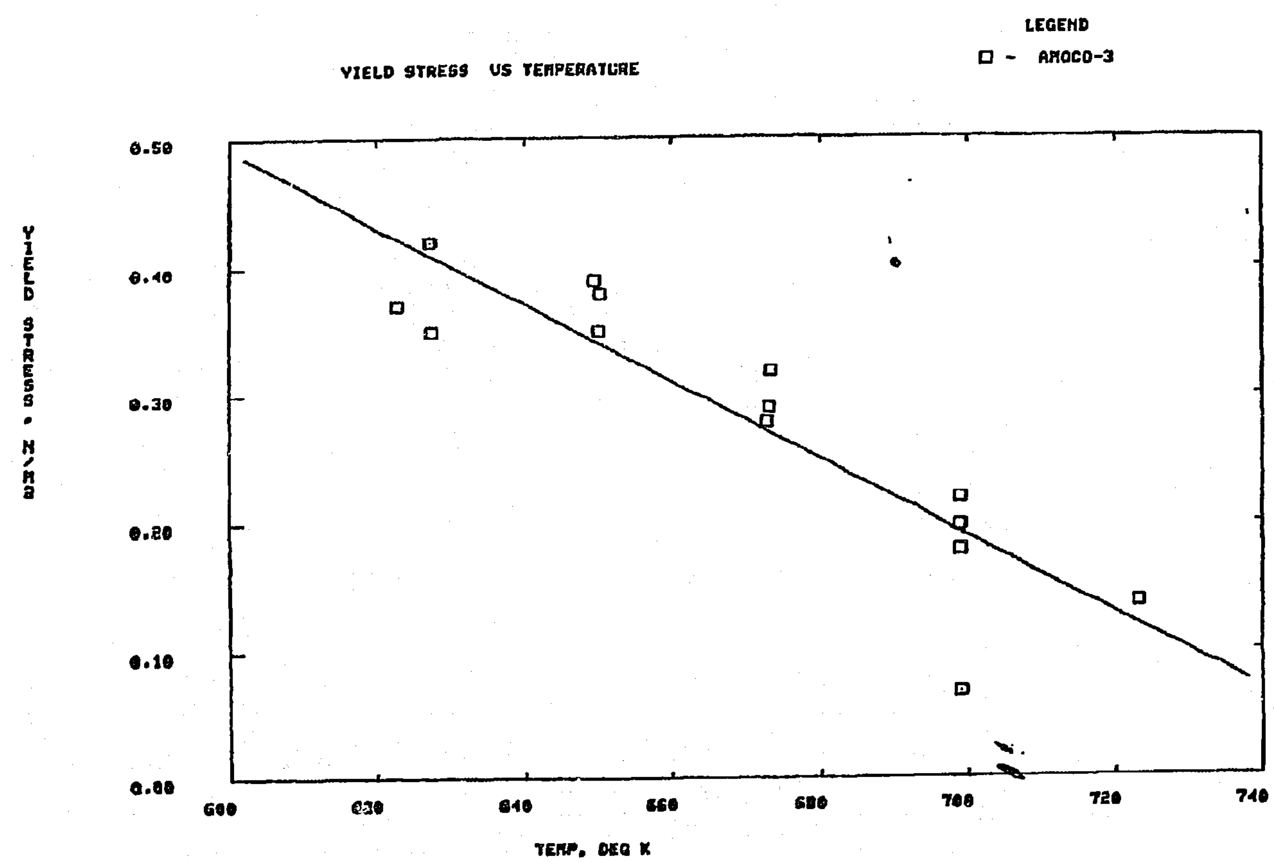
YIELD STRESS VS TEMPERATURE
LEGEND
□ - AMOCO-3
YIELD STRESS, N/M2
0.50
0.40
0.30
0.20
0.10
0.00
600
620
640
660
680
700
720
740
TEMP, DEG K

Figure F-8

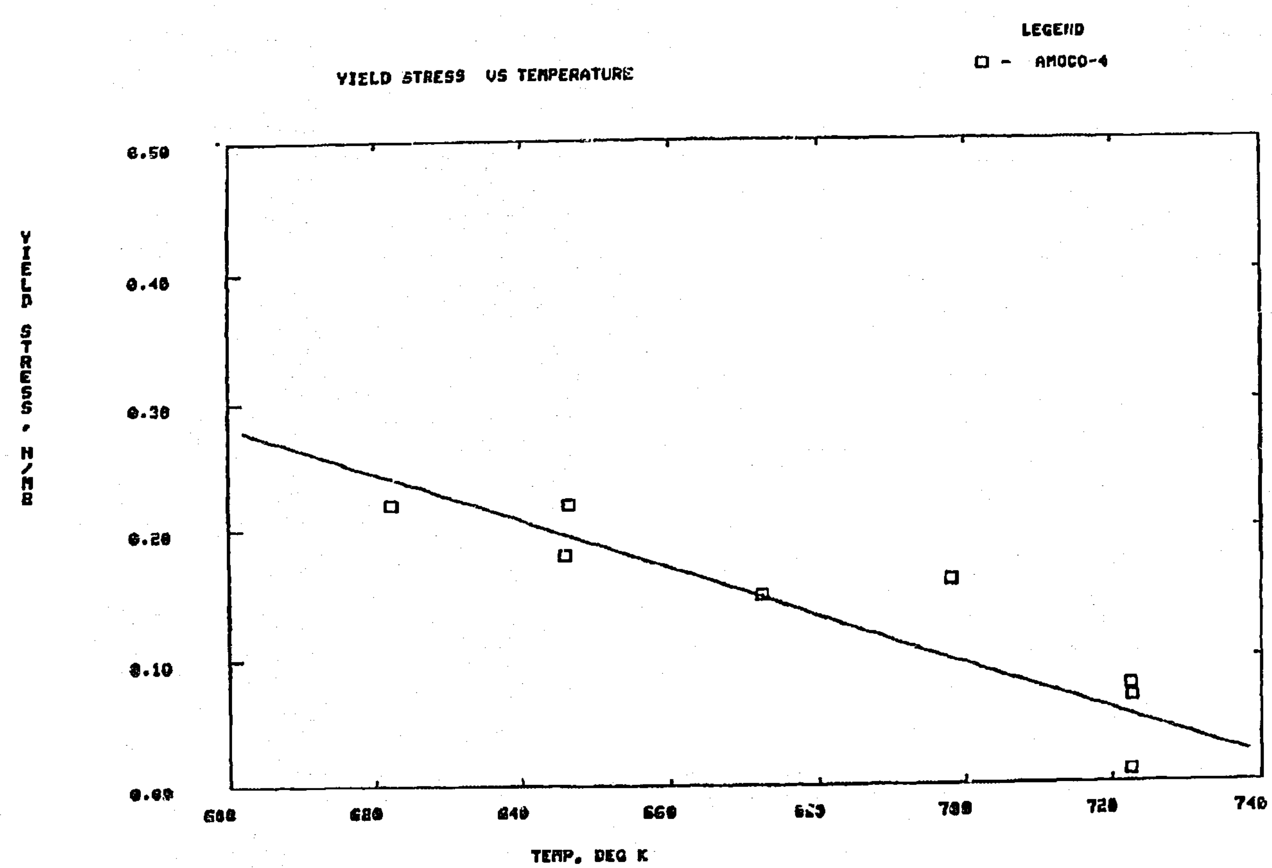
YIELD STRESS VS TEMPERATURE
LEGEND
□ - AMOCO-4
YIELD STRESS, N/M2
0.50
0.40
0.30
0.20
0.10
0.00
600
620
640
660
680
700
720
740
TEMP, DEG K

Figure F-9

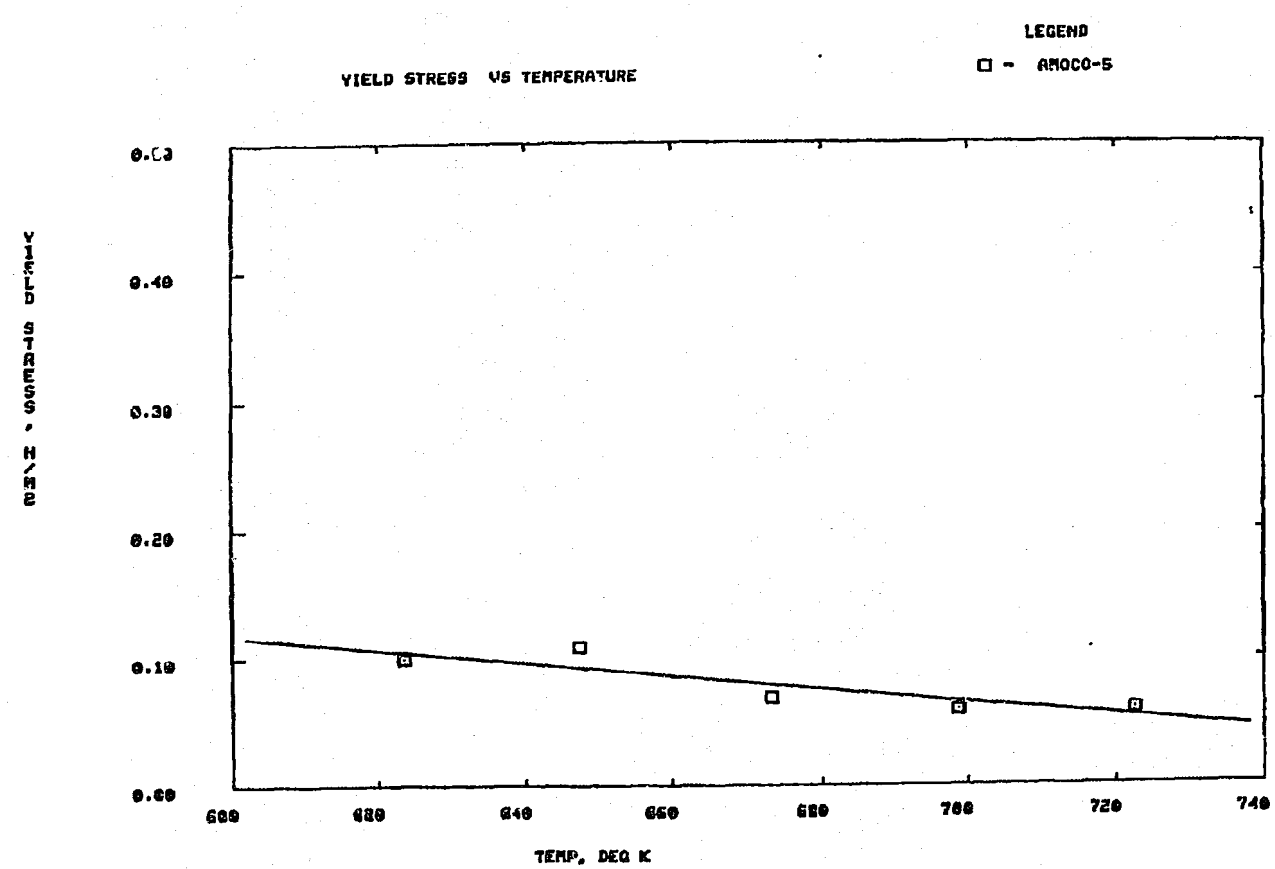
YIELD STRESS VS TEMPERATURE
LEGEND
□ - AMOCO-5
YIELD STRESS, N/M2
0.50
0.40
0.30
0.20
0.10
0.00
600
620
640
660
680
700
720
740
TEMP, DEG K

Figure-10

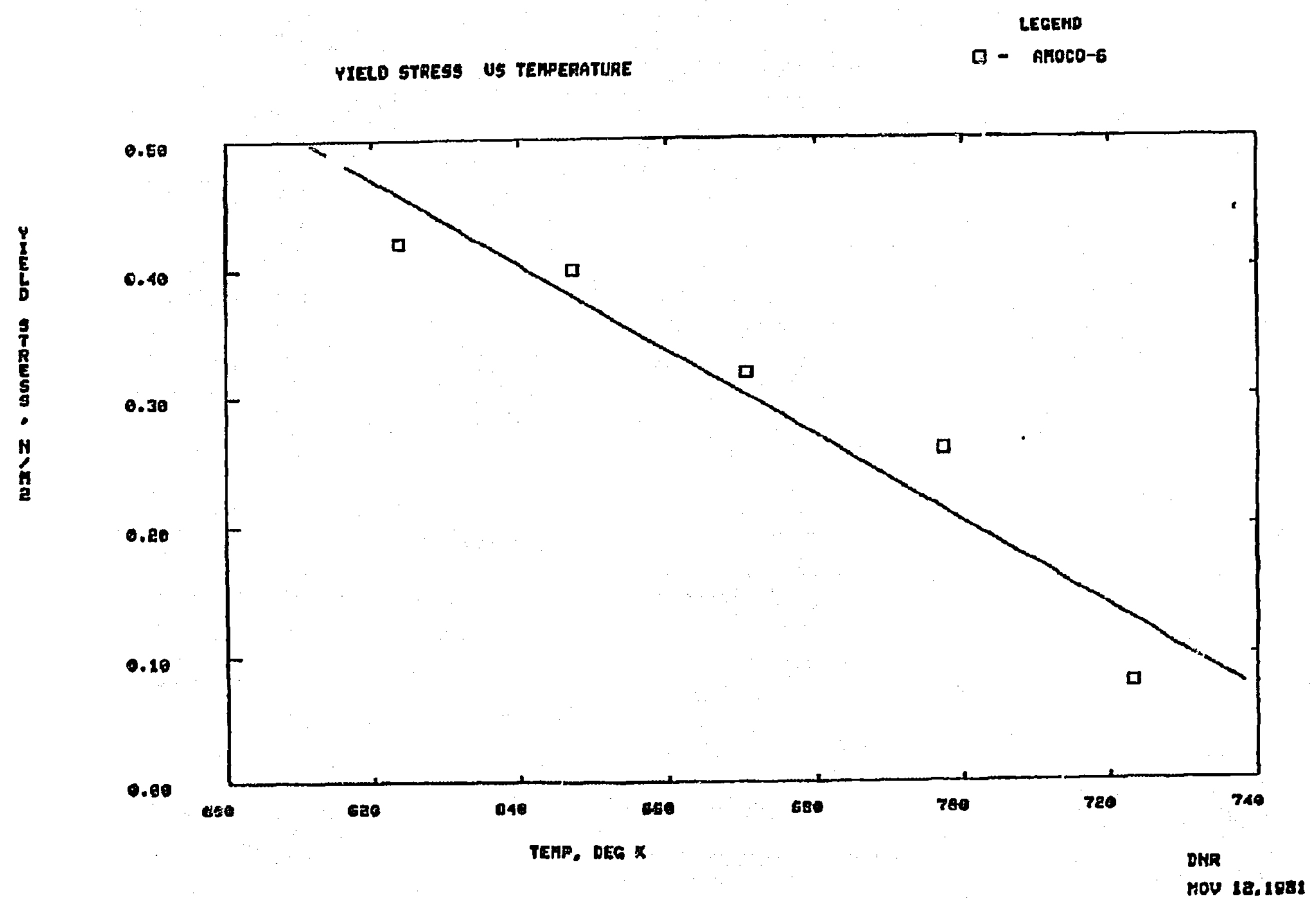
YIELD STRESS VS TEMPERATURE
LEGEND
□ - AMOCO-6
YIELD STRESS, N/M2
0.50
0.40
0.30
0.20
0.10
0.00
600
620
640
660
680
700
720
740
TEMP, DEG K
DNR
NOV 12,1981

Figure F-11

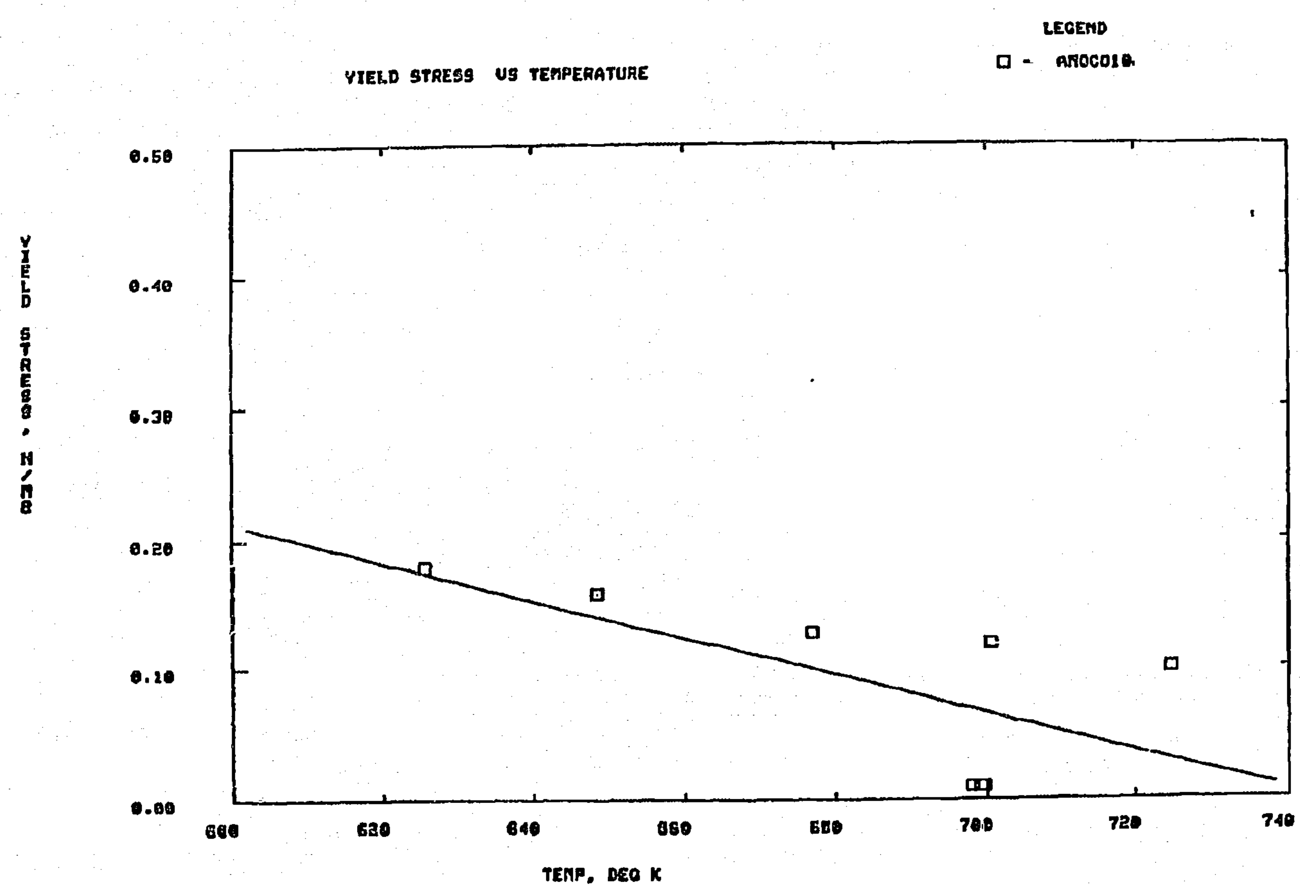

YIELD STRESS VS TEMPERATURE
LEGEND
□ - AMOCO10
YIELD STRESS, N/M2
0.50
0.40
0.30
0.20
0.10
0.00
600
620
640
660
680
700
720
740
TEMP, DEG K

Figure F-12

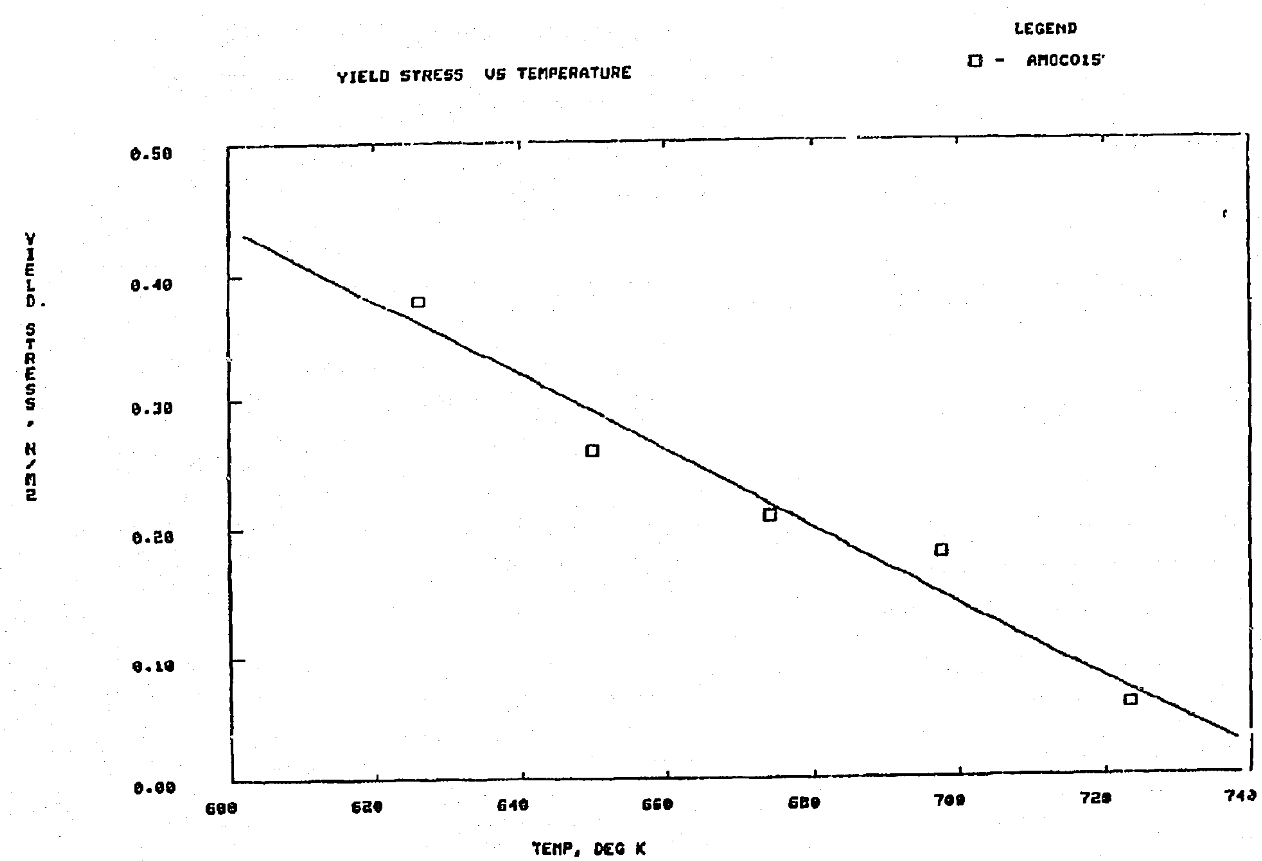
YIELD STRESS VS TEMPERATURE
LEGEND
□ - AMOCO15'
YIELD. STRESS, N/M2
0.50
0.40
0.30
0.20
0.10
0.00
600
620
640
660
680
700
720
740
TEMP, DEG K

Figure F-13

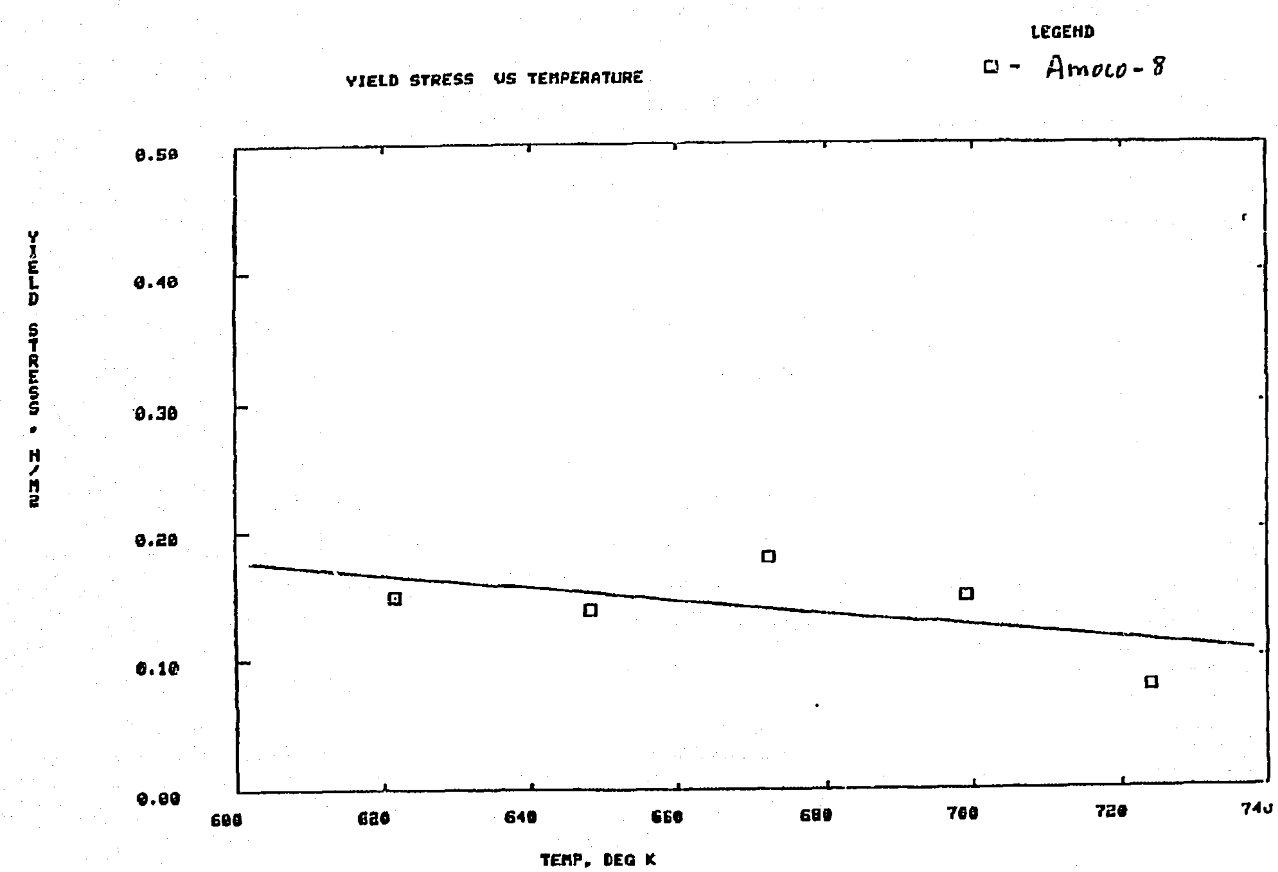
YIELD STRESS VS TEMPERATURE
LEGEND
□ - Amoco-8
YIELD STRESS, N/M2
0.50
0.40
0.30
0.20
0.10
0.00
600
620
640
660
680
700
720
740
TEMP, DEG K

Figure F-14

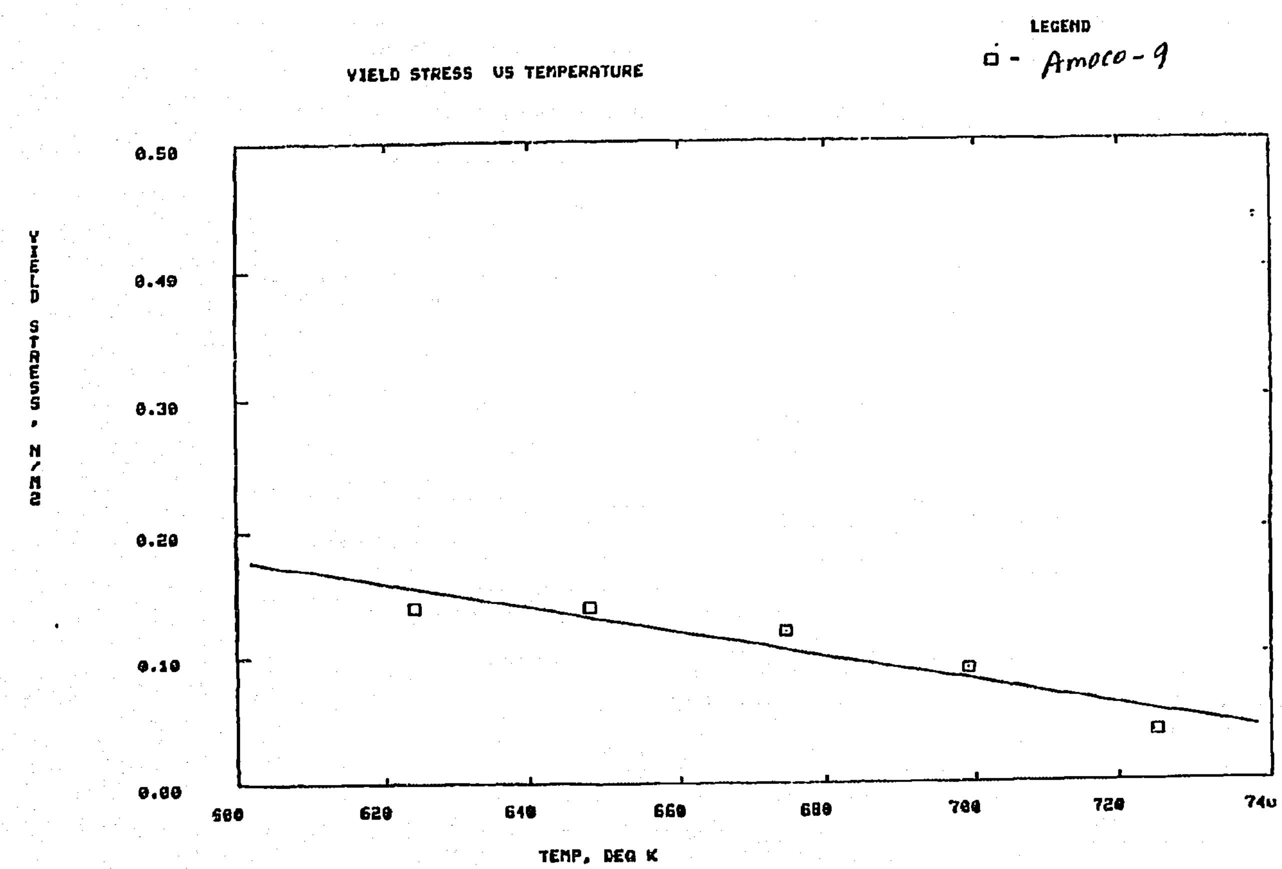

LEGEND
□ - Amoco-9
YIELD STRESS VS TEMPERATURE
0.50
0.40
0.30
0.20
0.10
0.00
YIELD STRESS, N/M2
600
620
640
660
680
700
720
740
TEMP, DEG K